University of Cincinnati

Date: 10/16/2015

I, Dusten Unruh , hereby submit this original work as part of the requirements for the degree of Doctor of Philosophy in Pathobiology & Molecular Medicine.

It is entitled:

Alternatively spliced tissue factor and pathobiology of pancreatic ductal adenocarcinoma: a novel biomarker and potential therapeutic target

Student's name: **Dusten Unruh**

This work and its defense approved by:

Committee chair: Vladimir Bogdanov, Ph.D.

Committee member: Fred Lucas, M.D.

Committee member: El Mustapha Bahassi, Ph.D.

Committee member: William Miller, Ph.D.

Committee member: Xiaoyang Qi, Ph.D.

19451

Alternatively spliced tissue factor and pathobiology of pancreatic ductal adenocarcinoma: a novel biomarker and potential therapeutic target

A dissertation presented
by

Dusten John Unruh
B.S., North Dakota State University, 2009

To

The Graduate School
of the University of Cincinnati
in partial fulfillment of the requirements for the degree of

Doctor of Philosophy

In the department of Internal Medicine, Division of Hematology-Oncology
of the College of Medicine

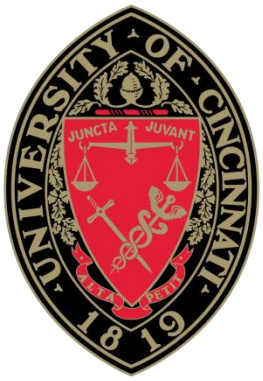

September 2015

Committee Chair: Vladimir Bogdanov, Ph.D.

Abstract

Background: Pancreatic ductal adenocarcinoma (PDAC) comprises ~75% of all diagnosed cases of pancreatic cancer – the 4th leading cause of cancer death and a growing public health problem. The incidence of PDAC continues to increase while the overall 5-year survival rate remains <5%. This extremely poor prognosis is largely due to the absence of effective treatments and late diagnosis, making the identification and testing of new therapeutic targets and biomarkers a high priority.

PDAC is marked by high expression of Tissue Factor (TF), the main physiologic trigger of blood coagulation. There are two forms of TF: full-length TF (flTF) that contains a transmembrane domain and alternatively spliced TF (asTF) that lacks a transmembrane domain and is secreted. In malignant tissues, the function of TF is known to extend beyond clotting. flTF triggers intracellular signaling via G protein-coupled protease-activated receptors (PARs), which leads to increased tumor growth predominantly by neoangiogenesis. It was later discovered that flTF expressed on cancer cells keeps β1-integrins in an inactive state and that FVIIa:TF binding releases this inhibition, rendering cancer cells more motile and responsive to integrin signaling. In striking contrast to flTF, asTF binds and activates integrins promoting cancer cell proliferation, resistance to apoptosis, and angiogenesis, suggesting that the asTF-integrin signaling axis may represent a novel therapeutic target.

Aim: To improve our understanding of the mechanisms regulating asTF-induced PDAC progression, examine circulating levels of asTF and assess the effectiveness of anti-asTF targeted therapeutics in hopes of improving PDAC treatment.

Methods: Tumor microarrays, PDAC specimens, and PDAC metastases were evaluated for asTF expression and/or monocyte infiltration. PDAC cell lines were implanted in the pancreases of mice and *in vivo* imaging studies performed. TF activity was measured using FXa chromogenic assay; TF levels were assessed using flow cytometry and ELISA. Anti-asTF monoclonal antibody RabMab1 was co-implanted with Pt45P1 cells and monitored for tumor progression.

Results/Conclusions: We report for the first time that asTF is expressed in human PDAC lesions exhibiting heavy monocyte infiltration, and demonstrate that asTF potentiates PDAC spread during early as well as late stages of disease. asTF enhances the procoagulant potential of PDAC cells and cell derived microparticles. asTF-β1 integrin interactions render PDAC cells more motile, likely via competing with laminin for β1-integrin binding; RabMab1 fully inhibits asTF-potentiated PDAC cell migration. Host-derived TF has no impact on the size of primary PDAC tumor, yet it contributes to tumor vascularization and, consequently, metastatic spread. When co-implanted with RabMab1, Pt45P1 cells grow much smaller tumors with fewer monocytes and blood vessels that release less asTF into the circulation. We also report that asTF at levels ≥0.2 ng/mL occurs more frequently in the plasma of patients with PDAC compared to healthy subjects, and PDAC patients whose plasma asTF levels are ≥0.2 ng/mL have a significantly lower chance to qualify for tumor resection, irrespective of initial pre-surgical diagnostic evaluation. Thus, asTF may serve as marker of aggressive PDAC phenotype, and antibody-based targeting of asTF may comprise a novel therapeutic strategy to stem PDAC progression.

Acknowledgments

It was with the help and support of many friends, colleagues, coauthors and others who made this work possible. I would like to express the deepest appreciation to:

My advisor, Dr. Vladimir Bogdanov who deserves thanks for many things. First and foremost, for creating the research environment in which I have performed my graduate studies. Vladimir, your enthusiasm, energy, and stories have made the laboratory a joy. You always provide insightful discussions and analogies about the research, which encourage critical thinking. Your input during key moments in my work while also allowing me to work independently provided a great environment. Without your guidance and confidence in me these last five years this dissertation would not have been possible.

My thesis committee members, Drs. Fred Lucas, Mustapha Bahassi, Xiaoyang Qi, and William Miller whom I am grateful for their willingness to endure my committee meeting presentations and provide feedback and encouragement. Your support and constructive feedback are greatly appreciated.

Because of the research environment sustained by Vladimir, I have crossed paths with many collaborators, students, and postdocs who have influenced and enhanced my research. My work has been strongly influenced by Dr. Ramprasad Srinivasan; a postdoc in the lab when I joined, who taught me lab techniques and multiple assays critical to completing this work. Timofey Sovershaev, a rotating student from Tromsø, Norway who became a close friend and provided new perspective on working projects. Kathleen LaSance, for all her help with mouse

imaging. Rotating students Robert Sturm and Ryan Keil for all their help and assistance. Zhengtao Chu for teaching me the orthotopic pancreatic cancer mouse model.

The Pathobiology and Molecular Medicine program, students and faculty for providing an enriching environment during my education. Also, I would like to thank Heather Anderson, the program coordinator for keeping me on track. Your support and encouragement are greatly appreciated.

My good friends Robert and Jamie Koncar, who were somewhat of psychologists during this journey keeping me sane, your friendship was one of the most rewarding outcomes from these past five years.

My parents, Wayne and Tangula, for all their love and encouragement. They instilled at an early age a love of nature and science, and supported me in all of my pursuits. You've taught me about hard work, persistence and having self-respect all which have created a good foundation to meet life. My sister, Sierra for your support and love, and who I am proud of and love very much.

Most of all, my wife Magaly, my love and companion whom I fell in love with during our senior year at North Dakota State University. You left your friends and job, so I could pursue graduate school. Your support and willingness to endure soporific presentation practices, and the fact that you proofread my thesis and may perhaps be the only person other than me who will read the entire thing. Without your support there would be no thesis.

Contents

List of Figures

Abbreviations:

ABP-280	actin-binding protein 280
ACS	acute coronary syndrome
Akt	protein kinase B
AREG	amphiregulin
Asn	asparagine
ASF/SF2	serine/arginine-rich splicing factor 2
asTF	alternatively spliced Tissue Factor
ATCC	American Type Culture Collection
BMP	bone morphogenetic protein
BRCA1 & 2	breast cancer 1 & 2
CA19-9	carbohydrate antigen 19-9
CD11b	cluster of differentiation 11b
CD68	cluster of differentiation 68
CD206	cluster of differentiation 206
CDKN2A	cyclin-dependent kinase inhibitor 2A
cDNA	complementary deoxyribonucleic acid
Clk1	CDC-like kinase 1
Clk4	CDC-like kinase 4
CRP	C-reactive protein
CT	computed tomography
CTGF	connective tissue growth factor
CTL4	cytotoxic T-lymphocyte-associated protein 4
Cyr61	cysteine-rich angiogenic inducer 61
Cys	cysteine
CXCL1	chemokine (C-X-C motif) ligand 1
CVM	Cell-Vue Maroon
DAB	3, 3-diaminobenzidine
DISPO	Disposition Impacted by Serial Point of Care Markers
DM	diabetes mellitus

DMEM	Dulbecco's Modified Eagle's Medium
DOPS	dioleoylphosphatidylserine
DOX	doxycycline
ECM	extracellular matrix
EGF	epidermal growth factor
EGFR	epidermal growth factor receptor
EFEMP1	epidermal growth factor-containing fibulin-like extracellular matrix protein 1
EGR-1	early growth response gene-1
ELISA	enzyme-linked immunosorbent assay
EMT	epithelial-to-mesenchymal transition
ESE	exonic splicing enhancer
E-selectin	endothelial-leukocyte adhesion molecule 1
FVII	coagulation factor VII
FVIIa	activated coagulation factor VII
FIX	coagulation factor IX
FX	coagulation factor X
FACS	fluorescence-activated cell sorting
FAK	focal adhesion kinase
FBS	fetal bovine serum
FDA	Food and Drug Administration
FDG	^{18}F-fluorodeoxyglucose
FFPE	formalin-fixed paraffin-embedded
FITC	fluorescein isothiocyanate
flTF	full-length Tissue Factor
GAPDH	glyceraldehyde 3-phosphate dehydrogenase
GEO	Gene Expression Omnibus
GM-CSF	granulocyte macrophage colony-stimulating factor
GTP	guanosine triphosphate
H&E	hematoxylin and eosin
HIF-1α	Hypoxia-inducible factor 1-alpha
HRP	horseradish peroxidase

hTF	human Tissue Factor
ICAM-1	intercellular adhesion molecule 1
IHC	immunohistochemistry
IFN-γ	interferon-gamma
IgG	immunoglobulin G
IL-1α	interleukin-1α
IL-6	interleukin-6
IL-8	interleukin-8
IMDM	Iscove's Modified Dulbecco's Medium
JNK	c-Jun N-terminal kinase
K-RAS	Kirsten rat sarcoma viral oncogene homolog
Le	Lewis antigen
LKB1	liver kinase B1
Lys	lysine
mAb	monoclonal antibody
MAPK	mitogen-activated protein kinase
M-CSF	macrophage colony-stimulating factor
Mdm2	mouse double minute 2 homolog
Mist1	muscle intestine and stomach expression 1
MLH1	MutL homolog 1
MPs	microparticles
MRI	magnetic resonance imaging
mRNA	messenger ribonucleic acid
mTF	murine Tissue Factor
mTOR	mammalian target of rapamycin
NAP5	nematode anticoagulant protein 5
NAPc2	nematode anticoagulant protein c2
NCBI	National Center for Biotechnology Information
NF-κB	nuclear factor kappa-light chain-enhancer of activated B cells
NF-Y	nuclear factor Y
NSCLC	non-small cell lung cancer

p14ARF	alternative reading frame protein 14
PanIN	pancreatic intraepithelial neoplasia
PAR-1	protease activated receptor 1
PAR-2	protease activated receptor 2
PARS	protease activated receptors
PBS	phosphate-buffered saline
PD-1	programmed cell death protein 1
PDAC	pancreatic ductal adenocarcinoma
PDGFRb	platelet-derived growth factor receptor b
Pdx1	pancreatic and duodenal homeobox 1
PET	positron emission tomography
PI3K	phosphatidylinositol 3-kinase
PKC	protein kinase C
pNET	pancreatic neuroendocrine tumor
PPP	platelet poor plasma
PRSS1	protease serine 1
PS	phosphatidylserine
PTEN	phosphatase and tensin homolog
PVDF	polyvinylidene fluoride
RalGDS	Ral guanine nucleotide dissociation stimulator
Ras-ERK	extracellular signal-regulated kinase
RhoA	Ras homolog gene family member A
RNA	ribonucleic acid
rNAPc2	recombinant nematode anticoagulant protein c2
ROS	reactive oxygen species
SapC	Saponin C protein
SC35	splicing component 35
SCID	severe combined immunodeficiency
SMA	superior mesenteric artery
SMAD4	mothers against decapentaplegic homolog 4
SR	splicing regulatory / serine-arginine rich

SRp40	Serine/arginine-rich splicing factor 5
SRp55	Serine/arginine-rich splicing factor 6
TAMs	tumor associated monocytes/macrophages
TF	Tissue Factor
TGF-β	transforming growth factor beta
TMA	tissue microarrays
TMB	3,3',5,5'-Tetramethylbenzidine
TNF-α	tumor necrosis factor-alpha
TP53	tumor protein 53
TP73	tumor protein 73
UCCI-TB	University of Cincinnati Cancer Institute's Tumor Bank
VCAM-1	vascular cell adhesion protein 1
VEGF	vascular endothelial growth factor
VEGF-A	vascular endothelial growth factor-A
VEGF-C	vascular endothelial growth factor-C
VTE	venous thromboembolism
WTA	whole transcriptome amplification

Chapter 1: Introduction

In solving a problem of this sort, the grand thing is to be able to reason backwards. That is a very useful accomplishment, and a very easy one, but people do not practice it much.

– Sherlock Holmes, in Sir Arthur Conan Doyle's
A Study in Scarlet

1.1 The pancreas – a brief history

The earliest known description of the pancreas is attributed to Herophilus of Chalcedon (300 B.C.), a Greek physician deemed to be one of the first human anatomists and adopter of the scientific method (1). Despite Herophilus's pioneering research on human anatomy, he received public criticism and was referred to as the 'butcher' of Alexandria – for his innumerable human dissections and gruesome vivisections performed before public audiences (2). The name 'pancreas' was later coined by Rufus (100 A.D.), another Greek physician, and etymologically translates as all flesh (pan: all, and kreas: flesh) – at the time the Greeks thought the pancreas was a fleshy cushion to protect the large blood vessels lying behind it (3). It wasn't until the 17th century that researchers discovered its glandular function. In 1642, during the dissection of an executed murderer, Johann Georg Wirsüng, the prosector of Padua, described the main duct of the pancreas and to this day it bears his name (4). Wirsüng achieved historical immortality with his discovery, and at the same time it was his ruin: one year following his discovery he was murdered by a co-worker, the result of a quarrel over who was the first to truly discover the duct (5). Although Wirsüng is credited with the duct's discovery, he never recognized the duct's function, and in a letter to a colleague he described it as an artery or vein that lacks blood (4).

The glandular function of the pancreas was first hypothesized by Reignier de Graaf. While studying at Leiden in 1664, De Graaf investigated pancreatic secretion via the method of collecting pancreatic juices by cannulation of the pancreatic duct (6). De Graaf was unable to identify the chemical composition of the collected pancreatic juice; he merely tasted it, and noted its 'insipid' and 'acid-salt' palate (3). Although De Graaf was wrong in believing that pancreatic juice was acidic (pancreatic fluid has a pH around 8.6), he hypothesized that its primary function was for the

segregation of food elements. This hypothesis was later supported and espoused upon by 19th century German chemists Willy Kuhne and Alexander Marcet, who discovered the pancreatic digestive enzymes trypsin and lipase. However, the French physiologist Claude Bernard is credited with clarifying the function of the pancreas when he demonstrated the ability of pancreatic juice to emulsify fatty foods and convert starch into sugar (3). These discoveries and experimental investigations summarized above are just a few of the important contributions in determining the anatomy and physiology of the pancreas.

1.2 Pancreas anatomy and physiology

The pancreas is a compound glandular organ, derived from the endoderm that is located in the retroperitoneum associated with several vital structures, which complicate diagnostic and therapeutic procedures. Normally it has an average weight of 90 g, and is shaped like a tadpole, that is divided into four main anatomical areas: head, neck, body, and tail (7). The pancreatic head is the thickest portion of the pancreas and lies within the C-loop of the duodenum, to the right of the superior mesenteric and portal veins. The neck of the pancreas is the narrowest portion of the gland with a width less than 2 cm; lengthwise it traverses the mesenteric blood vessels anteriorly, connecting the pancreatic head and body. The pancreatic body is located between the neck and tail of the pancreas, and sits above the superior mesenteric artery and vein. The pancreatic tail extends from the pancreas body to the splenic hilum. The pancreatic duct (duct of Wirsüng) traverses the entire pancreas lengthwise and joins with the common bile duct, which drains secretions from acinar cells and bile into the duodenum via the duodenal papilla (papilla of Vater) (**Figure 1.1A**).

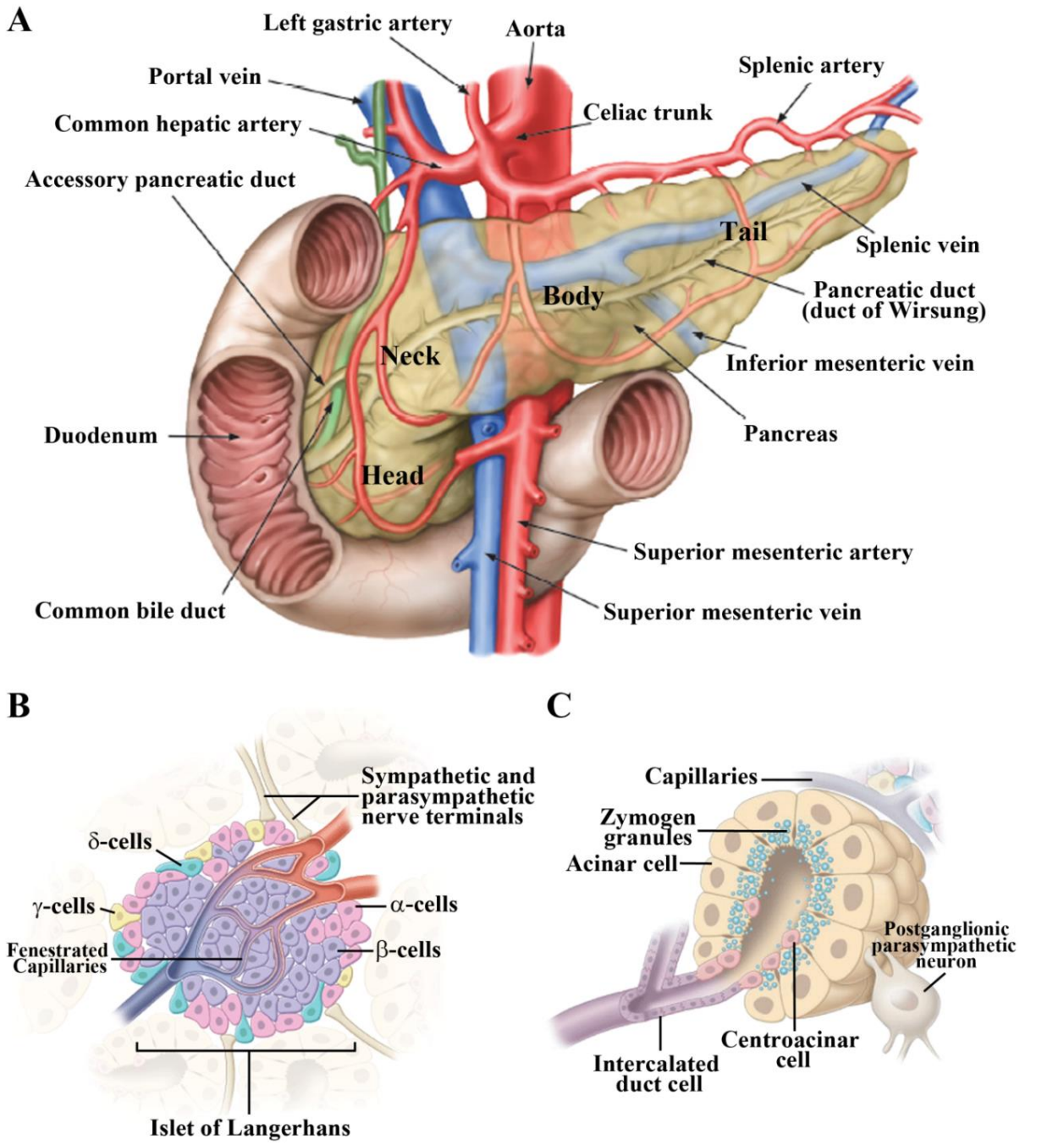

Figure 1.1: Anatomy and physiology of the pancreas. (***A***) Gross anatomy of the pancreas. (***B***) & (***C***) Exocrine and endocrine functional units of the pancreas. The pancreas participates in two major physiologic processes: digestion and glucose metabolism. (***B***) The endocrine portion of the pancreas, primarily responsible for regulating glucose homeostasis. (***C***) The exocrine portion of the pancreas, responsible for secreting digestive enzymes (zymogens) into the ducts. Adapted from (314).

As mentioned above, the pancreas functions as both exocrine and endocrine gland (a compound glandular organ) (**Figure 1.1B & C**). Approximately 85% of the pancreas is comprised of a branching network of acinar (meaning 'cluster of grapes') and duct cells. These cellular clusters make up the exocrine portion of the pancreas that produce and deliver digestive pro-enzymes, pancreatic fluid, and electrolytes into the gastrointestinal tract. Acinar cells synthesize and secrete zymogen granules that are released at the cell apex by exocytosis into the ductal system. Multiple defense mechanisms exist to prevent premature intra-acinar enzyme activation (a key feature of acute pancreatitis), by compartmentalization of zymogen granules from lysozymes, and by synthesizing trypsin inhibitors and antiproteases. Normally, activation of the zymogens occurs in the duodenum, by cleavage of trypsinogen to trypsin via duodenal mucosal enteropeptidase, which in turn activates other digestive enzymes.

The endocrine pancreas constitutes approximately 2% of the pancreatic mass, and is identified by small ovoid clusters of cells called islets of Langerhans found dispersed throughout the pancreas, that are somewhat more plentiful in the pancreatic tail. The islets are a highly perfused structure of cells in close proximity to fenestrated capillaries. There are four main endocrine cells that compose the islets: i) α-cells that secrete glucagon, which promotes cells in the body to release glucose into the blood stream, ii) β-cells that secrete insulin, which promotes cells in the body to absorb glucose, iii) δ-cells that secrete somatostatin, which inhibits insulin and glucagon production and suppresses the release of gastric digestive enzymes, and iv) γ-cells that secrete pancreatic polypeptide, which regulates both exocrine and endocrine pancreatic secretion activities. The remaining 13% of pancreatic mass is composed of extracellular matrix, nerves, and blood vessels.

1.3 Pancreatic cancer

1.3.1 Epidemiology

Pancreatic cancer is the tenth most common malignancy, and is the fourth leading cause of cancer related mortality in both women and men in the western world. It is predicted that by year 2020, pancreatic cancer related mortality will surpass that of colon and liver cancer, making pancreatic cancer the second leading cause of cancer related death, placing it just behind lung cancer (8)(9). The American Cancer Society estimates 48,960 new cases of pancreatic cancer for year 2015, and is estimated that 40,560 of these patients will succumb to the disease (8). These numbers highlight the extremely dismal diagnosis of pancreatic cancer, which has a median survival of <6 months and a 5-year survival rate below 5% (10). The majority of diagnosed pancreatic cancers are classified as pancreatic ductal adenocarcinoma (PDAC), which comprises roughly 85% of all diagnosed cases of pancreatic cancer, and is associated with a worse prognosis (11).

PDAC is associated with a variety of known demographic and environmental risk factors, which include smoking, advanced age, chronic pancreatitis, family history, obesity, and diabetes (12)(13)(14)(15)(16)(17). The median age at which PDAC is diagnosed is 71 years, and it is rarely diagnosed in people younger than 40 years of age (11)(15). At 80 years of age the risk factor for developing pancreatic cancer increases 40-fold (18). Computational models of PDAC that incorporate the number of somatic mutations, driver versus passenger events, and cellular proliferation as they acquire a cancerous phenotype, estimate that it takes an average of 11.7 years for initiating events that begin pancreatic carcinogenesis to develop into *in situ* cancer and a further 6.8 years for primary tumor to develop metastatic clones (19)(20). Once metastasis occurs patients

succumb to the disease, on average 2.7 years later (21); unfortunately, the majority of pancreatic cancer patients are diagnosed during the late-stage of disease making it difficult to provide therapeutic intervention. However, if these computational models of PDAC development are correct, it provides a large time-window of opportunity for early detection and potential cure.

Numerous studies have established the genetic basis for familial PDAC, and it is estimated that 5-10% of PDAC develops due to an inherited component (22)(23). Corresponding germline mutations have been linked to familial PDAC, which include cyclin-dependent kinase inhibitor 2A (*CDKN2A*) (24), breast cancer 1 & 2 (*BRCA1 & 2*) (25)(26), liver kinase B1 (*LKB1*) (27), protease serine 1 (*PRSS1*) (28), and MutL homolog 1 (*MLH1*) (29)(30). Mutations in cationic trypsinogen gene *PRSS1* has one of the highest incidence rates associated with PDAC, and increases risk by 53-fold (31). *PRSS1* mutations cause the cationic trypsinogen protein to be more effectively auto-activated, consequently leading to pancreatitis (31). Pathological processes such as pancreas exocrine organ dysfunction and inflammation are known to be an important risk factors in tumorigenesis, because they promote the release of growth factors, cytokines, and reactive oxygen species (ROS), and thus cause an increase in cell proliferation and accumulation of oncogenic mutations (30).

1.3.2 Morphological characteristics of PDAC

PDAC is a malignant epithelial neoplasm characterized by extensive desmoplasia. Most commonly, the disease arises in the head of the pancreas and infiltrates into surrounding tissues,

such as the lymphatics, peritoneum, and spleen (32). The most common sites for distal metastasis are the liver and lung; however, PDAC metastasis has been reported in virtually all organs (33)(34)(35). PDAC develops via a progressive model, and is defined by its histological and genetic pathology (**Figure 1.2**) (36)(19). The precursor lesions that eventually develop into bona fide PDAC are termed pancreatic intraepithelial neoplasia (PanIN). There are three classifications of PanIN characterized by increasing cytological atypia: PanIN-1, are composed of mucinous columnar epithelial cells with little cellular atypia; PanIN-2, are composed of papillary (rather than flat) epithelial cells and have some nuclear atypia; PanIN-3, have high-grade dysplasia and are referred to as carcinoma *in situ* (**Figure 1.2**) (19)(37).

The histopathology of PDAC resembles that of the ductal cells, and is where it derives its nomenclature. Although this nomenclature implies that the neoplasm originates from ductal cells, its exact cellular origin (histogenesis) is still debated. Studies in mice have allowed for the dissection of cellular lineages in their capability to develop into bona fide PDAC. By targeting the activating mutation of K-RAS^{G12D} to the entire pancreas via the pancreatic and duodenal homeobox 1 (*Pdx1*) promoter, mice were capable of developing PDAC histologically similar to human disease (38). This led to the speculation about the true cellular origin of PDAC. Premalignant acinar-to-ductal metaplasia is frequently observed in PDAC disease, and some hypothesize that this suggests a reprogramming of acinar cells to a duct-like phenotype as a possible mechanism for developing PDAC (39). Supporting this hypothesis and highlighting acinar cells extensive plasticity, researchers used an acinar-specific promoter *Elastase* or muscle intestine and stomach expression 1 (*Mist1*) to activate oncogenic K-RAS^{G12D}, which resulted in the development of PanIN lesions and eventually PDAC (40)(41)(42); in contrast genetic targeting

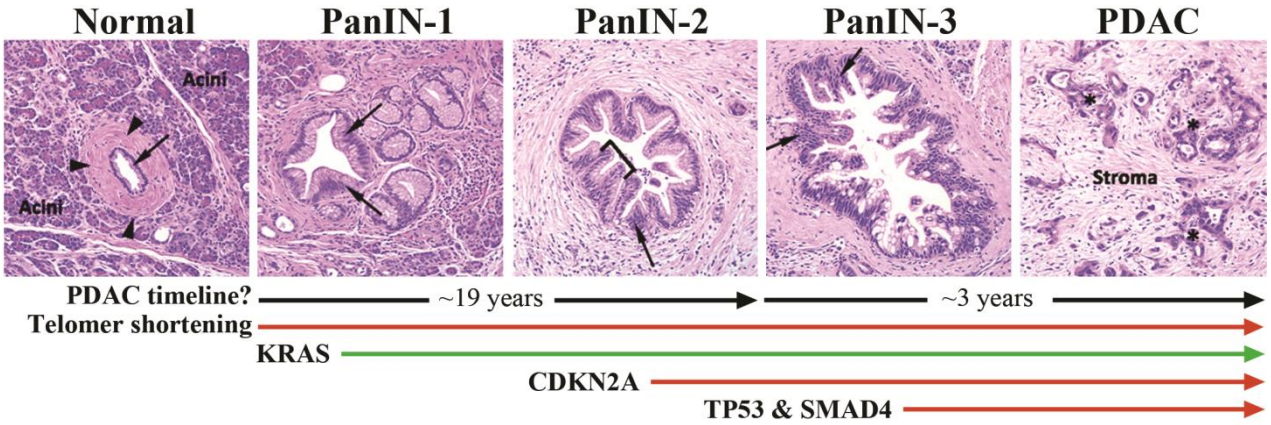

Figure 1.2: Morphological and genetic characteristics of PDAC progression. Pictured are examples of the histopathology of PDAC development. Normal ducts characterized by a single cell layer of low cuboidal epithelium (arrow) surrounded by periductal fibrotic tissue (arrowheads). Pancreatic intraepithelial neoplasia (PanIN); increasing grade (1-3) reflects increasing atypia, eventually leading to PDAC. PanIN-1 lesions present with elongation and mucinous hyperplasia of ductal cells (arrows), but lack cytological atypia. In contrast, PanIN-2 lesions present with nuclear abnormalities, crowding (arrow), and papillary folding (bracket). PanIN-3 lesions present with severe nuclear atypia, loss of cellular polarity (arrows), and frequent mitosis. PDAC is characterized by poorly formed neoplastic glands (asterisk), pronounced stroma, and invasive growth. The genetic alterations that accumulate in PDAC are thought to have temporal sequencing. Mutations are classified by the following: early (telomere shortening and Kirsten rat sarcoma viral oncogene homolog (*K-RAS*)), intermediate (*CDKN2A*), and late (tumor protein P53 (*TP53*) and mothers against decapentaplegic homolog 4 (*SMAD4*)). Green arrows indicate activation and red arrows indicate loss of function mutations (see section 1.3.3 genetic and molecular biology for more information). Adapted from (19); hematoxylin and eosin (H&E) images re-printed with permission.

of ductal cells with a ductal-specific promoter *Cytokeratin-19* to increase K-RAS expression, resulted in ductal cells that rarely gave rise to PDAC and were less susceptible to oncogenic K-RAS initiated tumorigenesis when compared to acinar cells (43). It has also been proposed that centroacinar cells could be the cell of origin of PDAC (44), but like ductal cells, centroacinar cells do not readily form PDAC (45). Others have hypothesized that pancreatic cancer stem cells, recently identified in PDAC (46), could be a possible candidate for PDAC cellular origin. PDAC stem cells were shown to be highly tumorigenic, but it is yet to be shown whether these cells can develop disease from a mutated stem cell, or if they are the result of a cell regaining stem cell-like properties (46). Thus, at least in mice, acinar cells exhibit a higher propensity to form PDAC in response to oncogenic mutation of K-RAS, whereas ductal and centroacinar cells are not as refractory to oncogenic transformation. Finally, it is possible that there is no unique cell of origin in the human disease, and mutations that accrue in pancreatic cells give rise to PDAC with indistinguishable tumor phenotypes.

1.3.3 Genetic and molecular biology

One of the earliest and most pervasive molecular events that occur in premalignant ducts and all stages of PanIN is telomere shortening and dysfunction (47)(48). Telomeres (TTAGGG sequences) become progressively shorter following cellular division. Telomeres prevent fusion between chromosome ends, and their attrition leads to genomic instability and chromosomal rearrangements through breakage-fusion-bridge cycles that promote amplification, translocations, and deletions (49)(50). Interestingly, it appears that telomere abnormalities occur more frequently in epithelial cancers and drive epithelial carcinogenesis (51). Importantly, premalignant cells can

avoid telomere shortening induced senescence by inactivating *TP53*-dependent DNA damage response (52), which cooperates with telomere dysfunction to promote the accumulation of oncogenic abnormalities (53). Studies of telomerase-knockout mice support the model of *TP53* cooperating with telomere dysfunction (54) and in breast tumors telomere length shortening correlates with *TP53* mutations (55).

Through molecular profiling of PanINs from pancreatectomy, researchers have reinforced the notion that PanIN-to-PDAC progression is highly associated with an accumulation of gene alterations, and that these genetic mutations associate with the histopathologic stages of PDAC (56). Unlike some malignancies that can be driven by a single genetic mutation, such as leukemia, PDAC has been shown to have an average of 63 genetic alterations (57)(58). Recent genome-wide sequencing of PDAC provided insight into its molecular biology, and revealed a set of 14 core signaling pathways and processes commonly altered in PDAC (56)(57)(59)(60) (**Figure 1.3**). Although these core pathways are commonly associated with PDAC, individual tumors vary vastly in terms of the pathways that are altered (57). Subsequent studies further highlight the vast heterogeneity of mutated genes in PDAC tumors, with 2,016 non-silent mutations and 1,628 copy-number variations (58). Despite this extreme heterogeneity among PDAC tumors, there are only a handful of genetic mutations that occur at a high frequency, suggesting that these mutations act as driver mutations for tumorigenesis. These commonly observed mutations include the following: *K-RAS*, *CDKN2A*, *TP53*, and *SMAD4*.

The most common genetic mutation in PDAC is the activating point mutation at codon 12 of the *K-RAS* gene. *K-RAS* encodes a GTP-binding protein that mediates a wide variety of

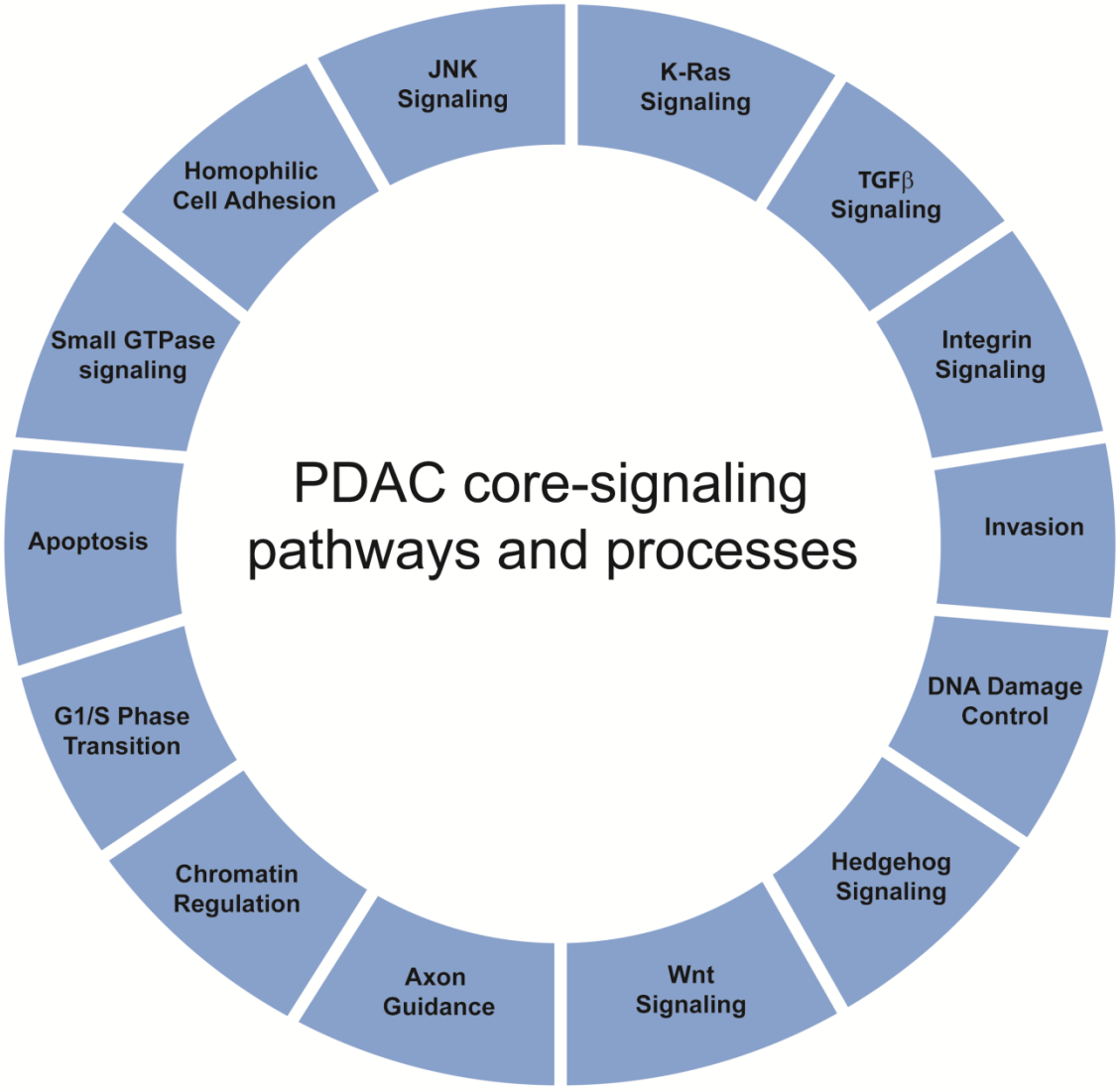

Figure 1.3. **PDAC core-signaling pathways and processes**. The fourteen signaling pathways and processes commonly associated with genetic alterations in the majority of PDAC. These pathways were determined by whole exome sequencing of PDAC tumors, and provide a new paradigm in the development of next-generation pleiotropic treatments and therapeutic strategies. Figure adapted from (56)(57)(58)(59)(60).

cellular processes, including induction of proliferation, survival, differentiation, and invasion (61). *K-RAS* mutations are one of the earliest genetic abnormalities to occur in pancreatic tissue, detectable in about 30% PanIN-1 lesions, and increase in frequency with disease progression, with the frequency rising to nearly 100% in advance disease (62)(63)(64). Of note, *K-RAS* mutations are also found in patients with chronic pancreatitis a risk factor for PDAC suggesting that *K-RAS* mutations are driving forces in the development of PDAC (65). Furthermore, genetically engineered mice with pancreatic specific K-RAS^{G12D} mutation develop PanIN lesions that progress to PDAC, albeit at a very slow rate (66)(67). K-RAS activation engages a multitude of effector pathways, such as extracellular signal-regulated kinase (Ras-ERK), mitogen-activated protein kinases (MAPK), Ral guanine nucleotide dissociation stimulator (RalGDS) and phosphatidylinositol 3-kinase/protein kinase B (PI3K/Akt) pathway, thereby acting on a variety of downstream targets such as transcription factor nuclear factor kappa-light chain-enhancer of activated B cells (NF-κB) and mammalian target of rapamycin (mTOR) promoting cell survival, proliferation, angiogenesis, and invasion (68)(69).

CDKN2A encodes for p16 protein, and regulates cell cycle progression from G1 phase to S phase. *CDKN2A* also encodes for alternative reading frame protein (p14ARF), which inhibits mouse double minute 2 homolog (Mdm2), thus regulating cell cycle by promoting TP53 activity. Inactivating *CDKN2A* mutations occur in 80-95% of PDAC tumors and comprise the second most frequent genetic mutation detectable in moderately advanced PanIN lesions (70)(71). Loss of *CDKN2A* function is associated with promoter hypermethylation, mutation, and deletion (71). Germline mutations of *CDKN2A* alleles confer a 13-fold increased risk for PDAC (72)(73). *K-*

RAS mutations promote an increase in p16 expression, and thus it is hypothesized that *CDKN2A* inactivation may be necessary to override cell senescence induced by K-RAS activation (74).

TP53 tumor suppressor gene encodes for protein TP53, which regulates multiple anticancer functions, such as apoptosis, DNA repair, and cell cycle. *TP53* mutations are commonly associated with single-point mutations and observed in 75% of PDAC (75)(76). *TP53* mutations appear in late-stage PanINs that have acquired features of dysplasia, which highlights its function in preventing malignant progression (77)(78)(79). Mice harboring pancreatic specific *K-RAS*^{G12D} activating mutation and deletion of *TP53*, have increased metastases compared to *TP53* wild-type mice (80). It appears that TP53 may drive the prometastatic phenotype by inhibiting tumor protein/nuclear factor Y (TP73/NF-Y) complex, which represses platelet-derived growth factor receptor b (PDGFRb) and that blocking PDGFRb with small molecule inhibitors and ribonucleic acid (RNA) interference prevented PDAC metastasis (81).

Another frequent PDAC associated mutation is the inactivation of *SMAD4*. SMAD4 plays a central role in transforming growth factor beta (TGF-β) and bone morphogenic protein (BMP) signaling pathways (82)(83). TGF-β signaling promotes fibroblast proliferation and epithelial-to-mesenchymal transition (EMT) (83)(84)(85). *SMAD4* deletion/mutation occurs in 50% of PDAC cases, and is thought to occur in late stage PanIN or PDAC (86)(87). Loss of *SMAD4* expression is highly associated with metastasis, and in PDAC patients, loss of *SMAD4* was observed in 22% of localized disease and 75% in patients with metastasis (88). It appears that loss of SMAD4 promotes tumor spread predominantly via TGF-β signaling and that antibodies to TGF-β stem PDAC metastasis, while exogenous addition of TGF-β signaling cytokines enhanced invasion

(89)(90). However, given the implication of BMPs in tumor metastasis in other malignancies, dysregulated BMP signaling may also contribute to PDAC spread, but currently is not as well studied in the PDAC setting (91)(92)(93)(94).

The outcome of genetic studies described above have several mechanistic implications for PDAC pathobiology. Although a core set of fourteen pathways is associated with PDAC, the pathway components that are altered in any individual tumor vary widely. The described PDAC tumor heterogeneity among these pathway components can explain the difficulty in developing a therapeutic panacea or 'magic-bullet' cure. A single therapeutic agent that is effective against a cancer cell containing the druggable target will give rise to subclones that lack the therapeutic target and thus are resistant. This suggests that the best therapeutic strategies for PDAC may comprise in agents that target multiple core processes and signaling pathways, rather than a single altered genetic component. Furthermore, the observation that PDAC develops sequentially by accruing mutations that promote PDAC progression and are associated with disease phenotype, may offer avenues for genomic and proteomic analysis that will aid in tumor typing and improve tumor classification, further improving patient specific therapy.

1.3.4 Clinical presentation and diagnosis

PDAC is a highly infiltrative malignancy with the majority of patients at the time of clinical diagnosis having lympho-vascular invasion and/or extensive metastasis. Patients are typically asymptomatic until late in the course of the disease, thus making early diagnosis and therapeutic intervention difficult. As mentioned earlier, the majority (60 – 70%) of PDAC tumors originate

in the head of the pancreas versus (20 – 30%) in the body and tail of the pancreas (95)(96). The presenting symptoms and prognosis are related to PDAC location. Patients with body or tail tumors tend to have decreased median survival compared to patients with tumors originating in the head of the pancreas (95)(96). The differences are thought to be due to frequency of metastatic disease, and early onset of symptoms. The most common presenting symptoms of PDAC are abdominal pain, weight loss, gastrointestinal symptoms, and asthenia (97). Jaundice is commonly associated with tumors originating in the head, due to compression of the common bile duct. Other physical symptoms of PDAC include palpable abdominal mass or gallbladder (98). New-onset diabetes is present in roughly 50% of patients with PDAC, and should raise suspicion to the possibility of pancreatic cancer (99)(100). An additional clinical finding is 'thrombophlebitis' or venous thromboembolism (VTE, Trousseau's syndrome) (101).

There is intense interest in identifying new pancreatic cancer biomarkers that go beyond screening and identifying disease. These new tumor markers could have predictive and prognostic value, which will aid in stratifying patients based on disease aggressiveness, help select patient subsets for clinical trials, and help identify those who will respond favorably to therapy (**Figure 1.4**). Currently, the most common marker for pancreatic cancer is carbohydrate antigen 19-9 (CA19-9). CA19-9 is currently the only Food and Drug Administration (FDA) approved biomarker for pancreatic cancer, and has a sensitivity of 70% and specificity of 87% (102)(103). Since pancreatic cancer has a relatively low prevalence among the general population, the ideal marker should have sensitivity and specificity that exceeds 99% to minimize false positives (104). Thus, CA19-9 is neither sensitive nor specific for screening and detecting pancreatic cancer, and it is typically used only for the follow-up of patients already diagnosed with the disease. A decrease

in postoperative levels of CA19-9 is the best index for improved patient prognosis, whereas in contrast, patients with increased CA19-9 after tumor resection have a significantly shorter median survival (105)(106). Increased levels of CA19-9 may be due to nonmalignant diseases, such as chronic and acute pancreatitis, biliary obstruction cholangitis, and liver cirrhosis (102). Furthermore, patients who are Lewis antigen negative (Le^{a-b-}) don't synthesize CA19-9 because of a genetic absence of the Le enzyme (fucosyltransferase 3), and thus cannot test positive for CA19-9 even during high tumor burden (107)(108)(109). Therefore, between 5-10% of the general population will have undetectable disease when screened for CA19-9 (108)(109).

Imaging has become a crucial tool for determining initial diagnosis and staging, tumor resectability, and treatment monitoring. Computed tomography (CT) is the single most important imaging tool for detecting and staging pancreatic cancer; however, other imaging technology, such as magnetic resonance imaging (MRI) and positron emission tomography (PET) have their advantages (110). The accuracy of modern CT for detecting PDAC is fairly high, with some reports suggesting a sensitivity of 76-92% (110)(111)(112). Primary PDAC tumors are typically not difficult to identify, due to their abundant fibrous stroma and hypovascularity. However, smaller tumors can pose a challenge for visual identification and other signs of a mass must be used, such as pancreatic ductal dilation, biliary ductal dilation, abnormal pancreas contour, and pancreatic atrophy (110)(113). CT also has the ability to determine venous and arterial involvement, with new technologies having resolutions of <0.4 mm, allowing for the evaluation of major and minor mesenteric branch vessel tumor involvement (114). Determining tumor vascular involvement is critical for identifying resect able and unresectable disease. Whereas CT is the primary imaging technology used to identify PDAC lesions, MRI also has its utility. MRI

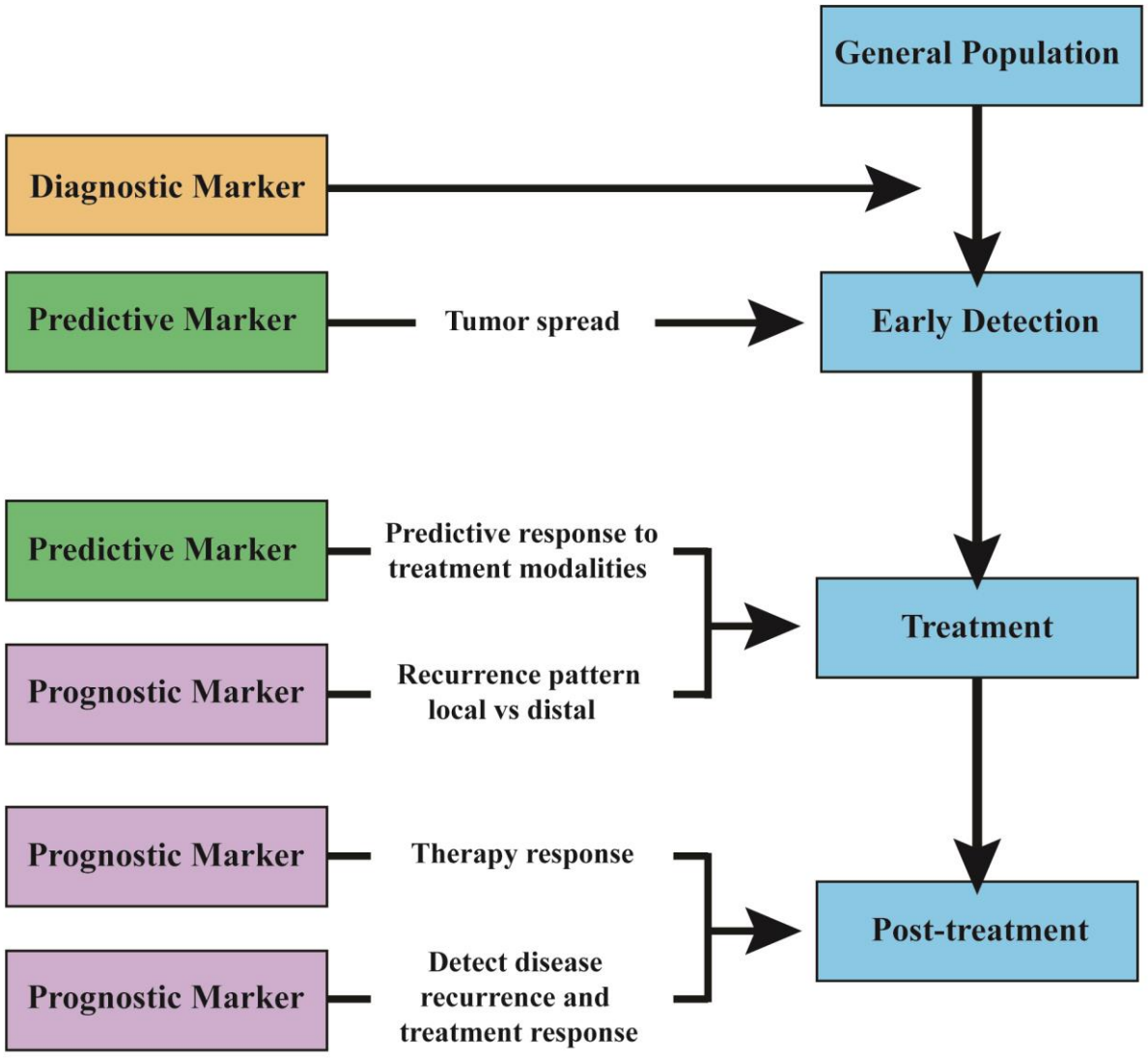

Figure 1.4: Integration of diagnostic, predictive, and prognostic biomarkers for management of patients with pancreatic cancer. There is an urgent need to develop predictive markers, markers that can identify subpopulations of patients who are likely to respond to a given therapy. In contrast, prognostic markers provide information on the likely course of the PDAC disease. Adapted from (109).

has greater soft-tissue contrast versus CT, and thus is useful in identifying small lesions (115)(116). Unlike the anatomic imaging techniques CT and MRI, PET uses a radiotracer ^{18}F-fluorodeoxyglucose (FDG), which is a glucose analog that accumulates in cancer cells. The sensitivity of PET is only 72%, and it is not recommended for screening; however, it does have value in differentiating between benign and malignant lesions, and may be superior to CT in evaluating therapeutic response (117).

1.3.5 Treatment and management

Currently, the only available curative treatment for PDAC is surgical resection. In order to determine tumor resectability it is critical to assess primary tumor involvement with local vessels, such as superior mesenteric artery and vein, celiac artery, portal vein, and hepatic artery (118). After determining tumor resectability the majority of patients do not qualify for surgery, only 10-20% of patients are considered to be candidates for surgical intervention, and many of these patients are found to have positive microscopic margins during surgery (119). The anatomic location of the tumor determines the type of surgery performed. Tumors located in the head and neck of the pancreas will undergo a pancreaticoduodenectomy (the Whipple procedure) (120). Tumors in the body or tail of the pancreas undergo left pancreatectomy, and it often includes a splenectomy (121). Operative mortality at high-volume clinical centers is low and ranges from 1-4% (122); however, post-operative morbidity is high with an average of 40% (123). Furthermore, the 5-year survival rate for patients who underwent tumor resection ranges from 15-25%, and it is estimated that 20% will develop local recurrence and more than 70% will develop metastatic disease (124).

Since the vast majority of PDAC patients do not qualify for tumor resection and have poor outcomes, chemotherapy remains the standard of care. Gemcitabine has been the primary adjuvant and palliative cytotoxic therapy for PDAC since its approval in 1996 (125)(126). However, gemcitabine alone has only a modest effect on overall survival (~6.7 months) (127), which suggests that drug monotherapy is inadequate to surmount the multitude of core-signaling pathways and processes associated with heterogeneous cancer cell populations. Recently, two trials of combination chemotherapy regimens have emerged showing a survival advantage versus gemcitabine monotherapy (128)(129). One trial incorporates the combination of fluorouracil, irinotecan, oxaliplatin, and leucovorin (FOLFIRINOX), and had a median survival rate of 11.1 months, which was a 4.4 months improvement over gemcitabine monotherapy (128). The second trial examined the combination of gemcitabine plus nanoparticle albumin-bound (nab)-paclitaxel, and had a median survival rate of 8.5 months versus the 6.7 months of gemcitabine alone (129). Both trials had a significant improvement in median survival, health status, and quality of life and currently are considered standard treatment for PDAC.

As our knowledge of PDAC core-signaling pathways and processes expands, new opportunities to develop targeted therapies are increasing. One such targeted therapy for pancreatic cancer is Erlotinib, a tyrosine kinase inhibitor of the catalytic domain of epidermal growth factor receptor (EGFR), which is over-expressed in 90% of pancreatic tumors (130). Erlotinib has been approved by the FDA for pancreatic cancer therapy, but following a Phase III study only showed marginal improvement when combined with gemcitabine versus gemcitabine only, with an overall survival benefit of roughly one month (131). Currently, other compounds are being evaluated in Phase II/III clinical trials that target tumor stroma, immune response, and signal transduction pathways. Pancreatic cancer is extremely stroma-rich, and this dense stromal

compartment is thought to act as a physical barrier that prevents therapeutic agents from reaching cancer cells (132)(133)(134). However, pharmacologic inhibitors that deplete tumor stroma had a worse overall survival, unrelated to drug toxicity (135). It was later determined that the tumor stromal compartment plays an important role in restraining tumor growth and spread (136). Immunotherapy approaches that target immune checkpoint inhibitors are gaining track in solid tumors, especially in melanoma where they have received FDA approval (127). However, therapies that target T-lymphocyte immunologic checkpoints in PDAC have been unfruitful, and studies of anti-cytotoxic T-lymphocyte-associated protein 4 (CTL4) and anti-programmed cell death protein 1 (PD-1) failed to demonstrate significant patient responses (137)(138). These results may be due to the low number of tumor-infiltrating T-lymphocytes in PDAC, and currently investigators are exploring how PDAC avoids immune surveillance (139)(140)(141). Researchers have also focused on targeting signal transduction pathways associated with PDAC. One of the most pervasive and earliest effector signal transduction pathways associated with PDAC is K-RAS, which is critical in promoting tumor initiation, progression, and tumor maintenance, thus making it a "holy grail" for PDAC therapy (142)(143)(144). K-RAS has proven to be a challenging therapeutic target for multiple reasons: it has a high binding affinity to guanosine triphosphate (GTP), feedback loops, and a poor therapeutic window (144). Recently, new compounds that can interact with the oncogenic mutant form K-RAS (cysteine-12 in G12C) have been identified, and are garnering hope for the identification of similar compounds that could interact with G12D and G13D K-RAS mutations (144)(145)(146). In sum, targeted therapy in PDAC is for the most part still in experimental stages, and has yet to become a clinical standard.

1.4 Tissue Factor

1.4.1 Tissue Factor introduction

Tissue Factor (TF) (also named thromboplastin, Factor III, or CD142), derives its name from the ability of tissue extracts to initiate coagulation upon contact with blood or plasma. In 1905 Paul Morawitz, described the classical theory of blood coagulation. This "classic" theory of blood coagulation describes four essential factors: thromboplastin, calcium, prothrombin, and fibrinogen (147). Morawitz postulated that three of these components are always present in circulating blood, and the triggering factor thromboplastin must be released either from solid tissues or blood components. Later in 1964, when additional coagulation factors were discovered two groups almost simultaneously described a new model of coagulation; the "waterfall" or "cascade" theory, which describes a sequential proteolytic activation of pro-enzymes that leads to the formation of thrombin (147)(147). In 1981 Ronald Bach, Yale Nemerson, and William Konigsberg purified TF apoprotein (148), and subsequently its cDNA was isolated and sequenced (149)(150), thus establishing the field of TF research.

TF is a 47 kDa transmembrane glycoprotein that functions as the primary physiological initiator of blood coagulation by binding plasma FVII/FVIIa (151). The TF:FVIIa complex promotes blood coagulation by activating both FX and FIX, which subsequently results in the generation of thrombin - forming a fibrin-rich hemostatic plug (151). TF is encoded by the *F3* gene, located on chromosome 1 (p22-p21), which contains 6 exons. These 6 exons of *F3* produce a precursor protein with 295 amino acids, which undergoes post-translational modification – whereby the 32 amino acid signal peptide is removed. The resultant mature protein consists of an extracellular domain (residues 1-219), transmembrane domain (residues 220-242), and a

cytoplasmic tail (residues 243-263) and is referred to as full-length TF (152)(150)(153) (154) (**Figure 1.5**).

In 2003, Bogdanov et al. described an alternatively spliced isoform of TF termed alternatively spliced TF (asTF) (155). asTF is the result of alternative splicing of the primary *F3* transcript, whereby exon 5 is omitted, resulting in the fusion of exon 4 and 6 creating a shift in the open reading frame and the generation of a unique 40 amino acid C-terminal domain (155)(156) (**Figure 1.5**). This unique C-terminus lacks a transmembrane domain, and thus is secreted. Since asTF retains the conserved Lysine (Lys) residues Lys^{165} and Lys^{166} (necessary for proteolytic activation of FVII and FX), some believe that asTF maintains FX activation, although at a diminished rate as compared to flTF due to the unique C-terminus causing a lower FVII affinity. However, its procoagulant function remains a matter of debate, some reports indicate asTF as being procoagulant and accruing in thrombi, but others exclude such a function, making its role in hemostasis and/or thrombosis unclear (155)(157)(158)(159). This discrepancy could be due to physiologically irrelevant conditions and the lack of validated and reliable assays for measuring asTF activity (160)(161). Although the extent of its hemostatic function is controversial, multiple reports indicate that asTF possesses non-hemostatic functions, which have (patho)physiological implications in cancer (162).

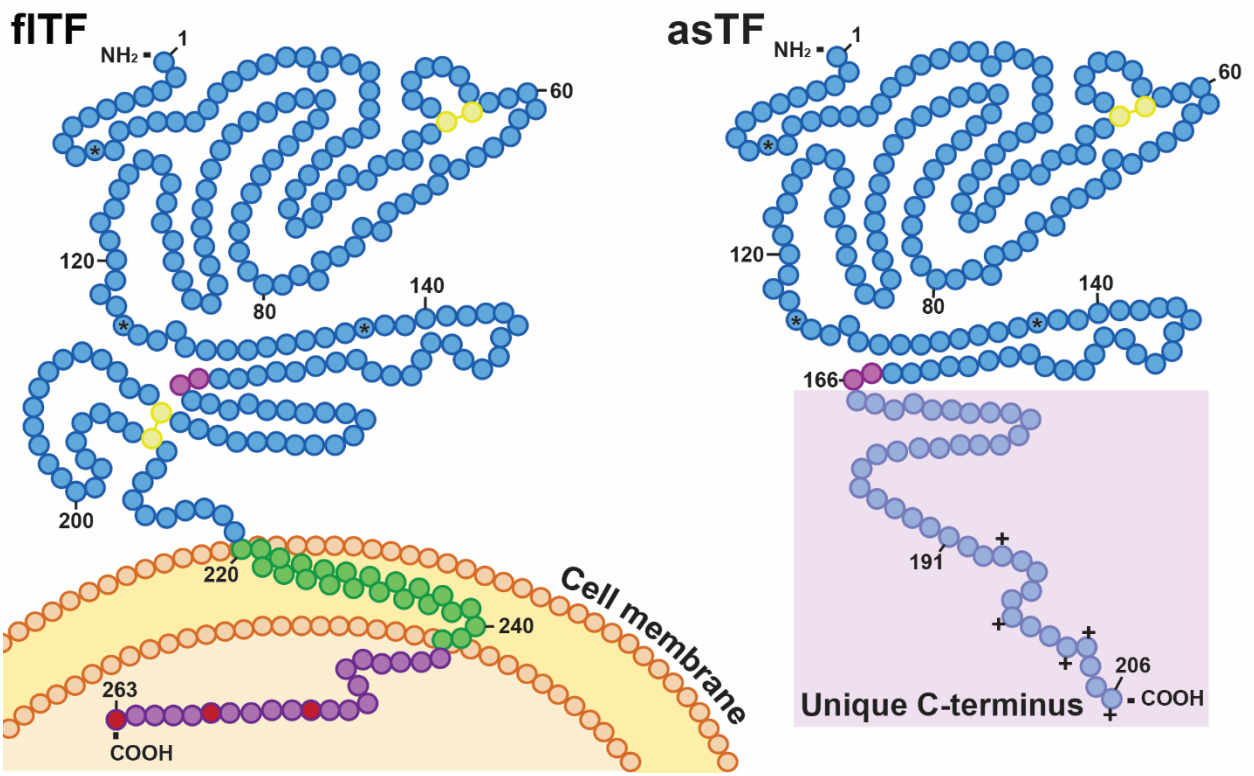

Figure 1.5: Structure of TF protein variants. Full-length TF (flTF) is an integral transmembrane protein, whereas alternatively spliced TF (asTF) is a soluble protein. Both isoforms contain the same first 166 residues, which share a N-terminal β-sandwich and the charged doublet Lys^{165}:Lys^{166} (Purple circles). There are 3 proposed Asparagine (Asn) glycosylation sites Asn^{11}, Asn^{124}, and Asn^{137} ("*" sign). Yellow circle represent disulfide bridges at Cysteine (Cys) - Cys^{49}-Cys^{57} and Cys^{186}-Cys^{209}. Through alternative splicing of the primary transcript, a frame shift occurs and generates a unique C-terminus in the asTF protein (highlighted in pink). asTF's C-terminus contains a cluster of 5 positively charged residues ("+" sign), thought to facilitate asTF's orientation on phospholipid surfaces. The flTF C-terminus contains three serine residues (red circles), which undergo phosphorylation.

1.4.2 TF and cancer

The molecular pathobiology of PDAC is marked by high expression of TF (163)(164)(165); which some hypothesize is the primary cause for elevated risk of thrombosis in patients with PDAC. The association between thrombosis and malignant disease has been recognized for well over a century (166). In 1865, the French physician Armand Trousseau described the relationship between cancer and venous thromboembolism (VTE) (also known as Trousseau's syndrome), and following Trousseau's observation studies have provided a multitude of evidence for VTE risk in cancer (166)(167). Cancer is responsible for roughly 20% of all new cases of VTE, and the risk for VTE is elevated 7-fold in certain malignancies, and for some the risk is up to 28-fold (166)(167).

TF is normally absent from quiescent endothelial cells, and is expressed in the adventitia and smooth muscle cells surrounding blood vessels. Aberrant TF expression occurs in a variety of tumors, the result of oncogenic events. In colorectal cancers mutations in *TP53* and *K-RAS*, which activate MAPK and PI3K signaling pathways, induce TF expression (168)(169). In human glioma cells, oncogenic EGFR and its mutant form EGFRvIII promote the expression of TF, protease-activated receptor (PAR-1), PAR-2, and ectopic synthesis of FVII, thus sensitizing the cells to TF/PAR-mediated signaling (170). The loss of phosphatase and tensin homolog (PTEN) and tumor hypoxia in glioblastoma upregulates TF expression and increases the risk of intravascular thrombotic occlusion (171). Also, other stimuli associated with malignant tissues such as TGF-β, tumor necrosis factor-alpha (TNF-α), interferon-gamma (IFN-γ), early growth response gene-1 (EGR-1), estrogen, Hypoxia-inducible factor 1-alpha (HIF-1α) are known to upregulate TF in cancer cells (172)(173)(174).

TF is highly expressed in PDAC as well as early PanIN lesions, and the expression of TF correlates with poor histologic grade and worse prognosis (175)(176). The function of TF is known to extend beyond hemostatic maintenance. In nonsmall cell lung cancer (NSCLC) and PDAC TF expression significantly correlates with microvascular density (177)(178). Both forms of TF play an important role in tumor growth and angiogenesis (162). However, both flTF and asTF mediate tumor progression via unique mechanisms. The flTF:FVIIa complex can enzymatically activate protein-coupled protease-activated receptors (PARS). The flTF:FVIIa binary complex can activate PAR-2 and the flTF:FVIIa:FXa ternary complex can activate PAR1, which induce signaling cascades involving protein kinase C (PKC), PI3K, and MAPK family, p44/42, p38, and c-Jun N-terminal kinase (JNK). These processes promote the production of pro-angiogenic factors, such as vascular endothelial growth factor (VEGF) A and C, connective tissue growth factor (CTGF), as well as chemokines and cytokines chemokine (C-X-C motif) ligand 1 (CXCL1), interleukin-8 (IL-8), and granulocyte macrophage colony-stimulating factor (GM-CSF) (179)(162). Blocking TF:FVIIa proteolytic function with a nematode anticoagulant protein (rNAPc2) diminishes vessel formation (180). Also of note, genetic deletion of flTF intracellular domain inhibits production of VEGF (181). Not only does flTF mediate tumor progression via pro-angiogenetic mechanisms, but it also influences tumor metastasis by regulating actin dynamics. In migratory cells, TF was shown to accumulate at the invasive edge, and actin-binding protein 280 (ABP-280) binds flTF's intracellular domain (182). flTF also regulates cell motility in a PAR-2 mediated mechanism, by upregulating Ras homolog gene family member A (RhoA) and cortactin proteins known to promote cell migration (183)(184).

In 2007, Hobbs *et al*. reported that asTF can facilitate angiogenesis, and showed that asTF overexpressing pancreatic cancer cells implanted into mice developed tumors associated with increased vessel density and size (185). However, the mechanism underlying this finding wasn't discovered until 2009 when van den Berg *et al*. reported that asTF mediates angiogenesis via non-proteolytic ligation of β1 and β3 integrins (186). Integrins are heterodimeric transmembrane receptors that function as adhesion molecules for cell-cell and cell-extracellular matrix (ECM) interactions, and can act as signal transduction platforms for a variety of biological processes (187). Integrins are a diverse family of proteins composed of an α and β subunit: in humans there are 18 "α" and 8 "β" monomers that can combine with each other to form 24 unique integrins that bind to a wide variety of ECM molecules, such as fibronectin, fibrinogen, von Willebrand factor, collagen, and laminin, thus regulating cell adhesion to ECM (188). Integrins also act as chemosensors to their microenvironment, nfluencing cell shape, survival, migration, and proliferation (188). Non-proteolytic asTF-integrin mediated signaling mechanism is in striking contrast to flTF, whose tumor promoting mechanism relies on proteolytic PAR-dependent signaling. Still, the role of asTF in tumor progression remains to be elucidated; with the knowledge that asTF interacts with integrins, we hypothesized that asTF enhances PDAC growth and spread as it accrues in the tumor stroma, acting as a non-proteolytic cell agonist.

Chapter 2: Alternatively spliced tissue factor contributes to tumor spread and activation of coagulation in pancreatic cancer

I am lost: the phlebitis that has just appeared tonight leaves me no doubt about the nature of my illness.

– Armand Trousseau
Malignancy, thrombosis and Trousseau: the case for an eponym

Alternatively spliced tissue factor contributes to tumor spread and activation of coagulation in pancreatic ductal adenocarcinoma

Dusten Unruh[1*], Kevin Turner[2*], Ramprasad Srinivasan[1*], Begüm Kocatürk[3], Xiaoyan Qi[1], Zhengtao Chu[1], Bruce J. Aronow[4], David R. Plas[5], Catherine A. Gallow[5], Holger Kalthoff[6], Daniel Kirchhofer[7], Wolfram Ruf[6], Syed A. Ahmad[9], Fred V. Lucas[2], Henri H. Versteeg[3*] and Vladimir Y. Bogdanov[1*]

[1]Division of Hematology/Oncology, Internal Medicine, University of Cincinnati College of Medicine, Cincinnati, OH, [2]Department of Pathology & Laboratory Medicine, University of Cincinnati College of Medicine, Cincinnati, OH, [3]Einthoven Laboratory for Experimental Vascular Medicine, Leiden University Medical Center, Leiden, The Netherlands, [4]Department of Biomedical Informatics and Developmental Biology, Cincinnati Children's Hospital and Medical Center, Cincinnati, OH, [5]Department of Cancer Biology, University of Cincinnati College of Medicine, Cincinnati OH, [6]University Hospital Schleswig-Holstein, Institute of Experimental Cancer Research, Kiel, Germany, [7]Department of Early Discovery Biochemistry, Genetech, Inc., San Francisco, CA, [8]Department of Immunology and Microbial Science, The Scripps Research Institute, La Jolla, CA, [9]Department of Surgery, University of Cincinnati College of Medicine, Cincinnati, OH

Citation: Unruh D, Turner K, Srinivasan R, Kocatürk B, Qi X, Zhengtao C, et al. Alternatively spliced tissue factor contributes to tumor spread and activation of coagulation in pancreatic ductal adenocarcinoma. Int J Cancer. 2014; 110(28):9-20.

2.1 Abstract

Alternatively spliced tissue factor (asTF) promotes neovascularization and monocyte recruitment via integrin ligation. While asTF mRNA has been detected in some pancreatic ductal adenocarcinoma (PDAC) cell lines and increased asTF expression can promote PDAC growth in a subcutaneous model, the expression of asTF protein in bona fide PDAC lesions and/or its role in metastatic spread are yet to be ascertained. We here report that asTF protein is abundant in lesional and stromal compartments of the five studied types of carcinoma including PDAC. Analysis of 29 specimens of PDAC revealed detectable asTF in >90% of the lesions with a range of staining intensities. asTF levels in PDAC lesions positively correlated with the degree of monocyte infiltration. In an orthotopic model, asTF-overexpressing high-grade PDAC cell line Pt45P1/asTF+ produced metastases to distal lymph nodes, which stained positive for asTF. PDAC cells stimulated with and/or overexpressing asTF exhibited upregulation of genes implicated in PDAC progression and metastatic spread. Pt45P1/asTF+ cells displayed higher coagulant activity compared to Pt45P1 cells; the same effect was observed for cell-derived microparticles (MPs). Our findings demonstrate that asTF is expressed in PDAC and lymph node metastases and potentiates PDAC spread *in vivo*. asTF elicits global changes in gene expression likely involved in tumor progression and metastatic dissemination, and it also enhances the procoagulant potential of PDAC cells and cell-derived MPs. Thus, asTF may comprise a novel therapeutic target to treat PDAC and, possibly, its thrombotic complications.

2.2 Background

Pancreatic cancer is the fourth leading cause of cancer associated death, and pancreatic ductal adenocarcinoma (PDAC) accounts for 85% of all forms of pancreatic cancer (189). Several forms of solid malignancies are associated with a hypercoagulant state, which is thought to be partially caused by increased tissue factor (TF) expression on tumor cells due to, e.g., activation of proto-oncogenes such as *K-RAS*, *EGFR* as well as inactivation of tumor suppressor genes such as *TP53* and *PTEN* (190). TF-bearing microparticles (MPs) have also been thought to play a critical role in malignancy-associated venous thromboembolism (VTE). Indeed, several studies indicate that cancer patients with VTE have significantly higher TF-MP activity and levels than cancer patients without VTE (191)(192), and such a link between TF-MP and VTE is confirmed by mechanistic studies (193). Alternatively spliced TF (asTF) is a minimally coagulant isoform of full-length tissue factor (flTF) that drives angiogenesis nonproteolytically through binding to integrins α6β1 and αvβ3 (155)(186). asTF-integrin interactions results in the activation of key signaling intermediates such as PI3K/Akt, p38 MAPK and FAK, resulting in endothelial neovascularization (186). Moreover, asTF binding to β1 integrins on microvascular endothelial cells activates the NF-kB pathway that results in the increased expression of major cell adhesion molecules such as E-selectin, VCAM-1 and ICAM-1, leading to enhanced monocyte adhesion to, and migration through, endothelial cells (194). Of note, α6β1 is expressed on PDAC cells, and the levels of this integrin are greatly potentiated by IL-1α; moreover, α6β1 induces Ras/ERK signaling resulting in the increased proliferation and migration of PDAC cells (195). To date, studies of asTF in the cancer setting have been focused largely on cervical cancer (186)(194), and lung cancer: in 2008, asTF mRNA was found to be increased in squamous cell carcinoma of the lung, as well as pulmonary adenocarcinoma (196). In tissues of non-small cell lung cancer, asTF mRNA

levels are highly predictive of patient outcome (197). Studies of asTF in the PDAC setting have thus far been limited. In 2006, screening of eight low- and high-grade PDAC-derived cell lines detected asTF mRNA expression in six cell lines (198). In 2007, Hobbs *et al*. reported that overexpression of asTF in a TF-null PDAC line MiaPaCa-2 enhances tumor growth in a subcutaneous model; however, this study suffered from lack of mechanistic insight as well as conceptual limitations inasmuch as asTF was studied in a nonphysiologic, flTF-null setting (185). While the expression of flTF is well documented in human PDAC (Ref (178) and work cited therein), it is yet to be established whether asTF mRNA and/or protein are expressed in bona fide human pancreatic cancer tissue. No data are available regarding the functional contribution(s) of asTF to PDAC pathobiology in physiologically relevant *in vivo* setting.

In this study, we report for the first time that asTF (*i*) is expressed in human PDAC tumor tissue exhibiting heavy monocyte infiltration, (*ii*) promotes tumor metastasis in an orthotopic model of PDAC, (*iii*) exerts autocrine/paracrine effects on PDAC cells resulting in global changes in gene expression and (*iv*) contributes to the procoagulant potential of PDAC cells and cell-derived MPs via distinct mechanisms.

2.3 Materials and methods

2.3.1 Reagents

Human anti-asTF rabbit polyclonal antibody suitable for immunohistochemical studies was described and characterized previously (194)(200), Custom rabbit monoclonal antibodies RabMab1 (asTF-specific) and RabMab95 (recognizing a TF region shared by asTF and flTF) were

employed in Western blotting and ELISA assays. For on-cell Western assays and flow cytometry analysis of intact cells and cell-derived MPs, flTF-specific mouse monoclonal antibody 10H10 (194), and the rabbit monoclonal antibody RabMab1 were used. Anti-GAPDH rabbit polyclonal antibody was from Trevigen, Inc. Isolectin B4 was from Invitrogen (Carlsbad, CA). Anti-integrin β1/β3 and EGFR antibodies were from R&D Systems (Minneapolis, MN) and Biolegend (San Diego, CA), respectively. TaqMan probe/-primer sets for EFEMP1, AREG and VEGF-A were from Roche Applied Science (Indianapolis, IN). Anti-EFEMP1 polyclonal antibody was from Thermo Scientific (West Palm Beach, FL). Anti-total MAPK/p-MAPK and total Akt/p-Akt antibodies were from Cell Signaling Technology (Beverly, MA). Anti-CD68 antibody was from Imgenex (San Diego, CA). Anti-F4/80 antibody was from Biolegend. Mouse monoclonal anti-human TF antibody 7G11 (200), was used as an inhibitory antibody in TF activity assays.

2.3.2 Tumor tissue specimens

Commercial tissue microarrays (TMA) were purchased from Imgenex Corporation (San Diego, CA). Use of de-identified specimens of human PDAC tissue was approved by the Institutional Review Board, University of Cincinnati. Twenty-nine specimens of primary PDAC tissue harvested from 26 patients were examined; in addition, five specimens of seminal lymph node metastases from four patients were available for and subjected to histological analysis. The summary of clinicopathological characteristics of the PDAC cohort is provided in **Figure 2.4**, Supporting Information. Immunohistochemical and fluorescence studies were performed as previously described (194); asTF staining intensity was annotated by two trained anatomical pathologists based on the strength of the reaction obtained by HRP color substrate DAB. PDAC

specimens were stratified into the weak, moderate and strong subcohorts based on the staining intensity of ≥75% of tumor cells whose staining pattern was predominantly intracellular in nature; extracellular/stromal staining, when present, was also considered in scoring.

2.3.3 Cell lines

Pt45P1 is a grade III human PDAC cell line that features key mutations characteristic of PDAC and has been previously shown to produce grade III tumors in nude mice (201). Capan-1, a grade I human PDAC cell line, was obtained from ATCC (Manassas, VA). Cells were cultured in IMDM (Capan-1) and DMEM (Pt45P1) supplemented with FBS in the presence of antibiotics/antimycotics and selective antibiotics, when appropriate.

2.3.4 Overexpression of asTF in Pt45P1 cells

asTF open reading frame was subcloned in pSecTagA (Invitrogen, Carlsbad, CA) using restriction sites NheI and AgeI, and the integrity of the resultant expression construct was verified using automated sequencing. The linearized construct was transfected into Pt45P1 cells using Fugene HD (Roche, Indianapolis, IN), and asTF-overexpressing clones were obtained using escalating concentrations of Zeocin as per the manufacturer's instructions, were pooled and expanded to establish asTF-overexpressing line Pt45P1/asTF+.

2.3.5 Western blotting

Cells were grown to confluence in six-well plates, washed twice with PBS, lysed using 2X sample buffer containing 2-mercaptoethanol and denatured at 95°C for 5 min. The lysates were loaded on 10% polyacrylamide gels and transferred to PVDF membrane. The membrane was blocked for 1 hr using 5% nonfat milk and probed with the appropriate primary and the corresponding HRP-conjugated secondary antibodies (Invitrogen) using conventional techniques. The blots were developed using LumiLight (Roche), and chemiluminescent bands were visualized by exposure to X-ray film. To verify equal loading, blots were then stripped and re-probed for GAPDH.

2.3.6 Flow cytometry, ELISA and on-cell western assays

Levels of various proteins and phosphatidylserine (PS) on the surface of nonpermeabilized cells and/or cell-derived MPs was measured using flow cytometry; in brief, PDAC cells and cell-derived MPs were suspended in 50 µl of PBS or Annexin V staining buffer (Invitrogen), to which 10 µg of the corresponding primary antibodies or 10 µL of Annexin V-FITC (Invitrogen) were added and incubated at RT for 30 min. The cells were then washed twice with PBS, resuspended in 500 µL of PBS, incubated with the corresponding secondary antibodies (excluding Annexin V-FITC samples) washed twice with PBS and analyzed; isotype IgG whole molecule preparations (Jackson Immunoresearch) served as negative/background controls. All flow cytometry studies were performed using FACS Calibur (Becton Dickinson). Levels of asTF in the conditioned medium were assessed using a sandwich ELISA; in brief, sample aliquots were placed in 96-well plates pre-coated with the capture antibody RabMab95 and incubated for 2 hrs; after subsequent washes, HRP-conjugated detection antibody RabMab1 was added for 1 hr, unbound antibody

washed away, o-Phenylenediamine was added and the plate was read at 405 nm in a colorimetric assay using a VersaMax microplate reader (Molecular Devices, Sunnyvale, CA). For on-cell Western assays, intact cells (2 X 10^4 cells per well, Pt45P1 and Pt45P1/asTF+) were seeded in 96-well plates, washed free of media with PBS and flash-fixed in 4% paraformaldehyde for 5 min at room temperature. Cell surfaces were then blocked with 1X Power-Block (Biogenex, CA) and probed with the monoclonal flTF-specific antibody 10H10 and secondary anti-mouse IR-dye-800 CW (LI-COR Biosciences, Lincoln, NE) to assess cell-surface flTF expression; imaging was carried using Odyssey IR scanner and quantified using Odyssey software (both from LI-COR).

2.3.7 Microarray analysis

Pt45P1 and Capan-1 cells were treated with recombinant human asTF preparations generated and characterized as previously described (186) for 4 hrs at a final concentration of 50 nM; equal volumes of 50% glycerol in PBS served as the vehicle control. Total RNA was isolated using RNAeasy Kit (Qiagen, Valencia, CA), reverse transcribed, amplified, fragmented and labeled for microarray analysis using the Nugen WTA Ovation FFPE kit and Encore biotin module (Nugen, San Carlos, CA) according to the manufacturer's instructions. The labeled samples were hybridized onto Affymetrix Human Gene 1.0 ST chips. Transcripts that were differentially expressed in Capan-1 and Pt45P1 cells - untreated and/or as a result of asTF treatment - were identified based on filtering for probe sets with Robust Multichip Average-normalized raw expression of at least 1.5-fold with $p < 0.05$ using a Welch t-test; the results of the analysis were uploaded to NCBI GEO (http://www.ncbi.nlm.nih.gov/geo/query/acc.cgi?acc=GSE45928). Differences in gene expression between Pt45P1 and Pt45P1/asTF+ cells were assessed using

RNAseq technology. Samples from each cell line were analyzed in duplicate using Illumina TruSeq mRNA cDNA libraries that were sequenced using single-end 50 base reads at a depth if ~20 million reads on an Illumina 2500 analyzer; the results were uplaed to NCBI (htpp://www.ncbi.nlm.nih.gov/sra?term=%28SRP020496%29). Gene list enrichment analysis was performed using ToppGene (http://toppgene.cchmc.org/).

2.3.8 Isolation of cell-derived MPs

5 X 10^5 Pt45P1 and Pt45P1/asTF+ cells were seeded in a T-75 flask and grown to confluence over 2 days. The cells were then switched to serum-free defined media for 4 days, after which the conditioned media was collected and precentrifuged at 5,200g for 1 hr to remove cell debris. The resultant MP-containing supernatant was ultra-centrifuged at 337,000g (NVTi 65.2 rotor, Beckman) for 2.5 hrs. The supernatant was carefully aspirated using a vacuum manifold and the remaining MP pellet was resuspended in PBS and used in flow cytometry analysis and/or Factor Xa generation assays.

2.3.9 Two-step FXa generation assay

5 X 10^3 intact cells or 70 µL of cell-derived MP resuspended in HBS were incubated with FVIIa (Enzyme Research Laboratories, South Bend, IN) at the final concentration of 10 nM for 15 min to pre-form a TF/VIIa complex. Subsequently, FX (Enzyme Research Laboratories) was added to the samples at the final concentration of 100 nM and allowed to incubate for another 15 min, after which $CaCl_2$ was added to initiate FXa generation. The reaction was stopped at 15 min

using EDTA-Bicine, and FXa substrate Pefachrome (Enzyme Research) was then added and OD 405 nm recorded over a period of 1 hr using VersaMax microplate reader (Molecular Devices). All reactions were performed at 37°C.

2.3.10 *In vivo* studies

Use of laboratory animals and the experimental protocols were approved by the Institutional Animal Care and Utilization Committee, University of Cincinnati. PDAC cells (1 X 10^6 in 150 µL PBS) were orthotopically implanted in the pancreases of nude mice (age: 8 weeks; source: Harlan Laboratories, Indianapolis, IN; n = 3 per cohort, three independent experiments); 3 weeks post-surgery, *in vivo* imaging was performed using *in vivo* multispectral imaging system FX (Kodak) employing a novel method to target tumors by Cell-Vue Maroon (CVM)-labeled, nanovesicle-coupled Saponin C protein fragment H2 (CVM-SapC[H2]-DOPS): such nanovesicles selectively target tumor cells as well as tumor vasculature enriched in externalized phosphatidylserine (202). For quantification of tumor spread to distal lymph nodes, the images were analyzed in the corresponding anatomical locations or projections above and below the limbs in the lateral view using Carestream MI software, background fluorescence subtracted, data converted to photons per second per mm^2, and the results averaged. Following imaging studies, animals were sacrificed by intracardiac puncture, tissue specimens were harvested, fixed in formalin, embedded in paraffin and 4-µm sections analyzed using conventional techniques.

2.3.11 Statistical analysis

Student's *t*-test was used to assess the statistical significance of the differences between the groups; $p < 0.05$ was considered significant. For multiple group comparisons, one-way ANOVA was used and Tukey post-hoc test was applied to derive *p* values.

2.4 Results

2.4.1 asTF protein levels in human PDAC tissue positively correlate with the density of stromal monocytic infiltrates

To assess whether asTF protein is detectable in several forms of solid malignancies including PDAC, we performed IHC staining for asTF in commercial microarrays (TMA) comprising PDAC (n = 10), breast (n = 10), urothelial (n = 10), prostate (n = 9) and ovarian (n = 10) carcinoma. asTF immunoreactivity was observed in all examined tumor tissues, including pancreatic intraepithelial (PanIN) - early-stage PDAC lesions - as well as advanced PDAC (**Figure 2.1A**). We also co-stained these tumor sections for CD68, a monocyte/macrophage marker, and observed strong asTF expression in tumor-infiltrating moncytes; nearly all tumor infiltrating monocytes expressed asTF, demonstrating that stroma cells, in addition to tumor cells, can also serve as a source of asTF in malignant tissue (**Figure 2.1B**). Among the solid tumors studied, PDAC had the most monocyte infiltration, approximately twofold over the other four solid malignancies ($p < 0.05$, **Figure 2.1C**); of note, eight out of 10 PDAC specimens had some degree of detectable monocyte infiltration, whereas in the other four groups of specimens, monocyte infiltration was observed in ≤4 out of ten per group. We then examined 29 specimens of resected PDAC tissue for asTF expression. There was no appreciable staining for asTF in the normal

pancreatic tissue (areas adjacent to the tumor lesions, available in ~30% of all PDAC specimens examined) with the exception of islets of langerhans exhibiting consistently weak staining; asTF expression was detectable in over 90% of PDAC specimens (**Figure 2.2 & 2.3A**). The tumor lesion as well as the associated stroma stained positive for asTF. Occasionally, (peri)nuclear staining pattern was observed for asTF in some PDAC cells (**Figure 2.3A**). In regional lymph node metastases, moderate levels of asTF expression were observed. Based on the staining intensity of asTF in tumor lesions, we stratified the 20 PDAC specimens into three categories (weak = five specimens from five patients, moderate = 19 specimens from 17 patients and strong = five specimens from four patients); CD68 staining of the specimens revealed significantly higher levels of CD68+ infiltrating monocytes in the "stong-asTF" subcohort compared to the "weak" and "moderate" subcohorts (**Figure 2.3B**). Isolectin B4 staining revealed paucity of vascularization in PDAC tissue specimens, which is consistent with the notion that PDAC is a hypovascular adenocarcinoma (203); still, one of the "strong-asTF' specimens exhibited a high degree of vascularization (**Table 2.1A**). We note that 100% of "strong-asTF" patients presented with perineural invasion, compared to 60% in the "weak-asTF" subcohort and 65% in the entire PDAC cohort (**Figure 2.4**).

2.4.2 asTF increases metastatic spread of high-grade PDAC cells *in vivo*

A. *charaacterization of asTF-overexpressing Pt45P1 cell line*. To ascertain the role of asTF in pancreatic tumor growth and metastasis, we used two well-characterized cell lines, namely Capan-1 and Pt45P1 cells which are grade I and grade III PDAC lines, respectively. Semi-

quantitative RT-PCR revealed that basal expression of asTF mRNA is higher in Pt45P1 cells compared to Capan-1 cells (**Figure 2.5A**); we then proceeded to overexpress asTF in Pt45P1 cells to establish the line we termed Pt45P1/asTF+, and verified asTF overexpression by RT-PCR and western blotting. flTF expression appeared somewhat higher in Capan-1 compared to Pt45P1, and in Pt45P1 compared Pt45P1/asTF+ (**Figure 2.5A**). flTF and asTF mRNA expression was then quantified using real-time PCR with reverse transcription, normalized to GAPDH (**Figure 2.5B**). Quantitative real-time PCR revealed no significant difference in flTF mRNA levels between Pt45P1 and Pt45P1/asTF+ cells, and Western blot analysis of total cell lysates revealed no difference in flTF protein levels among the three cell lines, yet asTF levels were higher in Pt45P1 than in Capan-1 cells with Pt45P1/asTF+ displaying the highest levels of asTF protein (**Figure 2.5C**). Annexin V staining revealed no significant difference in the levels of externalized phosphatidylserine among the three lines (**Figure 2.6A**).

B. *asTF overexpression increases the aggressiveness of PDAC in an orthotopic model*. Nude mice were injected with 1 X 10^6 cells of Capan-1, Pt45P1 and Pt45P1/asTF+ (n = 3) orthotopically into pancreases, and tumor growth was monitored periodically using CVM-SapC[H2]-DOPS-based *in vivo* imaging (**Figure 2.6B**). After 3.5 weeks of orthotopic xenograft, we observed tumor growth in all three sets of mice; statistically significant evidence of enhanced distal metastases was observed in mice injected with Pt45P1/asTF+ cells compared to the Pt45P1 cohort (**Figure 2.6C**). The animals were then euthanized and upon necropsy, it became apparent that in Pt45P1/asTF+ mice, tumor cells spread to distal lymph nodes; of note, there were no differences between the cohorts in terms of tumor volume and/or mass at this early stage (not shown). The excised tumors were then formalin-fixed, and paraffin sections stained for asTF

which showed various degrees of asTF expression; the lymph node metastases from the Pt45P1/asTF+ mice were also immunoreactive for asTF (**Figure 2.6B**). As we previously showed that asTF promotes angiogenesis (186), we tested the extent of neovascularization in the primary tumors and determined that Pt45P1/asTF+ tumors had the highest vessel density followed by Pt45P1 and Capan-1 tumors ($p < 0.001$) (**Figure 2.7A**). F4/80 staining of tumor specimens revealed progressively higher monocyte infiltration of tumor stroma with the increasing levels of asTF produced by tumor cells (**Figure 2.7B**), which is in agreement with the results obtained using human PDAC specimens (**Figure 2.3B**).

2.4.3 asTF induces global changes in gene expression in PDAC cells

Recently, it was reported that β1/β3 integrins - both engaged by asTF (155)(186) - synergize with EGFR to upregulate several kinases critical to cancer pathobiology (204)(205). To explore whether short-term exposure to asTF protein can elicit autocrine/paracrine changes in PDAC cells, we treated Capan-1 and Pt45P1 cells with recombinant asTF (50 nM) or vehicle control for 4 hrs and assessed gene expression using microarrays. Out of the 185 genes differentially expressed in Capan-1 and Pt45P1 cells, 19 were relevant to such processes as EGFR signaling, mesenchymal development and epithelial to mesenchymal transition (EMT) (**Figure 2.8A**); western blotting revealed upregulation of MAPK and Akt phosphorylation in response to asTF (**Figure 2.8B**), and expression of *EFEMP1* - the gene that promotes PDAC growth (206) - was upregulated in response to asTF in both PDAC cell lines (**Figure 2.8C**). To explore the gene expression shifts elicited by sustained overexpression of asTF, we compared transcriptomes of Pt45P1 and Pt45P1/asTF+ cells using RNAseq; the results, summarized in (**Figure 2.9**), show that

asTF promotes upregulation of cell migration, MAPK signaling, EMT and wound healing processes while downregulating cell adhesion, phosphatase activity, inhibition of MAPK cascade and apoptosis; again, upregulation of MAPK activity in response to heightened asTF levels was observed, and increased phosphorylation of Akt was observed in Pt45P1/asTF+ cells compared to Pt45P1 cells when cultures were maintained in low serum (**Figure 2.10A**). Interestingly, Pt45P1/asTF+ cells exhibited increased upregulation of *EFEMP1* as well as *AREG* - recently shown to promote proliferation of PDAC cells (207) - and *VEGFA* (**Figure 2.10B**); immunohistochemical evaluation of tissue specimens confirmed upregulation of EFEMP1 protein expression in Pt45P1/asTF+ cells (**Figure 2.10C**). Surface levels of β1/β3 integrins and EGFR did not differ in Pt45P1 and Pt45P1/asTF+ cells (**Figure 2.13B**).

2.4.4 asTF contributes to the procoagulant potential of PDAC cell lines

The procoagulant potential of asTF is still poorly defined and not universally recognized. asTF requires interaction with phospholipid surfaces to exert its weak procoagulant activity (155). We measured the TF-dependent procoagulant activity on PDAC cell surfaces using a standard endpoint two-step FXa generation assay. We observed a significant increase in TF activity in Pt45P1/asTF+ compared to Pt45P1 (**Figure 2.11A**). Cell-derived MPs isolated from conditioned media of Pt45P1/asTF+ cells also revealed a ~1.5-fold increase in TF activity compared to Pt45P1-derived MPs (**Figure 2.11B**). There was no difference in the total number of MPs generated by Pt45P1 and Pt45P1/asTF+ cells (**Figure 2.13C**). To confirm the specificity of our assay, we performed control experiments using monoclonal antibody 7G11, which inhibits the activity by

hindering TF/VIIa interaction (200). To address the possible contribution of altered flTF and/or asTF protein levels to the observed increase in procoagulant activity, we measured the surface level expression of flTF and asTF. While there was a trend toward a decrease in surface flTF levels on Pt45P1/asTF+ cells compared to Pt45P1 cells, it did not reach significance neither by FACS nor by on-cell western assay; however, MPs generated by Pt45P1 cells (**Figure 2.11C** and **Figure 2.13D**). Surprisingly, asTF was also detectable on the surface of Pt45P1 and Pt45P1/asTF+ cells and MPs; moreover, asTF surface expression was significantly increased in Pt45P1/asTF+ cells as well as MPs generated by them (**Figure 2.11D**); an approximately fivefold increase in the levels of free-secreted asTF protein was also seen in the MP-free conditioned media from the Pt45P1/asTF+ cells compared to Pt45P1 conditioned media (**Figure 2.11D**). There was no difference in the levels of β1/β3 integrins on MPs generated by Pt45P1 and Pt45P1/asTF cells (**Figure 2.13E**). By ELISA, plasma of mice bearing Pt45P1 and/or Capan-1 tumors (**Figure 2.12A**). Exogenous addition of recombinant asTF resulted in a dose-dependent increase in TF procoagulant activity in Pt45P1 cells, whereas there was no such increase in TF activity when recombinant asTF was added to Pt45P1-derived MP preparations (**Figure 2.12B**).

2.5 Discussion

In this report, we show for the first time that asTF protein is expressed in human PDAC lesions; asTF is evidently produced by the tumor cells as well as the infiltrating monocytes. Pancreatic tumors tend to by hypovascular in nature, and pharmacokinetics-related issues are commonly associated with the treatment of PDAC (203). While the human PDAC specimens in our study appeared largely hypovascular, a limitation of our study is that it involved a relatively

small number of PDAC specimens and, especially considering heterogeneity of PDAC tissue, better-powered studies involving (*i*) larger cohorts and (*ii*) in-depth examination of a larger tissue volume of each PDAC specimen are thus highly warranted. Still, we invariably found heavy infiltration of monocytes in the tumor stroma; notably, the degree of monocyte infiltration positively correlated with asTF protein levels in PDAC lesions (**Figure 2.3B**). The role of the flTF/asTF synergy in cancer pathobiology is very poorly understood. Inflammatory stromal cells and infiltrating monocytes are crucial mediators of lymph-angiogenesis. Lymphatic invasion of the tumor front and lymphatic metastasis is the major determining factor for PDAC metastasis (208). We previously showed that asTF could act as an inflammatory mediator, inasmuch as its activation of endothelial cells yields enhanced monocyte adhesion and transmigration under chemokine gradients (186). It is thus reasonable to propose that asTF expressed in the tumor cells and/or tumor-associated macrophages could play a role in PDAC metastasis.

In all biological settings described to date, flTF and asTF are co-expressed; thus, we assessed the role of asTF in pancreatic tumors in an orthotopic model of PDAC using an flTF-expressing PDAC cell line Pt45P1. We find that asTF promotes tumor spread in this model, and it also drives angiogenesis as revealed by the increase in vascular density. We observed an appreciable increase in macrophage infiltration in the orthotopically grown Pt45P1/asTF+ tumors, suggesting that our orthotopic model is suitable to study monocyte recruitment elicited by asTF in a PDAC setting (**Figure 2.3B**). Hobbs *et al.* (185) have shown that asTF induces pancreatic tumor growth and angiogenesis in a sub-cutaneous model, but flTF paradoxically had an inhibitory effect on both, in contrast to findings of others who have convincingly determined that flTF expression is positively associated with tumor growth and angiogenesis (168)(162). In this light, the

subcutaneous model employed by Hobbs *et al.* (185) has other serious limitations including, most significantly, a complete lack of recapitulation of the PDAC microenvironment and/or suitability in assessing metastatic potential. Furthermore, the MiaPaCA-2 cell line that was used by Hobbs *et al.* (185) lacks the TF gene expression; since asTF is not found in the absence of flTF, this model is not suitable for assessment of the role of asTF and/or flTF/asTF synergy in tumor growth and metastasis. We observed an increase in tumor vascularization in pancreatic tumors derived from asTF-overexpressing PDAC cell line, and it is reasonable to speculate that the underlying mechanisms of neovascularization are engaged by integrin-mediated signaling (186). Our microarray data highlight the signaling changes elicited by asTF in PDAC cell lines. asTF significantly activated various biological processes that are involved in tumorigenesis such as EGFR pathway and epithelial-mesenchymal signaling. One of the genes activated by asTF is *EFEMP1*, whose product is a ligand for EGFR and competes with EGF for receptor binding; EFEMP1 has been shown to activate MAPK and Akt in inducing pancreatic tumor growth (206)(209). Although PDAC tumors tend to be hypovascular, there is firm evidence that microvascular density in PDAC is comparable to that of other adenocarcinomas; moreover, VEGF expression levels are a significant and independent prognostic factor for advanced PDAC (210), and overexpression of asTF does increase *VEGFA* expression in PDAC cells (**Figure 4.10B**). In this light, the increase in vascular density in our mouse model might be due to asTF-mediated induction of *EFEMP1*, which has been recently shown to activate *VEGF* and, subsequently, increase microvascular density in a PDAC model (206); Thus, we plan to assess the significance of the *EFEMP1* expression for the asTF-PDAC axis with and without EGFR signaling inhibitors in future studies.

Pancreatic cancer is associated with increased thrombosis, and VTE is a risk factor of mortality in most forms of cancers (211). Haas *et al*. previously demonstrated that pancreas TF is substantially more immunoreactive in pancreatic cancer patients compared to those with chronic pancreatitis; importantly, plasma TF levels were heightened in patients with pancreatic cancer *vs*. controls and were particularly appreciable in patients that developed upper jugular and splenic vein thrombosis (198). A recent study by Wang *et al*. revealed that the major source of TF activity affording systemic activation of coagulation in PDAC in the tumor itself, whereby clotting factors enter the tumor through neovessels and activate coagulation in a TF-dependent manner (212). Our study shows that asTF may possibly synergize with flTF in promoting thrombosis in PDAC. We show that asTF overexpressing PDAC cells are more procoagulant and that MPs derived from these cells also display enhanced cell surface membrane retention of asTF, but no significant change was observed in flTF levels. The increased asTF retention on the cell membrane retention of asTF, but no significant change was observed in flTF levels. The increased asTF retention on the cell membrane is perhaps due to its interaction with integrins which is not likely to affect asTF's ability to bind FVIIa. Indeed, flTF in complex with β1 integrin on MPs appears to have full coagulant function, suggesting that the FVII binding site is preserved in integrin-bound TF (213). As asTF contains the FVIIa binding domain of flTF, it is possible that asTF binding to FVIIa leads to the overall augmentation of FX-to-FXa conversion in the presence of flTF on cell surfaces. We note that asTF retention may also be accomplished through direct interaction with phospholipid bilayers (155). As to the ability of asTF to increase flTF levels on PDAC cell-derived MPs, our findings closely echo those recently reported by Garnier *et al*., whereby promotion of EMT in colorectal cancer cells led to the release of extracellular vesicles carrying TF coagulant activity (214); addition of asTF to MPs derived from Pt45P1 cells did not augment total TF activity (**Figure**

2.12B), suggesting that the procoagulant potential of PDAC cell-derived MPs, while indirectly modulated by asTF, may very well be largely flTF-dependent. Further studies are required to evaluate the kinetics and avidity of asTF/FVIIa interaction and the evidently EMT-mediated mechanisms underlying the enhanced presence of flTF on MPs derived from PDAC cells overexpressing asTF. In sum, our results point to the role of asTF in the pathobiology of PDAC. The minimmaly coagulant asTF - a molecule that is not likely to significantly contribute to normal hemostasis yet may play a role in cancer-associated thrombosis as well as tumor spread - may serve as a novel target to treat PDAC and its thrombotic complications.

2.6 Acknowledgements

The authors thank Vallabaprabhu Subramanya for help with FACS analysis, Birgit Ehmer for help with microscopy, Katie LaSance and Evgeny Ozhegov for help with *in vivo* imaging studies, Neil Batra for help with intracardiac puncture procedure and Ryan Keil for help with tissue culture maintenance.

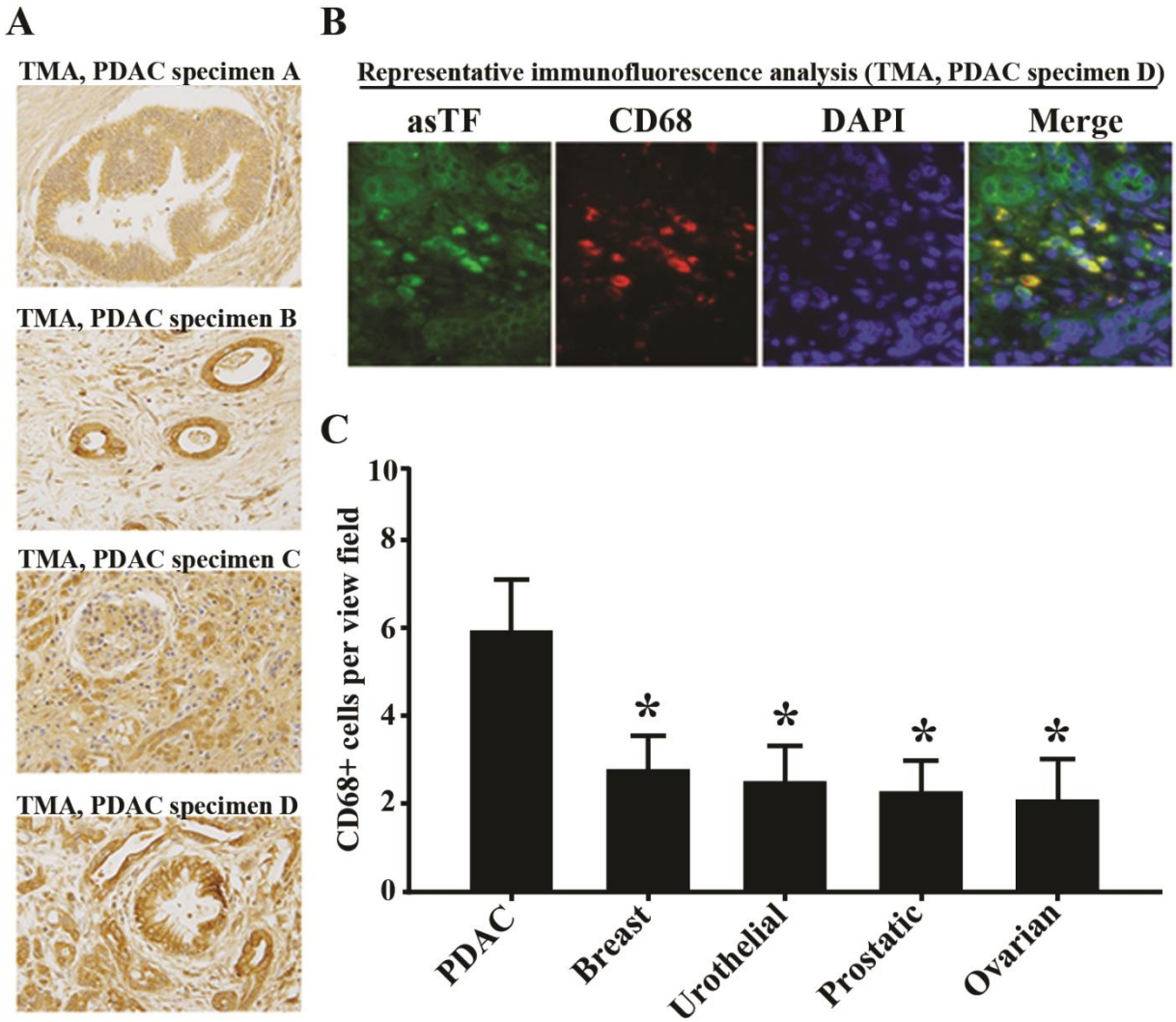

Figure 2.1: asTF expression and TAMs in human adenocarcinoma lesions. (original magnification: x40). (***A***) asTF expression in TMA: specimen A – a diffuse staining pattern of asTF in PanIN; specimen B – cell surface expression of asTF; specimens C and D – asTF expression in highly aggressive PDAC. (***B***) CD68 staining of specimen D (original magnification: x10, primary antibody was used at 2.0 µg/mL); asTF expression is observed in the lesion, stroma and infiltrating monocytes. (***C***) Monocyte infiltration in various solid tumors; *$p < 0.05$.

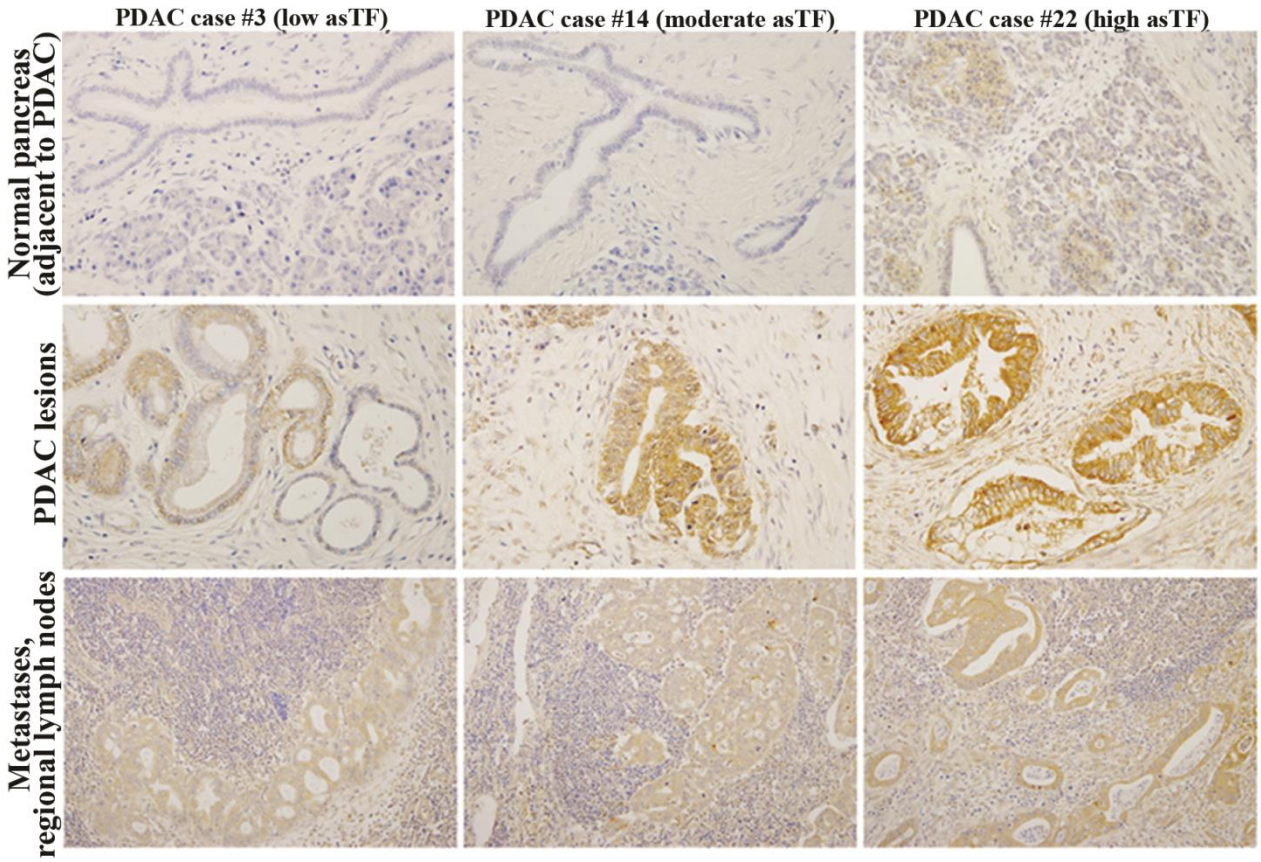

Figure 2.2: asTF expression in human PDAC lesions. (***A***) Representative images, top row: staining for asTF in non-malignant pancreas, *i.e.*, duct cells, islets of Langerhans (indicated by arrows) and acinar tissue; middle row, staining for asTF in PDAC lesions (weak staining, ~15%; moderate staining, ~70%; strong staining, ~15% of all tissue specimens, n = 29); bottom row, PDAC metastases in regional lymph nodes. Custom anti-asTF polyclonal antibody was used at 2.0 µg/mL; original magnification: x40.

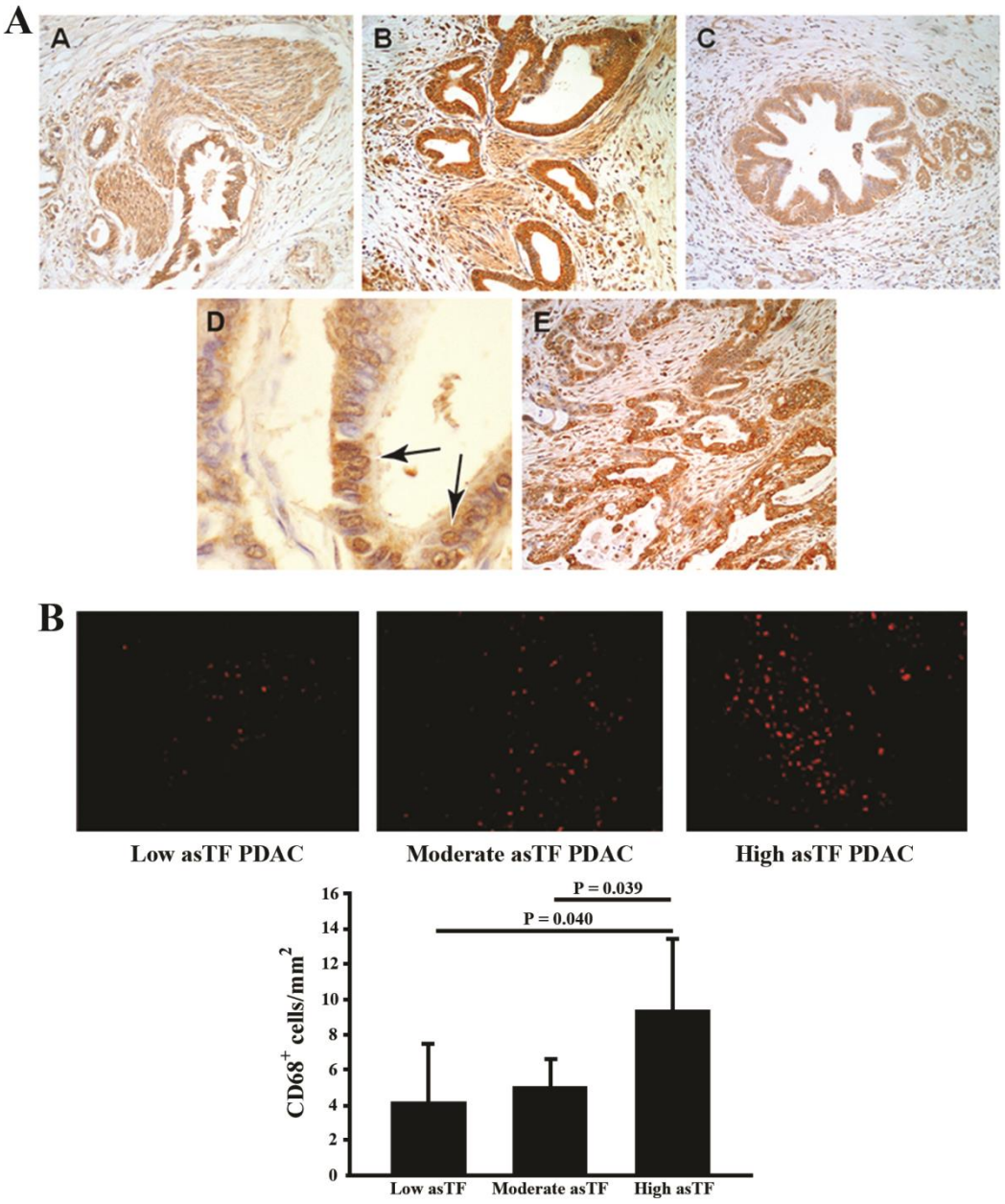

Figure 2.3: asTF expression patterns and TAMs in human PDAC lesions. (***A***) Expression patterns of asTF in PDAC. Representative histological sections showing asTF staining patterns in PDAC displaying perineural invasion (images A and B), pancreatic intraepithelial neoplasia lesions (image C) and (peri)nuclear staining occasionally observed in PDAC cells, arrows (image D). Intralesional variability of asTF protein expression was also observed in some PDAC specimens (image E). (***B***) CD68 staining in PDAC specimens exhibiting weak, moderate and strong staining for asTF (original magnification: x40, staining was carried out as in Fig. 2.1.

Characteristic	All patient (n = 26)	Weak asTF (n = 5)	Strong asTF (n = 4)
Median age, years (range)	65 (41 – 81)	62.5 (56 – 69)	57 (56 – 78)
Sex: M/F	11/15	3/2	3/1
pT category: T1/2/3	4/0/22	1/0/4	0/0/4
pN category: N0/1/2	7/18/1	2/3/0	1/3/0
Histological grade: G1/2/3	1/18/7	0/3/2	0/4/0
Pathological margin: Involved/ uninvolved	7/19	2/3	1/3
Perilymphatic, perivascular Invasion: yes/ no	4/21	1/4	1/3
Perineural invasion: yes/ no	17/9	3/2	4/0
Recurrence: yes/ no	11/15	3/2	1/3
Median time to recurrence, Months (range)	16 (10 – 22)	21 (16 – 22)	22

Figure 2.4: clinicopathological characteristics, PDAC cohort.

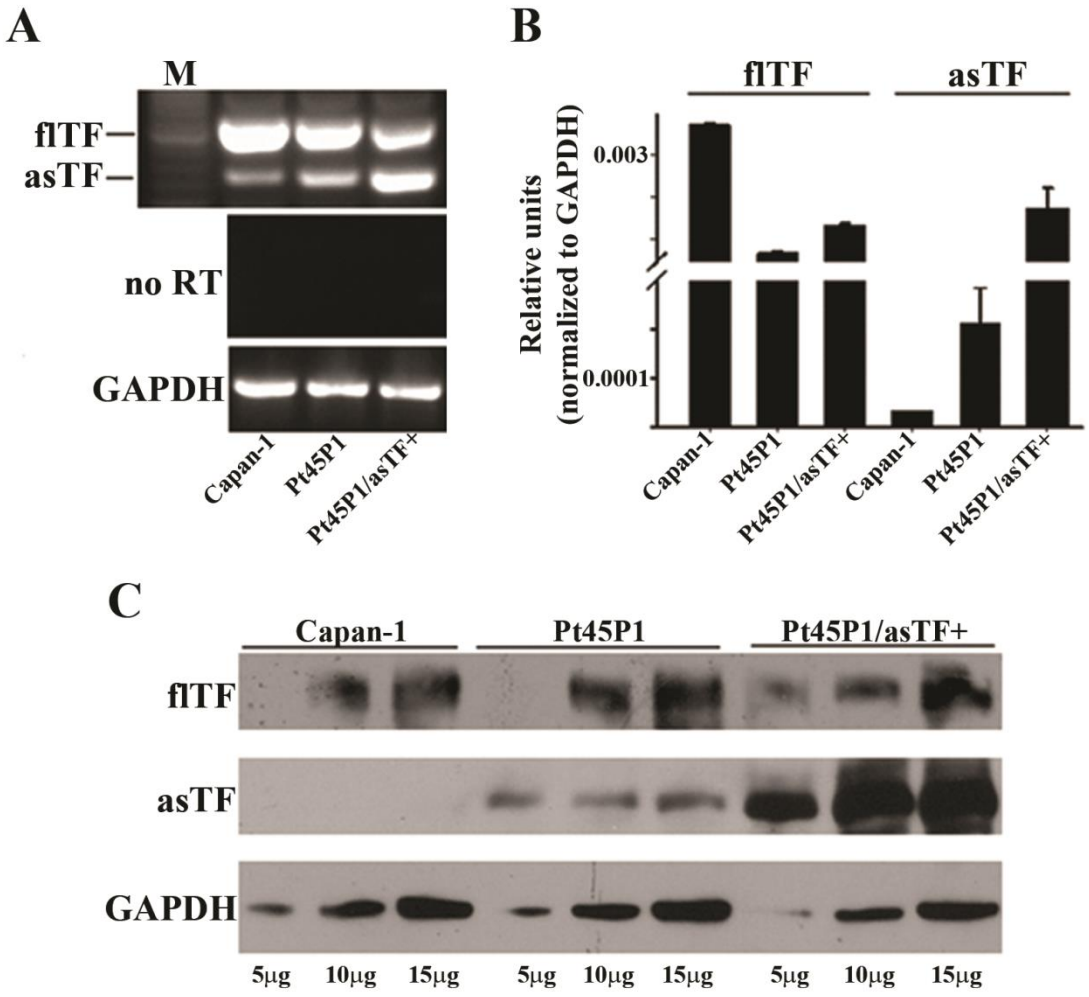

Figure 2.5: Verification of flTF/asTF expression levels in Grade I (Capan-I) and Grade III (Pt45P1) PDAC cell lines. (***A***, ***B***) flTF/asTF expression by conventional and quantitative real-time RT-PCR (n = 3). (***C***) flTF/asTF protein levels in cell lysates (total protein, µg).

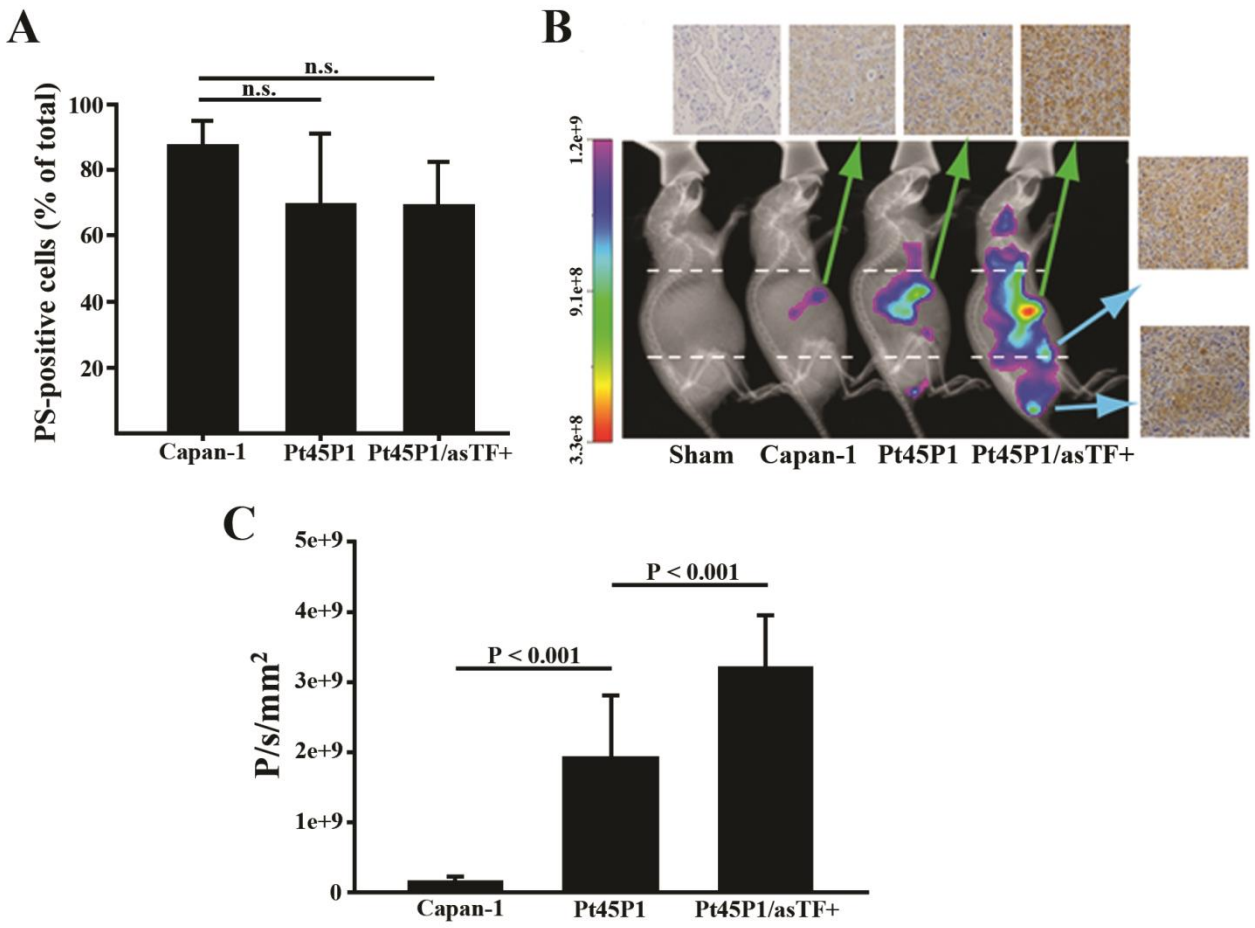

Figure 2.6: asTF promotes PDAC spread *in vivo*. (***A***) Annexin-V staining (PS levels) by flow cytometry (n=3). (***B***) PDAC cell lines were implanted orthotopically (three independent experiments, 3 mice per cohort), and 3.5 weeks post-surgery live animals were imaged using CVM-SapC(H2)-DOPS via tail injection. The mice were then sacrificed, tumors were excised, formalin fixed/paraffin embedded, and stained for asTF (top row); side panel – isolated Pt45P1/asTF+ lymph node metastases. (***C***) Quantification of tumor spread to distal lymph nodes (CareStream software, Kodak).

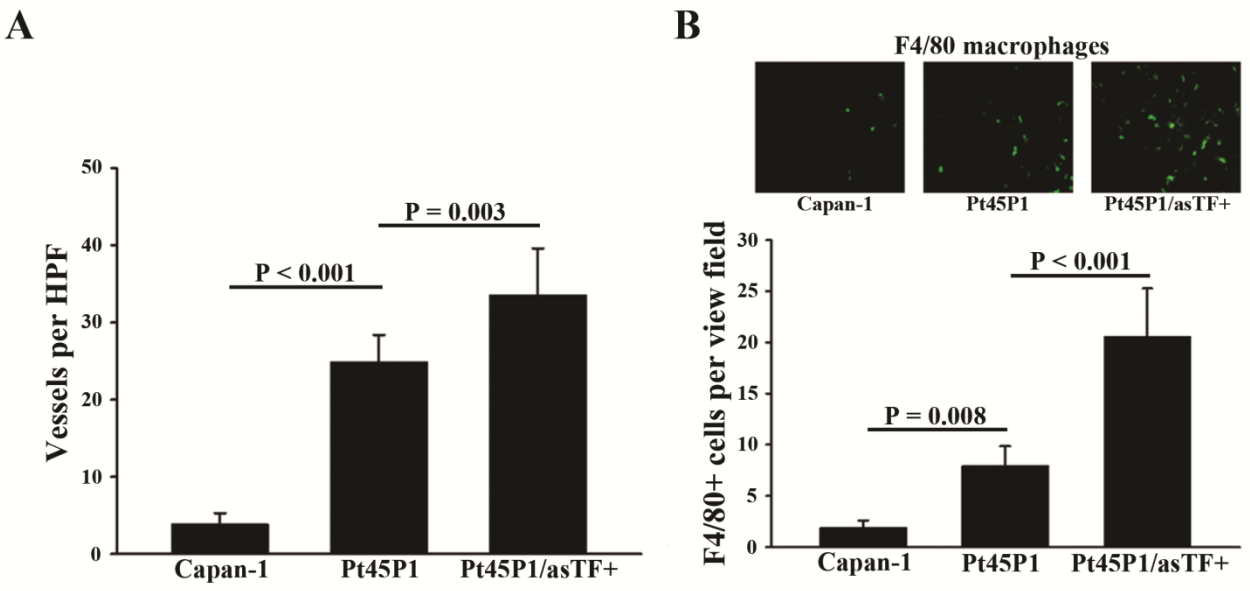

Figure 2.7: Orthotopically implanted PDAC line Pt45P1/asTF+ exhibits the highest level of monocyte infiltration, and vessel density. *(A)* Vessel density as assessed by isolectin B4 staining of the excised tumors. (***B)*** Infiltration of tumor stroma assessed by anti-F4/80 staining; representative images are shown on top, 8 view fields per specimen (n = 3 per specimen type) were counted and averaged; primary antibody was used at 10.0 μg/mL.

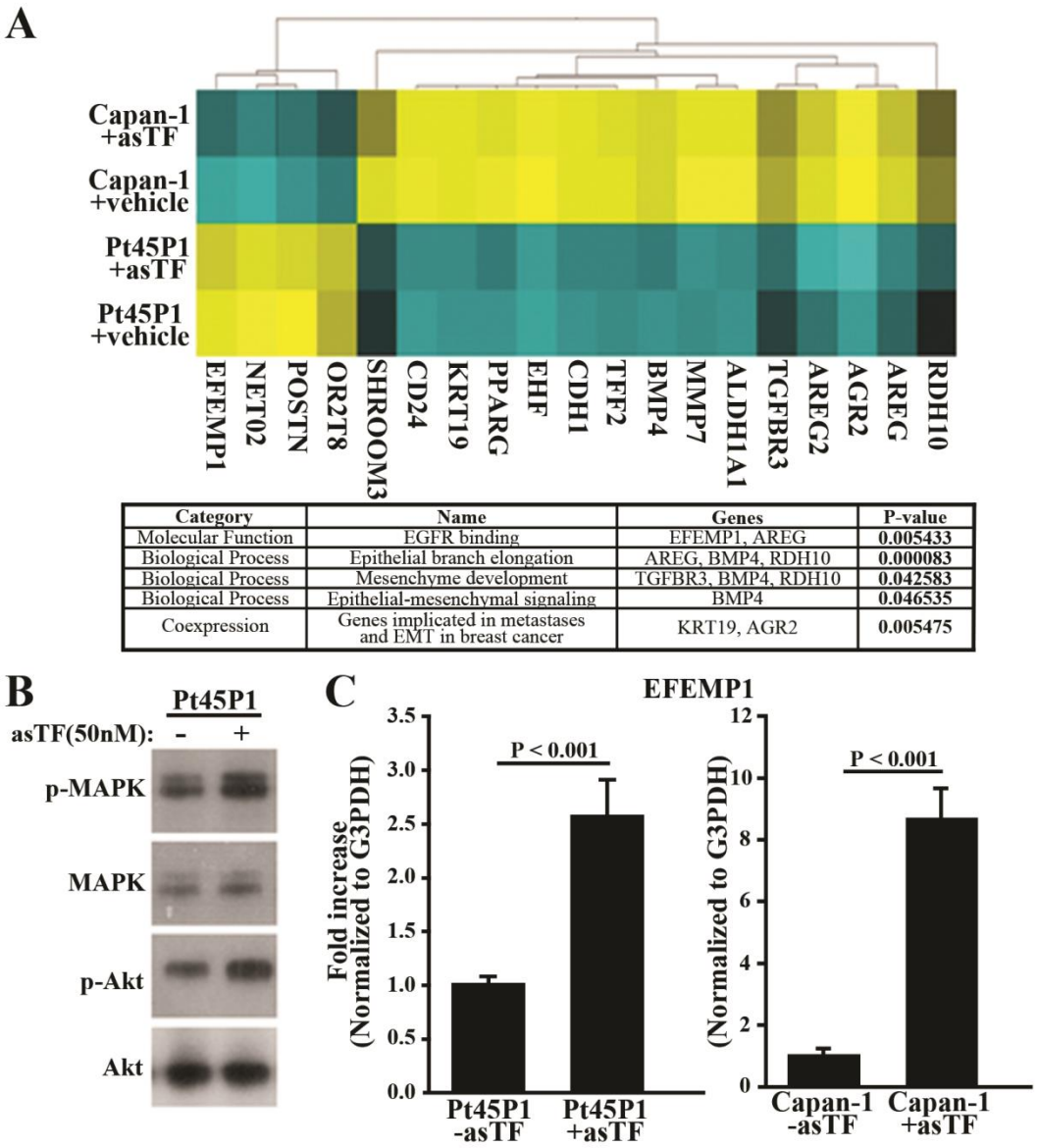

Category	Name	Genes	P-value
Molecular Function	EGFR binding	EFEMP1, AREG	**0.005433**
Biological Process	Epithelial branch elongation	AREG, BMP4, RDH10	**0.000083**
Biological Process	Mesenchyme development	TGFBR3, BMP4, RDH10	**0.042583**
Biological Process	Epithelial-mesenchymal signaling	BMP4	**0.046535**
Coexpression	Genes implicated in metastases and EMT in breast cancer	KRT19, AGR2	**0.005475**

Figure 2.8: asTF protein elicits changes in gene expression in PDAC cells. (representative data, two independent experiments in duplicate). (***A***) Heat map, Capan-1 and Pt45P1 cells were treated with recombinant asTF (50 nM) or vehicle control (PBS/glycerol) for 4 hours, total RNA was reverse transcribed, amplified, fragmented and labeled for microarray analysis; table: summary of the biological processes significantly altered in PDAC cells Capan-1 and Pt45P1. (***B***) Western blotting, phosphorylation status of MAPK and Akt in Pt45P1 cells treated with recombinant asTF or vehicle control; (***C***) real-time quantitative RT-PCR, levels of EFEMP1 transcripts in Capan-1 and Pt45P1 cells treated with recombinant asTF or vehicle control.

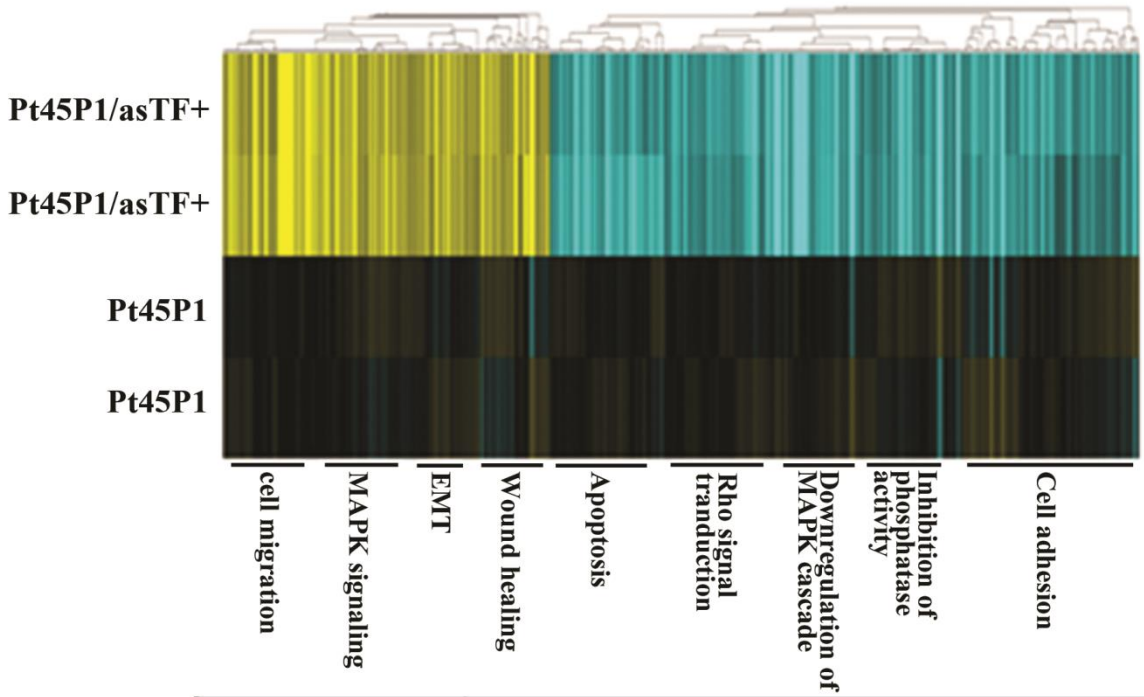

Category	Genes	*P*-value
enzyme linked receptor protein signaling pathway	EFEMP1, TGFBR2, LEF1, PMEPA1, OBSCN, FOXC2, ITPR2, CD3EAP, SERPINE1, SPRY1, SOCS2, TGIF2, RGMB, LTBP2, DUSP6, MAPKAPK3, FUT8, CGN, FOS, KRAS	2.83E-04
intracellular protein kinase cascade	TGM2, SPRY4, GJA1, TNFRSF11A, FGF13, HMGA2, GOLT1B, STK38L, PAK3, SPRY1, SOCS2, CARD9, DUSP9, DUSP6, DUSP2, MAPKAPK3, FOS, IKBKE, KRAS	7.53E-04
MAPK cascade	SPRY4, TNFRSF11A, FGF13, PAK3, SPRY1, CARD9, DUSP9, DUSP6, DUSP2, MAPKA, PK3, FOS, KRAS	5.52E-03
regulation of vascular wound healing	FOXC2, SERPINE1	4.64E-04
epithelial to mesenchymal transition	LEF1, GJA1, HMGA2, FOXC2, FOXF2	8.60E-04
negative regulation of cell adhesion	LEF1, SERPINE1, FXYD5, LAMB1, UBASH3B	1.73E-03
negative regulation of cell-cell adhesion	LEF1, FXYD5, UBASH3B	3.95E-03
cell migration	TGFBR2, LEF1, DOCK4, GJA1, TNFRSF11A, FGF13, SEMA3A, FOXC2, PODXL2, ITG, A2, SERPINE1, FUT8, LAMB1, KRAS, PPAP2B	1.67E-02

Figure 2.9: asTF protein elicits changes in gene expression in PDAC cells. (representative data, two independent experiments in duplicate). Heat map, differences in gene expression between Pt45P1 and Pt45P1/asTF+ cells; table: summary of the biological processes significantly altered in Pt45P1/asTF+ cells.

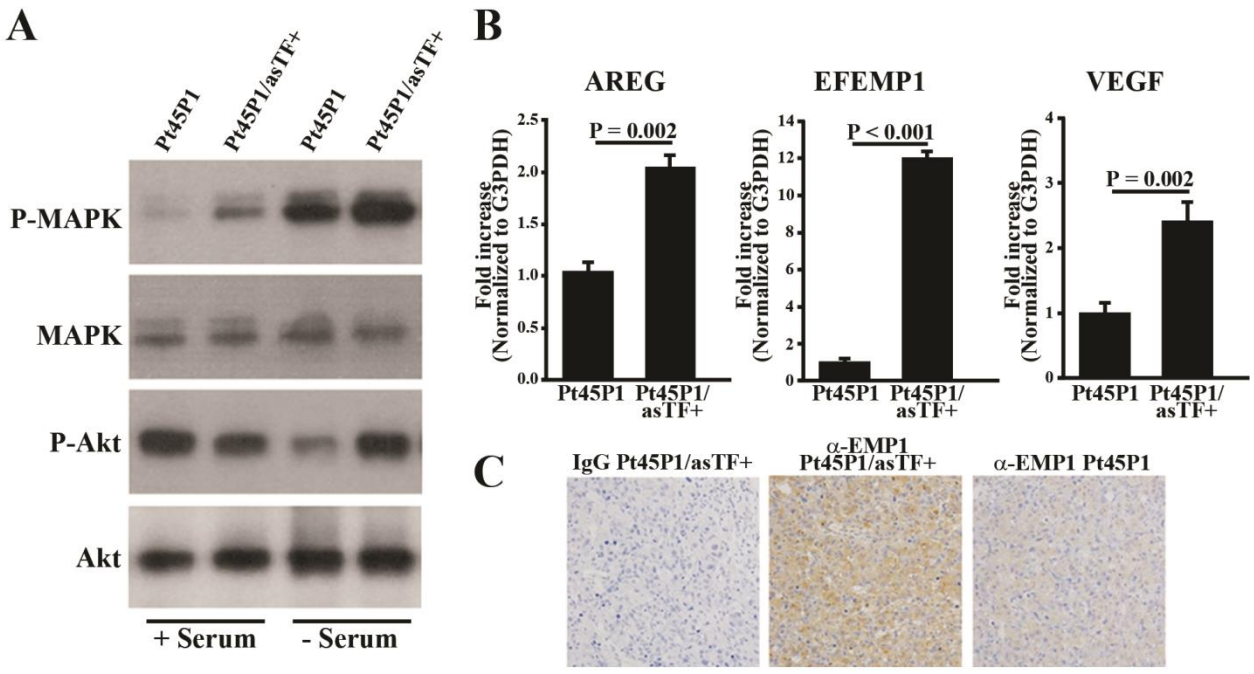

Figure 2.10: Assessment of EMT-associated gene expression / kinase upregulation in PDAC cells overexpressing asTF. ***(A)*** Western blotting, phosphorylation status of MAPK and Akt in Pt45P1 cells and Pt45P1/asTF+ cells. ***(B)*** Real-time quantitative RT-PCR, levels of EFEMP1, AREG, and VEGFA transcripts in Pt45P1 cells and Pt45P1/asTF+ cells. ***(C)*** Immunohistochemical analysis of EFEMP1 protein expression in Pt45P1 and Pt45P1/asTF+ cells.

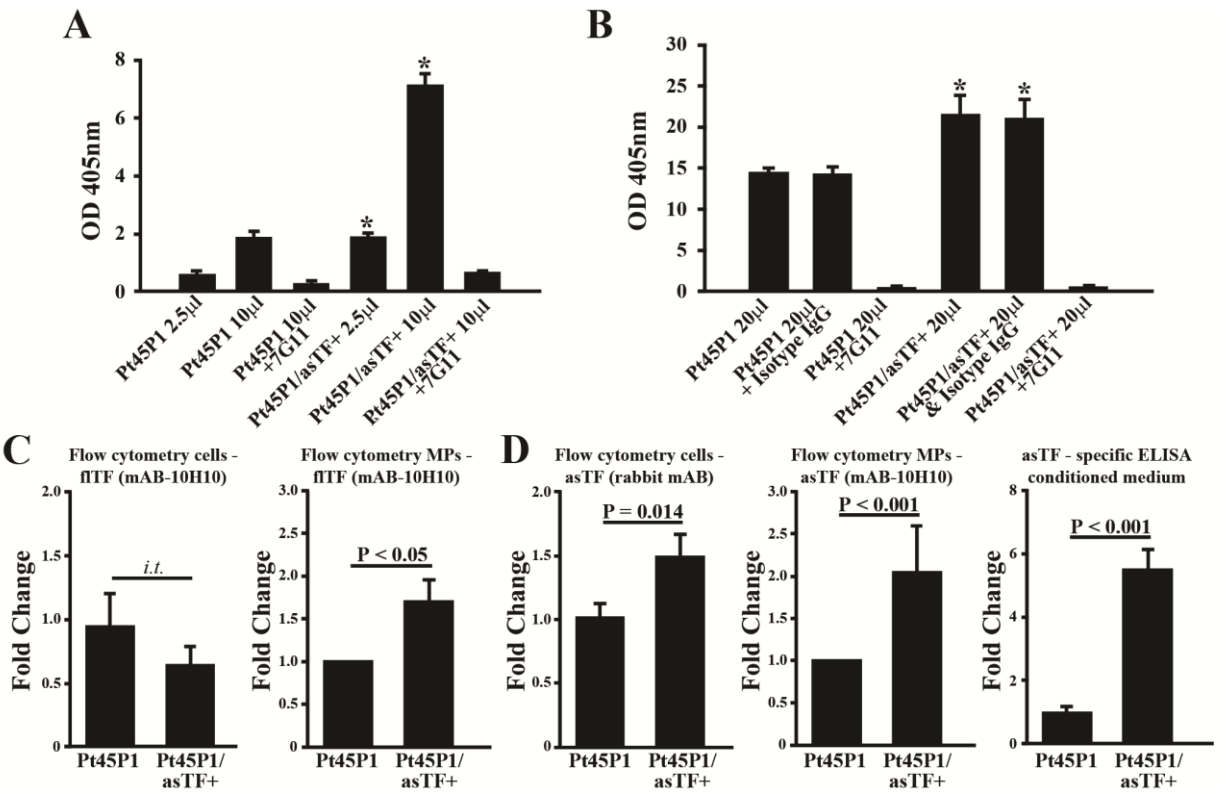

Figure 2.11: Analysis of procoagulant activity in PDAC cell lines and determination of TF isoform levels on nonpermeabilized cells and cell-derived MPs. ($n \geq 3$ experiments per each sample type). (***A***) TF activity on cell surfaces. (***B***) TF activity on cell-derived MP. (***C***) Cell-surface and MP expression of flTF protein. (***D***) Cell surface and MP expression of asTF protein; levels of asTF secreted in the culture media.

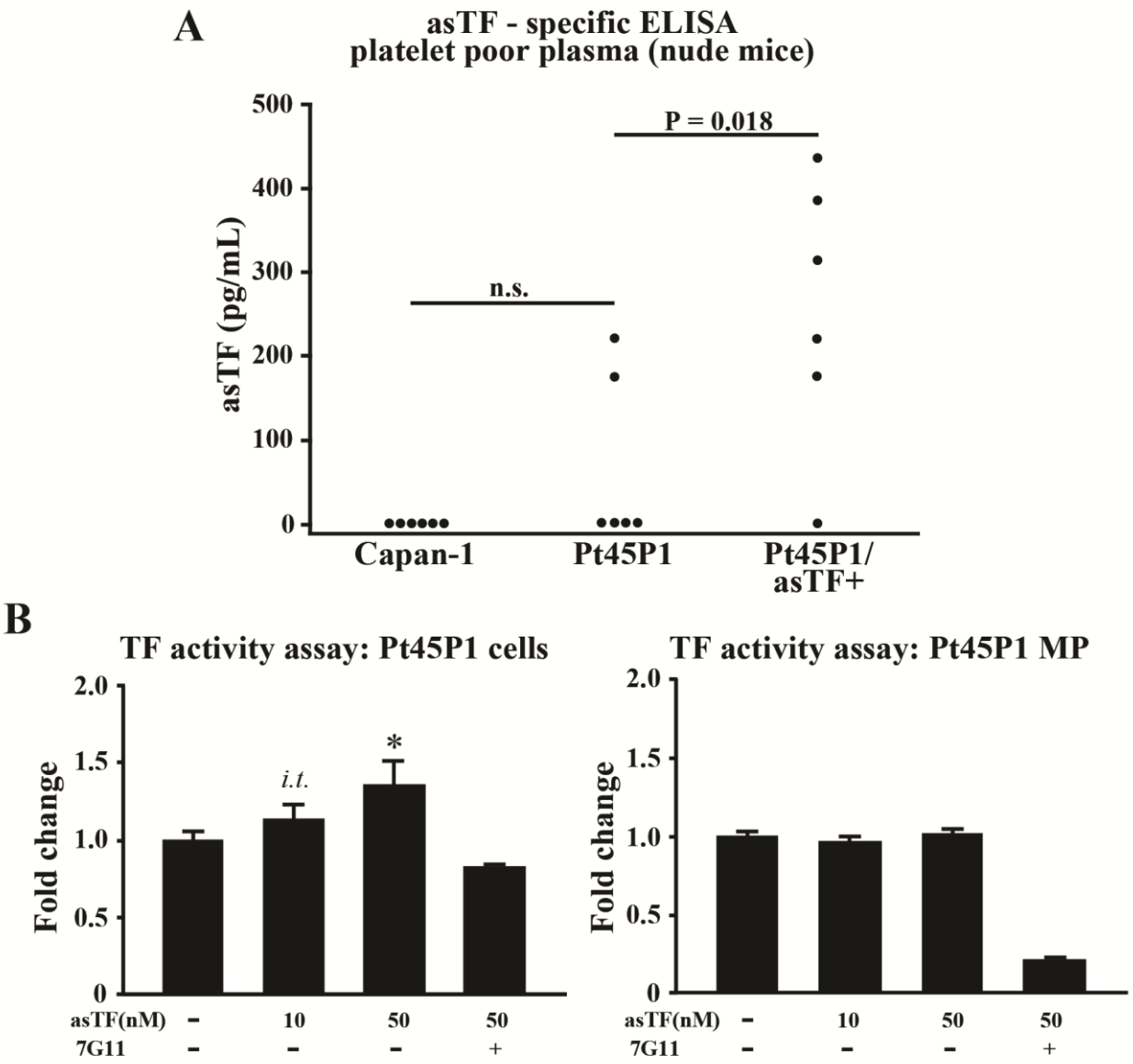

Figure 2.12: Circulating levels of arterial asTF and analysis of procoagulant activity of PDAC cells and MPs. ($n \geq 3$ experiments per each sample type). (***A***) Levels of asTF protein in the plasma of mice bearing tumors as indicated (six plasma samples per type, collected during two independent *in vivo* studies). (***B***) Effect of recombinant asTF on TF procoagulant activity on the surfaces of intact cells and cell-derived MP. $*p < 0.05$, *i.t.* – in-trend, $0.1 < p < 0.05$.

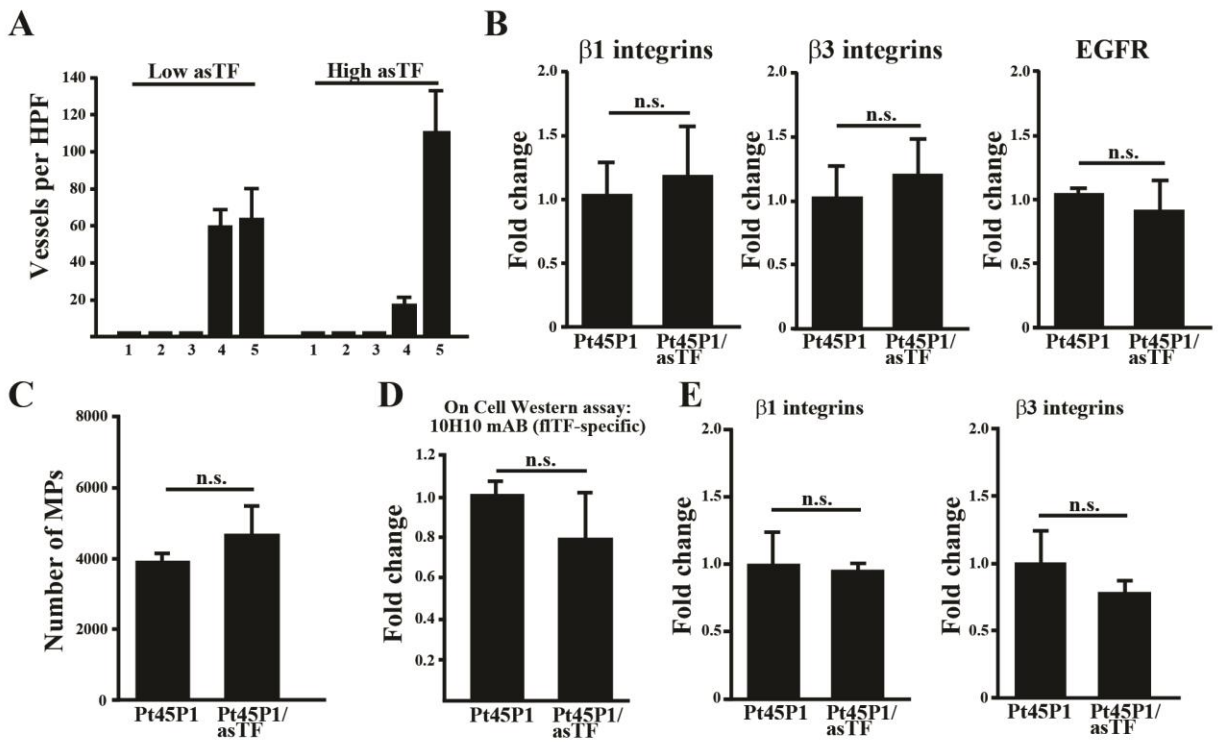

Figure 2.13: supplementary material. (***A***) Quantification of vessel density in the PDAC specimens stratified into weak asTF and strong asTF cohorts. (***B***) Levels of β1/β3 integrins and EGFR on the surface of Pt45P1/asTF+ cells ($n \geq 3$). (***C***) Total number of microparticles generated by Pt45P1 and Pt45P1/asTF+ cells ($n \geq 3$). (***D***) Levels of flTF protein on cell surfaces assessed using on-cell western assay ($n = 3$). (***E***) Levels of β1/β3 integrins on the surface of MP generated by Pt45P1 and Pt45P1/asTF+ cells ($n = 3$).

Chapter 3: Levels of alternatively spliced tissue factor in the plasma of patients with pancreatic cancer may help predict aggressive tumor phenotype

In the field of observation, chance favors the prepared mind.

– Louis Pasteur
Lecture, University of Lille, December 7, 1854

Levels of alternatively spliced tissue factor in the plasma of patients with pancreatic cancer may help predict aggressive tumor phenotype

Dusten Unruh[1], Farah Sagin[2], Mariette Adam[5], Patrick Van Dreden[5], Barry J. Woodhams[6], Kimberly Hart[3], Christopher J Lindsell[3], Syed A. Ahmad[4], and Vladimir Y. Bogdanov[1]

[1]Division of Hematology/Oncology, Internal Medicine, University of Cincinnati College of Medicine, Cincinnati, OH; [2]University of Cincinnati Cancer Institute Tumor Bank, University of Cincinnati College of Medicine, Cincinnati, OH; [3]Department of Emergency Medicine, University of Cincinnati College of Medicine, Cincinnati, OH; [4]Department of Surgery, University of Cincinnati College of Medicine, Cincinnati, OH; [5]Diagnostica Stago R&D, Gennevilliers, France; [6]Haemacon Ltd, Bromley, UK

Citation: Unruh D, Sagin F, Adam M, Van Dreden P, Woodhams BJ, Hart K, et al. Levels of alternatively spliced tissue factor in the plasma of patients with pancreatic cancer may help predict aggressive tumor phenotype. Ann Surg Onc. 2015

3.1 Abstract

Background. Circulating ('blood-borne') tissue factor (TF) is implicated in the pathogenesis of several chronic conditions, most notably cardiovascular disease, diabetes, and cancer. Full-length TF is an integral membrane protein, while alternatively spliced TF (asTF) can be secreted and, owing to its unique C-terminus, selectively detected in biospecimens. The predictive and/or prognostic value of asTF in the circulation is unknown. In a retrospective study, we measured levels of circulating asTF in healthy subjects and individuals with acute coronary syndrome (ACS), diabetes mellitus (DM), ongoing ACS + DM, and pancreatic ductal adenocarcinoma (PDAC). *Methods*. The prototype-tailored procedure (Diagnostica Stago) was used to measure asTF in plasma from 205 subjects. *Results*. There was no significant difference between the proportion of healthy subjects with asTF ≥200 pg/mL and those with ACS, DM, or ACS + DM. The proportion of pancreatic cancer patients (n = 43; PDAC: 42; pancreatic neuroendocrine tumor: 1) with asTF levels ≥200 pg/mL was significantly higher than in healthy subjects; asTF levels ≥200 pg/mL were detected more often in patients with unresectable disease irrespective of initial evaluation and/or preoperative carbohydrate antigen 19-9 (CA19-9) levels. *Conclusions*. While asTF levels ≥200 pg/mL are not observed with increased frequency in patients with ACS and/or DM, they do occur more frequently in the plasma of patients with pancreatic cancer and are associated with lower likelihood of tumor resectability, irrespective of the preoperative diagnosis. asTF may thus have utility as a novel marker of aggressive pancreatic tumor phenotype.

3.2 Background

Tissue Factor (TF) is a glycoprotein that serves as the primary initiator of blood coagulation. In the late 1990s, Key *et al*. and Giesen *et al*. demonstrated the presence of procoagulant TF in the blood of healthy individuals, which was contrary to the notion that TF only resided in the adventitia acting as a hemostatic envelope (215)(216). This paradigm shift was later confirmed by other groups demonstrating that blood monocytes in healthy individuals express low levels of TF (217). TF in cell-free plasma ('blood-borne' or circulating TF) occurs in two forms: full-length TF (flTF) which contains a transmembrane domain, and alternatively spliced TF (asTF) which lacks a transmembrane domain and can thus be secreted (155)(218). Circulating flTF is associated with blood cells and microparticles, whereas the unique C-terminal domain of asTF enables it to be released in a free form and circulate in the blood of humans and mice. asTF is detectable in a variety of healthy and diseased tissues, including spontaneously formed thrombi, atherosclerotic plaques, and cancer lesions (155)(219)(220).

Total circulating TF is elevated in diabetes mellitus (DM) (221), acute myocardial infarction (222), and pancreatic cancer (223). These diseases not only have elevated levels of TF antigen in the blood but also heightened levels of circulating TF activity, which increases the risk of thrombosis (221)(222)(223). TF is elevated in patients with acute coronary syndrome (ACS), and may be predictive of fatal and nonfatal cardiovascular events in patients with ACS (222)(224). DM plasma was reported to have heightened TF procoagulant activity (225); we note that approximately 80% of patients with DM will die from various forms of thrombosis (226). In contrast to circulating procoagulant flTF, which is elevated in benign disease (221)(222)(223)(224)(225)(226)(227), it is not known whether the same is true regarding

circulating asTF. Recently, asTF was shown to be present in the blood of metastatic breast cancer patients at concentrations exceeding 1 ng/mL (228), and overexpression of asTF by cancer cells promoted primary tumor growth and metastatic spread in an orthotopic model of pancreatic ductal adenocarcinoma (PDAC), the most common form of pancreatic cancer (>70%) (229). asTF acts as a cell agonist driving angiogenesis, cancer cell proliferation, and monocyte recruitment via integrin binding (186)(194)(224)(228)(229).

Non-proteolytic biological activity of asTF notwithstanding, there is currently no consensus as to whether asTF is able to contribute to normal hemostasis and/or thrombogenesis, or whether circulating asTF may serve as a biomarker in patients suffering from cardiovascular disease, diabetes, and/or cancer, including PDAC. The majority of patients with PDAC are unresectable; among the minority of patients initially deemed resectable, vascular invasion, metastatic spread to the peritoneal cavity, liver, lymph nodes and/or other distal sites are common and a substantial subset of patients with PDAC initially considered resectable will be deemed unresectable following exploratory laparotomy. Carbohydrate antigen 19-9 (CA19-9) is the only approved biomarker that appears somewhat helpful as a circulating preoperative indicator of unresectable PDAC (230); however, it has serious limitations in that Lewis-a-negative individuals do not express CA19-9, and it is thus absent in approximately 10% of the general population. Another limitation of CA19-9 is that it is elevated in several benign conditions, including liver cirrhosis, viral hepatitis, pancreatitis, and cholelithiasis.

Currently available assays for measuring circulating 'total TF' antigen and activity have varying sensitivity and specificity (231), and may or may not cross-react with asTF. Recently, we

reported that a newly developed asTF-specific sandwich enzyme-linked immunosorbent assay (ELISA) prototype can detect asTF in the plasma of mice bearing human PDAC tumors (232). Using this innovative ELISA, we have now measured asTF in the plasma of healthy subjects and patients with ongoing ACS, DM, ACS + DM, and PDAC to evaluate the potential of asTF as a PDAC-specific circulating biomarker.

3.3 Methods

3.3.1 Study subjects and sample collection

The study set comprised the following: platelet poor plasma (PPP) from subjects enrolled in the previously described Disposition Impacted by Serial Point of Care Markers in Acute Coronary Syndromes (DISPO-ACS) study (233); PPP from patients who donated their biospecimens to the University of Cincinnati Cancer Institute's Tumor Bank (UCCI-TB); PPP from patients with end-stage PDAC (Diagnostica Stago collection); and a cohort of age/sex-matched healthy individuals custom-ordered from Innovative Research, Inc. All plasma specimens were collected as per the approved protocols in their respective institutions. Power calculations were based on (223) to arrive at the minimum required number of subjects per each subcohort.

The DISPO-ACS group comprised 142 subjects. Specimens were selected to include (i) persons presenting to an emergency room with chest pain but who had no disease diagnosed and a negative troponin test, no history of coronary artery disease, and no history of DM (n = 38); (ii) ACS as determined by positive troponin levels (n = 39); (iii) self-identified DM (n = 40); and (iv)

combined ACS + DM (n = 25); subjects with cancer were excluded. Venous blood was drawn into tubes containing heparin; the presence of heparin does not affect the sensitivity of asTF ELISA (data not shown). Blood samples were centrifuged at 3,000 rpm for 15 min at 4°C; PPP was collected and stored at -80°C until use.

The pancreatic cancer group comprised 39 PPP samples from patients (PDAC: n = 38; pancreatic neuroendocrine tumor [pNET]: n = 1) who underwent treatment at the University of Cincinnati (UCCI-TB cohort), and four cases of end-stage PDAC from the Diagnostica Stago collection. In the UCCI-TB cohort, 25 patients, including the single case of pNET, were confirmed resectable/underwent surgery, and 14 patients were deemed unresectable due to locoregional spread identified during laparoscopic examination. The four PPP samples from the Diagnostic Stago collection were from patients suffering from end-stage PDAC/metastases to distal sites. Resectability was defined as no involvement of superior mesenteric artery, less than 180° involvement of superior mesenteric vein, no involvement of hepatic artery, no involvement of celiac artery, and no locoregional metastases. None of the patients were jaundiced prior to surgery; average tumor volume was 12.01 ± 12.10 cm^3 (smallest specimen: 1.21 cm^3; largest specimen: 56.88 cm^3). Among the 25 patients who underwent tumor resection, lymphatic/vascular involvement was identified in 11 patients; six received neoadjuvant chemotherapy (two gemcitabine, three gemcitabine/ abraxane, one gemcitabine/ cisplatin), and four underwent chemoradiaotherapy prior to surgery. PPP samples from healthy controls were provided by Innovative Research, Inc., and comprised 20 age/sex-matched prescreened subjects. Venous blood was collected in acid citrate dextrose tubes and processed as above.

3.3.2 Enzyme-linked immunosorbent assay (ELISA) and statistical analysis

PPP samples were assayed for asTF using a custom sandwich ELISA as previously described (232). In brief, 96-well plates were coated with an anti-asTF rabbit monoclonal capture antibody and probed with an asTF-specific peroxidase-conjugated detection antibody. In healthy individuals, circulating asTF levels were reported to be ≤100 pg/mL (234). The asTF ELISA sensitivity cutoff was 50 pg/mL; for the purposes of intracohort statistical analyses of prevalence, the threshold was set at 200 pg/mL - near the lowest concentration range at which asTF begins to exert its integrin mediated (patho)biological activity (194).

PPP samples from the UCCI-TB cohort were also assayed for CA19-9 using a commercial ELISA (Calbiotech, catalogue number CA199T). A CA19-9 level of 130 U/mL was treated as the optimal cutoff value useful in non-invasive determination of PDAC resectability (230). Kruskkal-Wallis one-way analysis of variance was used to test for differences; Chi square or Fisher's exact test was used to compare the proportion of PPP samples with the levels of asTF ≥200 pg/mL. Statistical analyses were performed using GraphPad and SigmaPlot 13.0 software packages and p values <0.05 were deemed significant.

3.4 Results

Levels of asTF ≥200 pg/mL were detected in the plasma of 7/38 (18 %) subjects in the DISPO-ACS control cohort, 5/39 (13 %) in the ACS cohort, 2/40 (5 %) in the DM cohort, and 4/25 (16 %) in the ACS + DM cohort. asTF concentrations were non-normally distributed, and

there was no significant difference in the mean asTF concentrations (p = 0.310) and/or the proportion of subjects with plasma asTF levels ≥200 pg/mL between the four DISPO-ACS cohorts (p = 0.272; **Figure 3.1**). The demographics and prior medical history of DISPO-ACS subjects whose asTF levels were ≥200 pg/mL, and those with asTF levels <200 pg/mL, did not differ significantly (**Figure 3.2**).

In the UCCI-TB pancreatic cancer cohort there was a significantly higher proportion of subjects with levels of asTF ≥200 pg/mL compared with age/sex-matched healthy subjects, i.e. 16/39 (41 %) patients with pancreatic cancer versus 3/20 (15 %) healthy subjects (p = 0.037) (**Figure 3.3**). As in the DISPO-ACS cohorts, asTF concentrations were non-normally distributed; following exploratory laparoscopy, 11 of 36 UCCI-TB patients initially deemed resectable were deemed unresectable due to locoregional spread. When the UCCI-TB cohort was split into bona fide resectable (n = 25) and unresectable (n = 14) subcohorts, asTF levels ≥200 pg/mL were significantly more prevalent in the unresectable subcohort irrespective of the results of initial evaluation; unresectable disease was identified in 9 of the 16 patients with asTF ≥200 pg/mL, and in 5 of the 23 patients with asTF levels <200 pg/mL (56 % vs. 22 %; p = 0.006). Diabetes, vein resection, and/or nodal metastases were not significantly more prevalent in the unresectable subcohort (**Figure 3.4**).

Absolute levels of asTF were measured in the PPP of matched healthy subjects (n = 20): resectable (n = 25) and unresectable (n = 14) patients comprising the UCCI-TB cohort, and also patients with end-stage disease (Diagnostica Stago collections, n = 4). As shown in **Figure 3.5**, a trend toward the increase in absolute asTF levels was discernible (resectable vs. unresectable

patients), which reached strong statistical significance when the resectable subcohort was compared with the end-stage disease subcohort.

CA19-9 levels ≥130 U/mL were detected in 12 of the 39 (31 %) PPP samples from the UCCI-TB cohort, of which 7 (58 %) had unresectable disease (**Figure 3.6**). There was no significant correlation between CA19-9 levels and asTF levels (**Figure 3.7**).

3.5 Discussion

In our study, circulating asTF levels ≥200 pg/mL was not significantly associated with ACS and/or DM. The lack of a difference between subjects without ACS and those with ACS and/or ACS + DM likely indicates that asTF is not elevated in the circulation during the acute phase of ACS, yet it remains to be definitively ascertained whether asTF is elevated in the circulation of patients with cardiovascular disease; we note that asTF is found in abundance in lipid-rich atherosclerotic plaques and may increase their destabilization as it is proangiogenic and promotes monocyte recruitment (194).

Circulating asTF levels ≥200 pg/mL were significantly more frequent in patients with pancreatic cancer compared with age- and sex-matched healthy subjects and all other subject groups examined (41 % vs. 5-18 %, respectively), and patients with plasma asTF levels ≥200 pg/mL were significantly less likely to qualify for tumor resection. The current standard in staging PDAC is anatomic imaging, but its accuracy in determining resectability is only 75 %, resulting in approximately 25 % of patients undergoing unnecessary laparotomy (235). Moreover, the 5-year

survival rate following tumor resection is less than 20 % (236) and new biomarkers that help detect more aggressive PDAC phenotypes are thus much needed. Currently, the only approved FDA biomarker is CA19-9, a sialylated Lewis-a antigen produced by exocrine epithelial cells of the digestive tract. CA19-9 may act as a ligand for E-slectin but its precise biological role and contribution to PDAC pathogenesis are not clear. Lewis-a-null individuals do not express CA19-9, and it is thus unusable as a biomarker in approximately 10 % of the population; another limitation is that CA19-9 can be elevated in benign disease (237)(238). While CA19-9 may be a suboptimal general screening tool in PDAC, preoperative CA19-9 levels have shown some promise in determining resectability in PDAC patients; a study designed to determine the optimal preoperative CA19-9 cutoff level associated with tumor unresectability reported that such value is 130 U/mL. Of the 262 pancreatic cancer patients enrolled in that study, 55 % had CA19-9 levels ≥130 U/mL, and 26 % of these were determined to be unresectable (230). Plasma asTF levels ≥200 pg/mL were present in 41 % of the pancreatic cancer patients in the UCCI-TB cohort, and 56% had unresectable disease, indicating that plasma asTF levels ≥200 pg/mL are likely non-inferior to CA19-9 in predicting unresectability. Interestingly, there was no correlation between plasma asTF and CA19-9 and, among the 14 UCCI-TB PDAC patients with unresectable disease, five had asTF ≥200 pg/mL, threee had CA19-9 ≥130 U/mL, and only four had both. We note that none of the resectable patients had asTF ≥200 pg/mL and CA19-9 ≥130 U/mL.

A significant limitation of our study is that the numbers of subjects in all cohorts we examined were small, rendering it difficult to draw definitive conclusions at this time. However, our observations regarding plasma asTF levels in pancreatic cancer patients vis-à-vis their

eligibility for tumor resection are qualitatively novel and will thus serve as an impetus for our group and, hopefully, other investigators to explore asTF's utility in larger cohorts.

3.6 Conclusions

Measuring asTF in plasma may help identify pancreatic cancer patients with more aggressive disease, yet low CA19-9 levels in circulation. Plasma asTF, a protein that, unlike CA19-9, is known to promote PDAC progression (229), may thus comprise a novel biomarker of aggressive disease with a potential utility in non-invasive determination of tumor resectability yet evidently no drawback of being elevated in benign conditions traditionally ascribed to plasma TF. A prospective study to determine whether plasma asTF may also be useful in longer-term patient stratification is currently underway.

3.7 Acknowledgment

The authors are grateful to Dr. Opeolu Adeoye (University of Cincinnati) and the team of DISPO-ACS investigators for making the DISPO-ACS PPP samples available for our study. This work was supported in part by a seed grant from the GIVEHOPE Foundation, Cincinnati, OH, USA.

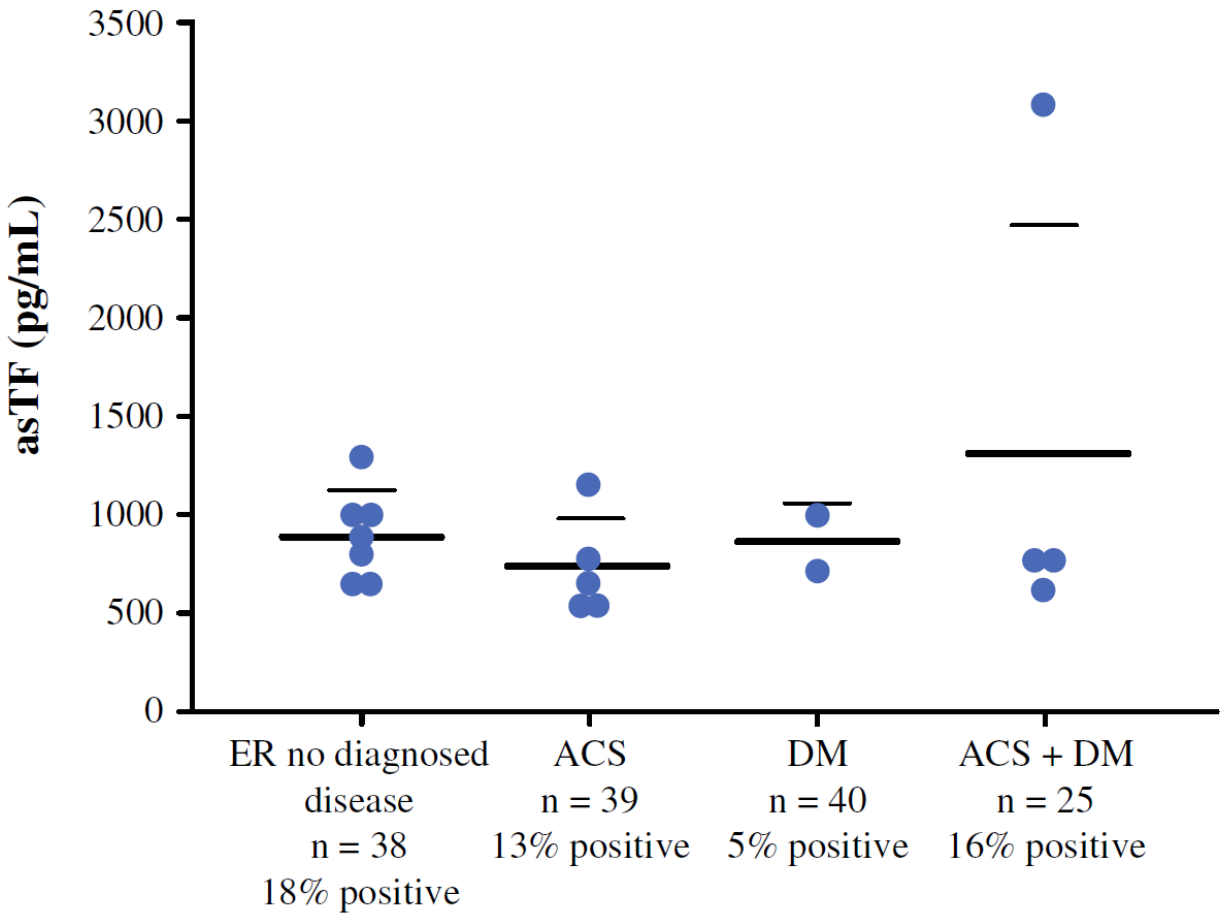

Figure 3.1: Plasma asTF levels, DISPO-ACS study. Dot-plot, circulating asTF (pg/mL). *Thick bars* indicated mean asTF concentrations; *thin bars* indicate SD. *SD* standard deviation, *CAD* coronary artery disease, *MI* myocardial infarction, *asTF* alternatively spliced tissue factor, *DISPO-ACS* Disposition Impacted by Serial Point of Care Markers in Acute Coronary Syndrome, *ACS* acute coronary syndrome, *DM* diabetes mellitus.

	asTF (≥200 pg/mL) N=18	asTF (<200 pg/mL) N=124	P Values
Age – Mean ± SD	66 ± 13	64 ± 15	0.674
Race – N (%)			0.676
Caucasian	4 (22.2)	35 (28.2)	
African American	11 (61.1)	82 (66.1)	
Other	3 (16.7)	7 (5.6)	
Sex – N (%)			0.208
Male	12 (66.7)	63 (50.8)	
Female	6 (33.3)	61 (49.2)	
Past medical history – N (%)			
Family history of CAD	8 (44.4)	53 (42.7)	1.000
Prior MI	6 (33.3)	31 (25.0)	0.565
Hypertension	12 (66.7)	94 (75.8)	0.505
Insulin dependent diabetes	2 (11.1)	20 (16.1)	0.739
Non-insulin dependent diabetes	5 (27.8)	40 (32.3)	0.792

Figure 3.2: Subject demographics, DISPO-ACS study. Demographics and characteristics of the subjects comprising the DISPO-ACS subcohorts. *SD* standard deviation, *CAD* coronary artery disease, *MI* myocardial infarction, *asTF* alternatively spliced tissue factor, *DISPO-ACS* Disposition Impacted by Serial Point of Care Markers in Acute Coronary Syndrome, *ACS* acute coronary syndrome, *DM* diabetes mellitus.

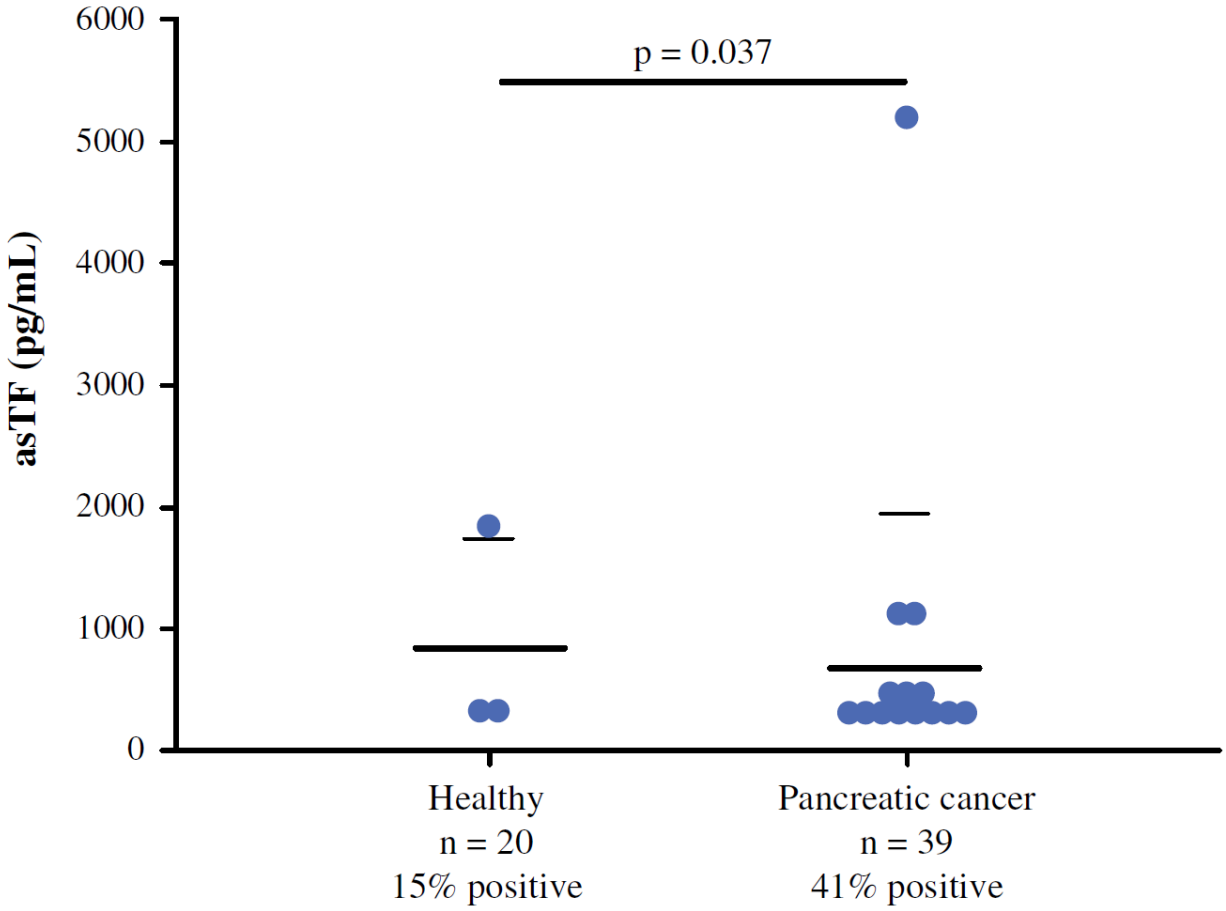

Figure 3.3: Plasma asTF levels, UCCI-TB pancreatic cancer cohort and age/sex-matched healthy subjects. Dot-plot, circulating asTF (pg/mL). *Thick bars* indicate mean asTF concentrations; *thin bars* indicate SD. *SD* standard deviation, *asTF* alternatively spliced tissue factor, *UCCI-TB* University of Cincinnati Cancer Institute's Tumor Bank.

		asTF (≥200 pg/mL)	asTF (<200 pg/mL)	P value
UCCI-TB cohort - N (%)		16 (41.0)	23 (59.0)	
Age - Mean ± SD		60 ± 8.92	64 ± 9.37	0.470
Race - N (%)				1.000
	Caucasian	14 (35.9)	21 (53.8)	
	African-American	2 (5.1)	2 (5.1)	
	Other	0 (0)	0 (0)	
Sex - N (%)				0.023
	Male	12 (30.8)	8 (20.5)	
	Female	4 (10.3)	15 (38.5)	
Diabetes - N (%)				1.000
	Yes	4 (10.3)	12 (30.8)	
	No	7 (17.9)	16 (41.0)	
Portal or mesenteric vein resection - N (%)				1.000
	Yes	1 (4.0)	6 (24.0)	
	No	4 (16.0)	14 (56.0)	
Nodal metastasis - N (%)				0.274
	Yes	7 (28.0)	0 (0)	
	No	13 (52.0)	5 (20.0)	
Resectability - N (%)				0.043
	Yes	7 (16.3)	18 (41.9)	
	No	9 (30.2)	5 (11.6)	

Figure 3.4: Subject demographics, UCCI-TB pancreatic cancer cohort and age/sex-matched healthy subjects. Demographics and characteristics of the subjects comprising the UCCI-TB cohort. *SD* standard deviation, *asTF* alternatively spliced tissue factor, *UCCI-TB* University of Cincinnati Cancer Institute's Tumor Bank.

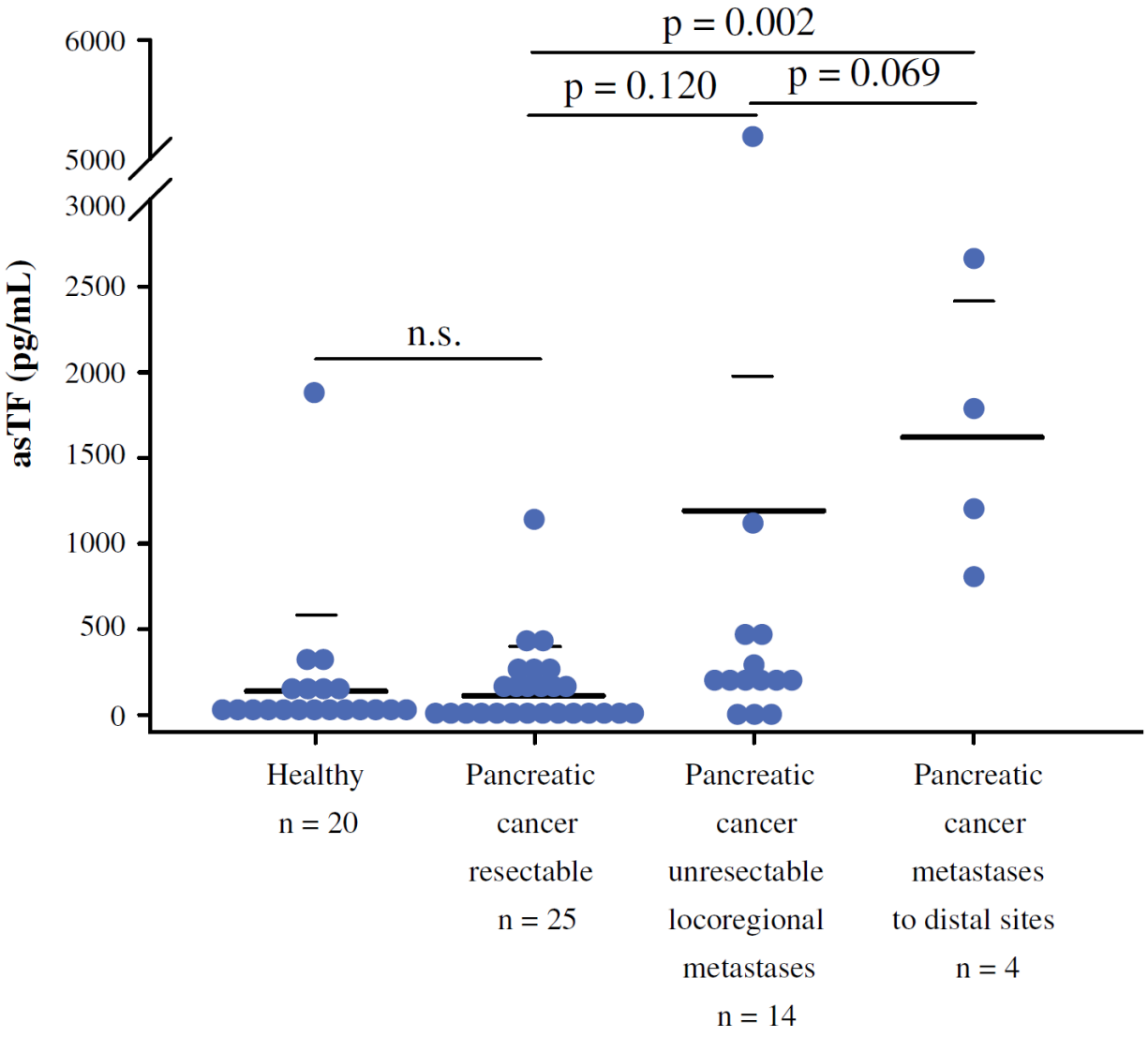

Figure 3.5: Absolute levels of asTF in PPP of age/sex-matched healthy subjects, patients who underwent tumor resection, patients deemed unresectable and patients with end-stage disease. *Thick bars* indicate mean asTF concentrations; *thin bars* indicated SD. *asTF* alternatively spliced tissue factor, *SD* standard deviation, PPP platelet-poor plasma, *n.s.* not significant.

	CA19-9 (≥130 U/mL)	CA19-9 (<130 U/mL)	P value
UCCI-TB cohort - N (%)	12 (30.8)	27 (69.2)	
Age - Mean ± SD	61.18 ± 7.04	62.36 ± 10.14	0.7270
Race - N (%)			1.0000
Caucasian	11 (28.2)	24 (61.5)	
African-American	1 (2.6)	3 (7.7)	
Other	0 (0)	0 (0)	
Sex - N (%)			0.4801
Male	8 (20.5)	12 (30.7)	
Female	4 (10.3)	15 (38.4)	
Resectability - N (%)			0.0331
Yes	5 (12.8)	20 (51.3)	
No	7 (17.9)	7 (17.9)	

Figure 3.6: Plasma CA19-9 levels and subject demographics, UCCI-TB cohort. Subject demographics and characteristics. *CA19-9* carbohydrate antigen 19-9, *UCCI-TB* University of Cincinnati Cancer Institute's Tumor Bank, *asTF* alternatively spliced tissue factor.

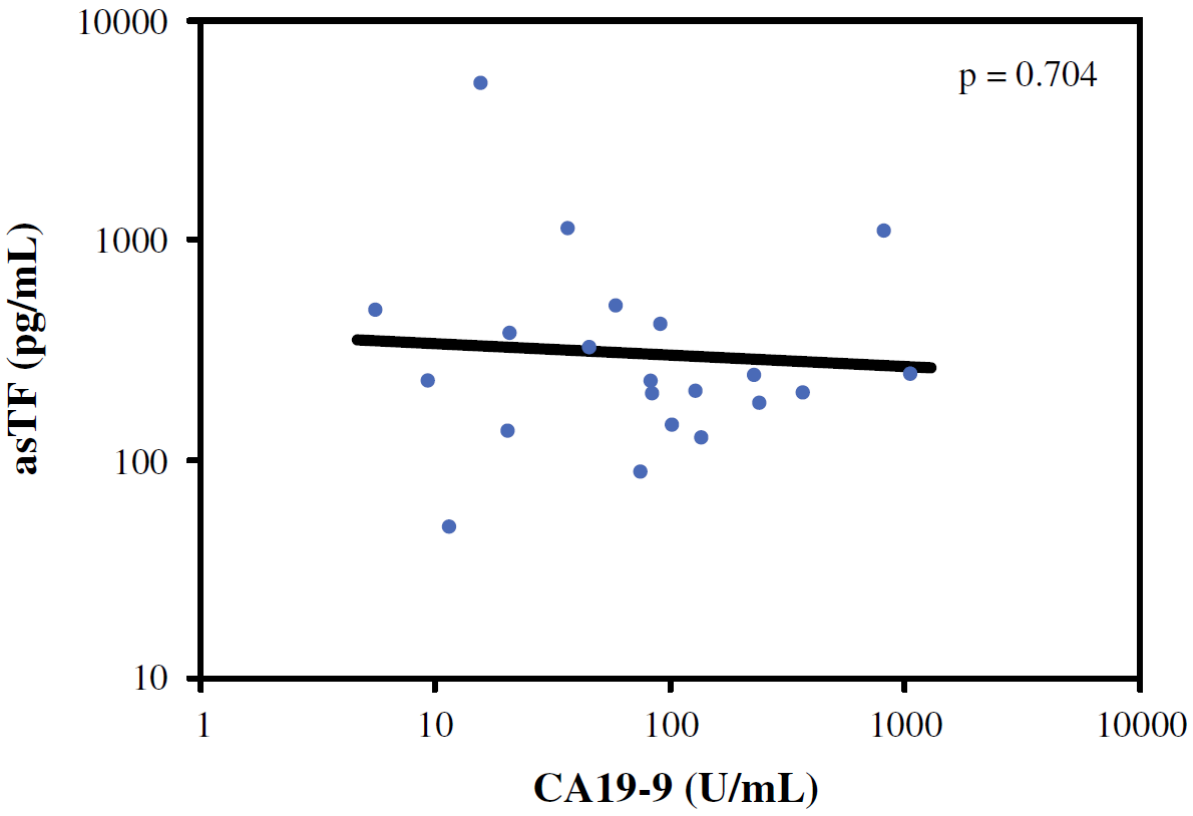

Figure 3.7: Plasma CA19-9 levels and subject demographics, UCCI-TB cohort. Correlation analysis, circulating asTF and CA19-9 levels. *CA19-9* carbohydrate antigen 19-9, *UCCI-TB* University of Cincinnati Cancer Institute's Tumor Bank, *asTF* alternatively spliced tissue factor.

Chapter 4: Antibody-based targeting of alternatively spliced tissue factor: a new approach to impede the primary growth and aggressiveness of pancreatic ductal adenocarcinoma

Cancer therapy is like beating the dog with a stick to get rid of his fleas.

– Anna Deavere Smith
Let Me Down Easy

Antibody-based targeting of alternatively spliced tissue factor: a new approach to impede the primary growth and aggressiveness of pancreatic ductal adenocarcinoma

Dusten Unruh[1], Betül Ünlu[2], Xiaoyang Qi[1], Zhengtao Chu[1], Robert Sturm[1], Ryan Keil[1], Syed A Ahmad[1], Timofey Sovershaev[3], Mariette Adam[4], Patrick Van Dreden[4], Barry J Woodhams[5], Divya Ramchandani[6], Georg F Weber[6], Janusz W Rak[7], Nigel Mackman[8], Henri H Versteeg[2], Vladimir Y Bogdanov[1]

[1] College of Medicine, University of Cincinnati, OH, USA; [2]Leiden University Medical Center, Leiden, The Netherlands; [3]The Arctic University of Norway, TromsØ, Norway; [4]Diagnostica Stago R&D, Gennevilliers, France; [5]Haemacon Ltd, Bromley, UK; [6]College of Pharmacy, University of Cincinnati, OH, USA; [7]McGill University Health Centre, Montreal Children's Hospital, Montreal, Canada; [8]University of North Carolina at Chapel Hill, NC, USA

Oncotarget (in minor revision)

4.1 Abstract

Alternatively spliced Tissue Factor (asTF) is a secreted form of Tissue Factor (TF) that is expressed in several forms of solid cancer, including pancreatic ductal adenocarcinoma (PDAC). asTF binds to β1 integrins on PDAC cells, whereby it promotes tumor growth, metastatic spread, and monocyte recruitment to the stroma. We determined the effect of antibody-based targeting of asTF in PDAC would significantly impact tumor progression. We here report that asTF-β1 integrin interactions, when disrupted by the anti-asTF monoclonal antibody that we recently developed and characterized, curtail experimental PDAC progression. Moreover, we show that tumor-derived asTF is able to promote PDAC primary growth and spread during earlier as well as later stages of the disease. In addition, we show that TF expressed by host cells plays a significant role in PDAC spread. Together, our data demonstrate that targeting asTF in PDAC is a novel strategy to stem PDAC progression and spread.

4.2 Background

Pancreatic ductal adenocarcinoma (PDAC) survival rate remains dismal, with 5-year survival <5%, and by 2020 is predicted to be the third leading cause of cancer-related death (239). Pancreatic cancer is commonly associated with thrombotic events, which contribute to its morbidity and mortality (240)(241). Cancer coagulopathy is thought to be partially due to the up-regulation of Tissue Factor (TF), the primary initiator of blood clotting (162)(242). Multiple oncogenic events that are characteristic of PDAC, e.g. activation of the proto-oncogene K-RAS and inactivation/loss of p53 and PTEN, promote TF expression (168). Recently, we reported that TF's secreted isoform termed alternatively spliced TF (asTF) is expressed in early-stage PDAC

lesions (pancreatic intraepithelial neoplasia, PanIN) and abundant in advanced PDAC, in contrast to normal pancreas (229). Our groups recently demonstrated that asTF acts on cancer cells in an auto/paracrine manner via β1 integrins, promoting disease progression by fueling cancer cell proliferation, survival, metastatic spread, neovascularization, and monocyte accumulation to the tumor stroma (228)(229).

Unlike the much-studied major form of TF termed full-length TF (flTF), asTF is minimally coagulant, and triggers cellular signals through non-proteolytic mechanisms by binding to α6β1 and αvβ3 integrins, and thereby activating PI3K/Akt, MAPK, and FAK signaling pathways (186). Integrin subunits α6 and β1 are up-regulated in PDAC, and play a crucial role in promoting PDAC aggressiveness (243). We reported that asTF-β1 integrin interaction on endothelial cells increases the expression of cell adhesion molecules VCAM-1, ICAM-1, and E-selectin, which facilitates monocyte recruitment (194). Levels of asTF positively correlate with the number of tumor associated monocytes/macrophages (TAMs), which are known to significantly contribute to tumor progression and resistance to chemotherapy (228)(229)(244). Tumor cell-derived asTF fuels PDAC primary growth and spread via upregulation of various signaling pathways (229); however, it is not known whether host-derived TF plays a discernible role in PDAC progression. In addition, it is not known whether tumor cell- and/or host-derived asTF can be targeted with a monoclonal antibody to stem PDAC tumor progression.

In this study, we sought to i) examine the novel asTF-integrin nexus as a potential therapeutic target in PDAC, including the activity of the novel asTF-specific neutralizing antibody RabMab1 ii) delineate the mechanisms underlying asTF-induced PDAC progression; and iii)

elucidate the relative significance of host-derived TF in PDAC. We employed a doxycycline (Dox)-inducible asTF transgene system to rule out the possibility of cell line and/or clonal selection variability influencing experimental outcomes. Using this approach, we investigated whether delayed-onset upregulation of asTF yields a phenotype that is distinct from that obtained via constitutive overexpression. The effectiveness of antibody-based targeting of asTF in PDAC was assessed using an orthotopic mouse model.

4.3 Materials and methods

4.3.1 Cell lines

Human PDAC cell line Pt45.P1 is classified as grade III, harbors K-RAS / p53 / p16 mutations, and has been extensively characterized (201) / authenticated by short tandem repeat analysis (ATCC). A modified cell line termed Pt45.P1/asTFi was generated by permanently co-transfecting Pt45.P1 cells with i) linearized pTet-On Advanced vector, and ii) pTRE-Tight vector (both from Clontech) with a human asTF expression cassette cloned into the plasmid's multiple cloning site. Fugene HD (Roche) was used to transfect the constructs; cells were maintained in G418 and seven G418-resistant clones were harvested, expanded, and the consistency of the levels of doxycycline (Dox)-inducible asTF mRNA/protein overexpression was verified before the clones were pooled (data not shown). All cell lines were grown in DMEM (Cellgro) supplemented with 10% fetal bovine serum (HyClone), 100 IU/mL penicillin, 100 µg/mL streptomycin, and 0.25 µg/mL amphotericin at 37°C in a humidified incubator (5% CO_2).

4.3.2 *In vivo* studies

All animal studies were done in compliance with the protocol approved by the Institutional Animal Care and Utilization Committee, University of Cincinnati. Pt45.P1/asTFi cells were orthotopically transplanted in the pancreases of 5-week-old female nude athymic mice, (n=5/cohort) (Harland Laboratories). Mice were subdivided into three cohorts: 1) animals that began receiving Dox (2 μg/mL in water/sucrose) on day 1 of the study ("Dox"), 2) day 25 of the study ("Late Dox"), and 3) sucrose water alone ("No Dox") for 5 weeks. Pt45.P1 cells were also orthotopically implanted into mice rescued from embryonic lethality caused by murine TF (*Cf3*) deficiency with a human TF (hTF) mini-gene: rescued mice ($mTF^{-/-}$,$hTF^{+/-}$, hereafter TF-Low) express only ~1% of TF levels compared to 50% expressed by their heterozygous counterparts ($mTF^{+/-}$/$hTF^{+/-}$, hereafter TF-Het) and were backcrossed into severe combined immunodeficiency (SCID) background (n=6/cohort) (245)(246).

In vivo efficacy studies of Rb1 were carried out as follows. Pt45.P1 cells were resuspended in PBS containing 100μg of Rb1 or rabbit IgG isotype control, and implanted in the pancreases of nude athymic / TF-Low/Het mice. Tumor progression was monitored via SapC-DOPS imaging over 7 weeks or when otherwise specified as previously described (n=8/cohort) (202). In brief, a multispectral imaging system FX (Kodak) was used to visualize tumor growth and spread employing Cell-Vue Maroon (CVM)-labeled, nanovesicle-coupled Saponin C protein fragment H2 (CVM-SapC[H2]-DOPS) injected via tail vein; this compound selectively binds to tumor cells as well as tumor vasculature enriched in externalized phosphatidylserine (202). Quantification of tumor spread was analyzed with Carestream MI software, background fluorescence normalized to sham-operated mice, and fluorescence was converted to photons per second per mm^2. At the end

of the study animals were sacrificed, necropsy was performed, and tumors were harvested and processed for protein, RNA, and histology (FFPE) analysis.

4.3.3 Quantitative RT-PCR

Total RNA was isolated from cells / tissue flash-frozen in LN_2 using the RNeasy kit (Qiagen) as per the manufacturer's instructions; cDNA was synthesized using Transcriptor (Roche). Quantitative RT-PCR was performed using our validated TaqMan probe and primer sets for asTF and flTF (229); GAPDH was used as a housekeeping gene.

4.3.4 Western blotting

Cells were trypsinized, washed with PBS, and pelleted. Cell pellets were resuspended in PBS supplemented with Protease Inhibitor I cocktail (Roche) and lysed in Laemmli buffer with 2-Mercaptoethanol. Samples were denatured at 95°C for 10 min, loaded on 12% polyacrylamide gels (Life Technologies) and transferred to PVDF membranes. Membranes were blocked overnight at 4°C and probed with primary and corresponding HRP-conjugated secondary (Invitrogen) antibodies. Blots were developed using LumiLight (Roche), and chemiluminescent bands were visualized with X-ray film. Anti-pAkt T308 antibody (clone D25E6, Cat. No. 13038), anti-pAkt S473 (Cat. No. 9271), anti-total Akt (Cat. No. 9272), anti-total MAPK (Cat. No. 9102), and anti-pMAPK p42/44 (Cat. No. 9101) were from Cell Signaling.

4.3.5 Migration studies

Gap closure/scratch assay was performed in triplicates by seeding 12-well plates with Pt45.P1/asTFi cells at $1x10^5$/well. Doxycyclin at a concentration of 2 µg/mL was added to induce asTF a day before the scratch was made and the expression levels of asTF were checked by Western blot in the presence and absence of dox. After cells adhered and reached confluence, the wells of the plate were scratched at the center using a P200 pipet tip. The generated gaps were analyzed for closure at 0, 18, 24, 48 hours. The results were quantified using Image J software (NIH) by measuring the area (in pixels) that remained unoccupied at each time point. The area at 0 hours was set to 100%.

Transmigration assay was carried out using 24-well plates / inserts with 8.0 µm diameter pores (BD Bioscience) pre-coated with 50 µg/mL laminin (Sigma-Aldrich Cat# L4544) in Hank's Balanced Salt Solution (HBSS; Cellgro) for 1.5 hrs. Excess laminin was removed from the inserts, following which $7.5x10^4$ Pt45.P1/asTFi cells were pre-incubated with anti-asTF antibody Rb1, anti-integrin β1 (R&D Systems), anti-integrin α6 (R&D Systems) or isotype control antibodies (Jackson ImmunoResearch) for 30 min, added to the inserts, and allowed to migrate for 5 hrs at 37°C, 5% CO_2 toward serum placed in the lower chamber. Afterwards the inserts were fixed in ice-cold methanol, and non-migrated Pt45.P1/asTFi cells were removed from the luminal side with a cotton swab. Inserts were excised, stained, and preserved with Vectashield / DAPI (Vector Labs). Images were captured on fluorescent microscope Keyence BZ-9000 (BIOREVO) at 20x; 6 representative fields per insert (n=3 inserts per each condition) were captured and results were analyzed using Image J.

4.3.6 ELISA

Platelet-poor murine plasma derived from whole arterial blood was assayed for asTF protein levels using our custom sandwich ELISA as described (232); in brief, samples were placed in 96-well capture plates and incubated for 3 hours at RT. Wells were washed and probed with asTF-specific detection antibody (Rb1) conjugated to HRP for 2 hours at RT. TMB substrate was then added and plate was incubated in the dark for 60 minutes; reaction was stopped with sulfuric acid and the plate was read at 405 nm. Serial dilutions of recombinant asTF in mouse plasma were used as standards in each run.

4.3.7 Tissue harvesting and histological analyses

Harvested tumor specimens were fixed in formalin overnight prior to paraffin embedding. Paraffin embedded tumors were sectioned (4 μm), baked for 1 hour at 63°C, and rehydrated. Sections were placed in Antigen Retrieval Citra Solution (BioGenex) for 20 minutes in a pre-heated steamer at 95°C; afterwards, slides were allowed to cool and rinsed in wash buffer (Dako). Slides were blocked for 12 min with a blocking cocktail, washed, and incubated with the primary antibodies: rabbit polyclonal anti-CD31 (Abcam); rabbit polyclonal anti-CD206 (abcam); monoclonal anti-β1 (R&D systems); monoclonal anti-α6 (R&D systems) were applied for 3 hours, slides washed and incubated with appropriate secondary antibodies for 30 minutes and Vectashield / DAPI. Images were captured using BZ-9000 BIOREVO (Keyence) and analyzed using BZ-II analyzer and Image-J software.

4.3.8 Statistics

Mean values were compared using Student's *t*-test between two groups, and for multiple group comparisons one-way ANOVA was used; $p<0.05$ was considered significant. All statistical analyses were performed using SigmaPlot v12.5. Data are represented as the mean ± standard deviation.

4.4 Results

4.4.1 asTF-integrin interactions promote PDAC cell migration

We recently reported that constitutive asTF overexpression in Pt45.P1 cells promotes metastatic spread *in vivo* (229); here we sought to investigate the mechanisms responsible and specifically whether asTF increases cell motility. We examined the expression levels of asTF in Pt45.P1/asTFi cells; when treated with Dox, Pt45.P1/asTFi cells had significantly higher levels of asTF mRNA and protein, while flTF mRNA and protein levels remained unchanged ($p<0.001$) (**Figure 4.1A & B**). Scratch assay was then performed; Dox-treated Pt45.P1/asTFi cells had completed gap closure by 24 hours, whereas Dox-untreated cells still had unoccupied area at 48 hours (**Figure 4.1C**). asTF-integrin α6/β1 interactions are known to promote cancer cell proliferation (228). To verify this enhanced scratch closure activity was due to cell migration and not cell proliferation, we performed a short-term cell migration analysis towards a serum chemo-gradient using laminin-coated transmembrane inserts and Pt45.P1/asTFi cells. Laminin is abundantly expressed in PDAC stroma and is known to bind α6β1 integrins (247). As in the scratch assay, Dox-treated cells exhibited a significantly higher migration rate compared to Dox-

untreated cells. Notably, when Dox-untreated Pt45.P1/asTFi cells were pre-incubated with the inhibitory anti-asTF antibody RabMab1, the basal rate of their migration was significantly reduced (**Figure 4.1D**), indicating that even the relatively low basal levels of asTF constitutively expressed in Pt45.P1/asTFi cells significantly contribute to their migratory potential. Pre-incubating Pt45.P1/asTFi Dox+ with anti-α6 inhibitory antibody yielded a partial reduction of cell migration, whereas pre-incubation with anti-β1 or anti-β1/anti-α6 fully inhibited cell migration (**Figure 4.1D**). Thus, expression of asTF in PDAC cells enables integrin mediated onset of cellular motility, a hallmark of progression and metastasis.

4.4.2 asTF promotes primary tumor growth and spread in vivo at early and later stages of tumor development

To examine the temporal effect of asTF overexpression on tumor dynamics *in vivo*, we orthotopically implanted $1x10^6$ Pt45.P1/asTFi cells into the pancreases of nude mice (n=5/group) and allowed tumors to develop over a period of 5 weeks. Mice received Dox (2μg/mL) in sucrose drinking water at day 1 ("Dox"), day 25 ("Late Dox"), or sucrose alone ("No Dox"), and tumor progression was monitored periodically *in vivo* using CVM-SapC[H2]-DOPS imaging (**Figure 4.2A**). At the end of the experiment, tumor growth was observed in all mice except one animal in the "Late-Dox" cohort. No appreciable distal metastases was observed in the "No Dox" cohort compared to the other two cohorts; the macroscopic spread outside primary tumor was significantly reduced in "Late Dox" mice compared to "Dox" mice ($p = 0.010$), yet it was in-trend higher in "Late Dox" mice compared to "No Dox" mice ($p = 0.082$) (**Figure 4.2A & H**). Mice were then euthanized and primary tumors resected and examined for weight and volume. "Dox"

tumors were significantly larger in both weight and volume compared to “Late Dox” and “No Dox” tumors (**Figure 4.2B & C**). These observations indicate that asTF expression can promote PDAC progression during early as well as late stages of the disease, resulting in larger tumors and increased spread.

4.4.3 asTF levels are associated with changes in tumor stromal composition

Next, we compared the histology of “No Dox”, “Late Dox”, and “Dox” Pt45.P1/asTFi tumors for vessel density (CD31) and the levels of stromal M2-polarized tumor associated macrophages (TAMs) (CD206). Both "Late Dox" and "Dox" tumors had significantly increased vessel density when compared to "No Dox", yet vessel density of “Late Dox” tumors was comparable to that of “Dox” mice; which suggests that PDAC vasculature plateaus relatively early during tumor development (**Figure 4.2D**). In addition to "No Dox" tumors having decreased vessels, they also had significantly fewer TAMs, as did “Late Dox” when compared to "Dox" tumors (**Figure 4.2E**).Consistent with our *in vitro* asTF expression levels, histological evaluation of asTF showed a relative increase in "Dox" vs "No Dox" tumors, and appeared to co-localize with β1-integrin (**Figure 4.2F**). Remarkably, asTF protein was present in circulation of mice in “Late Dox” as well as “Dox” cohorts at levels exceeding 1ng/mL (**Figure 4.2G**). Lastly, we analyzed the tumors for the levels of collagen deposition (Masson’s trichrome): “Late Dox” and “Dox” tumors had comparable collagen deposition, which was significantly higher compared to that in “No Dox” tumors ($p=0.043$) (**Figure 4.2I & J**). These observations suggest that asTF has a

multifaceted role in tumor stroma remodeling, whereby it increases TAMs, vessel density and collagen deposition.

4.4.4 Targeting asTF with RabMab1 impedes tumor progression

To assess whether treatment with RabMab1 can stem the growth of PDAC cells in the orthotopic setting as we found to be the case for breast cancer cells (228), we co-implanted Pt45.P1 cells with asTF inhibitory antibody RabMab1 or isotype control IgG using the same cell number and RabMab1 quantity that we previously employed in our breast cancer studies, i.e. 100µg/6x10^5 cells, and tumor growth was monitored periodically using CVM-SapC[H2]-DOPS *in vivo* imaging over 7 weeks (n=8/cohort) (**Figure 4.3A**). Tumors co-implanted with RabMab1 had a lower take compared to other cohorts (RabMab1: 4/8; IgG: 6/8; PBS: 7/8). Like PT45.P1/asTFi cells grown in mice not receiving Dox, Pt45.P1 cells did not exhibit significant spread even when grown for 7 weeks; however, when co-implanted with RabMab1, they produced significantly smaller tumors ($p<0.001$) (**Figure 4.3B & C**). RabMab1-treated tumors were also less vascularized and had ~3.5 fold fewer stromal macrophages compared to the cells co-implanted with vehicle (PBS) and/or isotype control IgG ($p=0.009$) (**Figure 4.3D & E**). Mice in the Pt45.P1/RabMab1 cohort had ~2 fold decrease in the levels of circulating asTF compared to mice in the Pt45.P1/PBS and/or isotype IgG cohorts (0.27ng/mL vs 0.60/0.54 ng/mL; $p<0.001$). Thus, antibody-based targeting of asTF may comprise a novel therapeutic strategy to stem PDAC progression.

4.4.5 Host-TF contributes to PDAC progression

We next sought to evaluate the contribution of host TF to PDAC growth and spread in our model using TF-Het (control) and TF-Low SCID mice. In light of our findings in nude mice pointing to a limited spread of Pt45.P1 cells in the setting of $1x10^6$ cells grown for 5 weeks (**Figure 4.2**) and/or $6x10^5$ cells grown for 7 weeks (**Figure 4.3**), we sought to augment the cells' ability to spread in this experiment and thus orthotopically implanted $1x10^6$ Pt45.P1 cells into TF-Low/Het mice and monitored tumor growth *in vivo* over 7 weeks. In agreement with prior studies pointing to SCID mice as a better platform to study the metastatic capacity of human tumor cells compared to nude mice (247), we observed significant systemic spread of Pt45.P1 cells in TF-Het mice (**Figure 4.4A & D**), and the fraction of mice with lung metastasis was higher in TF-Het mice than in TF-Low mice (4/6 vs 1/6) (**Figure 4.6A & B**) Pt45.P1 tumors grown in TF-Low/Het mice were comparable in weight and volume (**Figure 4.4B & 4C**); however, tumor spread was significantly diminished in TF-Low mice (p=0.007) (**Figure 4.4A & 4D**). Tumors in TF-Low mice also had lower vessel density (p=0.033) and had fewer M2 polarized TAMs (p=0.011) (**Figure 4.4E & F**). Notably, TF-Low tumors had decreased collagen deposition compared to TF-Het tumors (p=0.018) (**Figure 4.4G & H**). These TF-Low mice indicate that host-derived TF contributes to tumor spread and stromal remodeling.

4.4.6 RabMab1 suppresses tumor growth equally in TF-Het and TF-Low mice

To compare the relative contribution of tumor-derived asTF and host TF to tumor progression in our model, we analyzed Pt45.P1 tumor growth in TF-Low/Het mice treated with RabMab1 and isotype control IgG. In the presence of RabMab1, Pt45.P1 cells implanted in TF-

Low as well as TF-Het mice grew tumors that were significantly smaller compared to IgG control. We previously reported that constitutive overexpression of asTF in PT45.P1 cells induces MAPK and Akt phosphorylation (229); in this study, the MAPK p42/44 phosphorylation was unaffected by RabMab1 treatment (data not shown), yet a significant decrease in pAKT-T308 was observed ($p=0.002$), while the levels of pAKT-S473 were unaffected (**Figure 4.5C**). (**Figure 4.5A & B**) Moreover, RabMab1 reduced tumor vascularization and quantity of TAMs equally well in TF-Het and TF-Low mice (Fig 5C, 5D). Thus, RabMab1 works equally well in stemming PDAC tumor growth in SCID mice, which is in agreement with our findings in nude mice.

4.5 Discussion

In this study, we report the following set of novel findings: i) asTF-β1 integrin interactions render PDAC cells significantly more motile; ii) asTF is able to promote PDAC progression during early and late stages; iii) RabMab1-mediated targeting of asTF inhibits basal as well as asTF-potentiated migration of PDAC cells; iv) host-TF contributes to PDAC spread and influences the stromal composition of primary PDAC tumors; v) tumor-derived asTF is a more significant contributor to PDAC progression compared to host-TF.

Progress in treating patients suffering from PDAC has remained relatively stagnant since the approval of gemcitabine in 1996. Over the last several years, different formulations and combinations of cytotoxic agents have improved the median survival rate by 4.4 months over gemcitabine monotherapy (127). Despite these advances there remains a severe need for new therapeutic modalities that can target host immunity, stromal microenvironment, and cancer cell

signal transduction pathways (127). Our groups recently reported the potential for asTF to be a promising target in breast cancer (228); in this study, we show for the first time that inhibition of asTF-integrin interactions holds much promise in stemming PDAC progression. asTF promotes migration of PDAC cells; we posit that asTF-β1 interactions may render PDAC cells more motile via asTF competing with laminin for β1 integrin binding as well as promoting outside-in integrin signaling. It is also possible that, as we recently described in the breast cancer setting, asTF modulates binding and/or migration on laminin, similarly to how flTF modulates migration on laminin (228); an even more intriguing scenario might be envisioned whereby asTF competitively blocks flTF-dependent inhibition of β1 integrins on laminin. Our asTF-specific inhibitory monoclonal antibody RabMab1 inhibits basal and asTF-potentiated PDAC cell migration. Here we show that, in addition to promoting tumor cell migration, asTF alters the tumor microenvironment by increasing the number of TAMs, vessel density, and collagen deposition. In the presence of RabMab1, Pt45.P1 cells grew significantly smaller tumors with fewer TAMs, blood vessels, and reduced collagen content; future studies will investigate whether systemic and continuous administration of RabMab1, as opposed to cancer cell co-implantation, will have a major impact on PDAC progression: given the hypovascular, scar-like structure of desmoplastic PDAC tumors, antibody penetration of solid tumors remains a concern. Currently, we are defining the protein domain(s) of human asTF critical to its binding to β1 integrins in hope that molecular mapping of asTF-β1 integrin interactions will aid in the development of short inhibitory peptides as well as small-molecule compounds which may have superior capacity in PDAC tissue penetrance.

There is considerable interest in therapeutic targets that can attenuate aberrant signaling transduction pathways in PDAC. The PI3K/Akt pathway mediates a variety of cellular processes,

such as cell proliferation, survival, and motility (248). The PI3K/Akt pathway is activated in PDAC and is implicated in promoting resistance to apoptosis-inducing chemotherapies, and targeting the PI3K/Akt pathway can overcome resistance to chemotherapy (249). Our earlier studies showed that asTF-integrin interactions promote AKT phosphorylation (229)(186). In our *in vivo* study of RabMab1, we observe an inhibition of the phosphorylation of Akt at T308, which suggests that a reduction in tumor growth and spread may be in part due to the suppression of the Akt-dependent pro-survival pathways. Interestingly, we did not observe a change in the levels of pAkt-S473 post-treatment with RabMab1; the relative abundance of pAkt-S473 and pAkt-T308 is known to differ between various PDAC cell lines (250) yet no definitive information is available as to the relative importance of either site in PDAC pathobiology. Still, a recent study examining the pAkt-S473 / pAkt-T308 status demonstrated that compared to pAkt-S473, higher phosphorylation of pAkt-T308 as a more reliable biomarker for smoking and alcohol induced progression of head-and-neck small cell carcinoma (251); we note that smoking and excessive alcohol consumption are the two well-established risk factors for PDAC (127).

Therapies targeting macrophage recruitment, polarization and activation may also prove effective therapeutic strategies based on numerous *in vivo* data and preclinical findings (252). For multiple malignancies, high densities of TAMs are associated with poor clinical outcomes (253). M2-polarized TAMs, identified by mannose receptor CD206 (254)(255), but not CD68 correlate with negative outcome (256). In addition to being a more selective TAM marker, CD206 is associated with immunosuppression and release a variety of tumor-promoting growth factors that correlate with poor patient prognosis (256)(257). Here, we show that RabMab1 treatment reduces $CD206^+$ TAMs in our orthotopic PDAC mouse model and decreases metastasis. The amelioration

of metastasis may in part be indirectly related to a decrease in TAMs. Studies have demonstrated that M2 TAMs can promote epithelial-mesenchymal transition (254), and other *in vivo* tumor mouse models that deplete monocyte/macrophages exhibit diminished metastasis (252). Tumor cell TF-induced coagulation, which results in fibrin formation, may promote premetastatic niches by making distal sites more receptive to growth through the recruitment of $CD11b^+$ monocyte/macrophages (258). CD11b macrophage recruitment is mediated through the binding of CD11b to clot components and activated endothelium (259); we previously show that asTF-integrin interactions on microvascular endothelial cells can mediate macrophage accumulation independent of coagulation (194). It remains to be determined to what extent asTF directly influences metastasis and how much is influenced through indirect TAM mediated metastasis.

PDAC is characterized by extensive desmoplasia and much of the tumor mass is thus comprised of (extra)cellular components other than cancer cells, some of which may serve as a "host source" of TF in the tumor microenvironment. Currently, the relative contribution of host vs tumor-derived TF to PDAC progression is unknown. In our study, severe depletion of host TF had no significant impact on primary tumor weight and/or volume; however, we did observe a significant decrease in vessel density and TAMs in the tumors grown in TF-Low SCID mice and most strikingly, the spread was also dampened in TF-Low mice. Still, inhibition of tumor derived asTF had a much more significant effect on PDAC progression compared to low levels of non-tumor cell derived TF. Our data suggests that asTF may act as an important regulator of the inflammatory microenvironment known to play essential role in K-RAS driven progression of PDAC (260). In our hands K-RAS expressing PDAC cells exhibit low levels of TF but cooperate with exogenous asTF and host TF in formation of proinflammatory, prometastatic and collagen-

rich (desmoplastic) milieu. It is possible that in addition to cancer cells themselves, inflammatory cells and blood vessels (186), asTF also regulates the activity of pancreatic stellate cells implicated in PDAC-related fibrosis (261), a subject of interest for our future explorations. Since fibrosis and inflammation are regarded as elements of therapeutic intractability and resistance of PDAC to cytotoxic and targeted therapies (262), our results with the RabMab1 antibody suggests that this agent could act as therapeutic sensitizer in these various contexts, and possibly as a function of asTF detected in the circulation.

Aside from improving PDAC therapy per se, it is increasingly critical to identify reliable circulating biomarkers that can non-invasively determine the feasibility of surgical intervention (e.g. resectable/unresectable disease), or aid in patient stratification for clinical trials and/or therapeutic regimens. Multiple studies show that increased levels of circulating TF are associated with an increased risk for thrombosis in patients with cancer (263). However, it remains to be determined whether circulating "total TF" is an adequate cancer biomarker with an overall prognostic utility. Similar to other malignancies, PDAC exhibits aberrant pre-mRNA processing, which is likely to influence the relative expression of flTF and asTF. Splicing regulatory (SR) proteins ASF/SF2 and SRp55 are essential for biosynthesis of flTF whereas SR proteins SC35 and SRp40 promotes asTF biosynthesis in human monocytic cells (199)(264). Increased expression of various SR proteins has been implicated in the progression of tumors of the breast (265), lung (266), colon (267), and ovaries (268). Thus, it is reasonable to propose that aberrant pre-mRNA processing in cancer cells, including PDAC, is likely to perturb the splicing of TF pre-mRNA thereby increasing the levels of asTF. Using our newly developed asTF-specific ELISA, we show here that asTF is detectable at high levels in the circulation of mice bearing orthotopic PDAC

tumors. Importantly, RabMab1 was able to significantly reduce circulating levels of asTF to ~200 pg/ml: recently, we reported that pre-operative circulating levels of asTF ≥200 pg/ml can help identify PDAC patients with a more aggressive disease (269). We are currently conducting a prospective study to determine whether circulating asTF may also help in identifying recurrence in PDAC.

In sum, our findings show asTF-β1 integrin play a major role in pathobiology of PDAC, and that antibody-based targeting of asTF may comprise a novel strategy to stem PDAC progression. Because asTF is i) dispensable to normal blood clotting, ii) expressed at higher levels in malignant tissues, and iii) able to promote tumor progression, it may very well comprise the preferred isoform to target in a cancer setting.

4.6 Acknowledgments

The authors are grateful to Fred Lucas, MD, and Meggan Peak, MD, PhD, for their helpful suggestions concerning histological evaluation of tissue specimens. This works was supported in part by NIH/NCI grants R21 CA160293 and R01CA190717 to V.Y.B and NWO VIDI grant 91710329 to H.H.V.

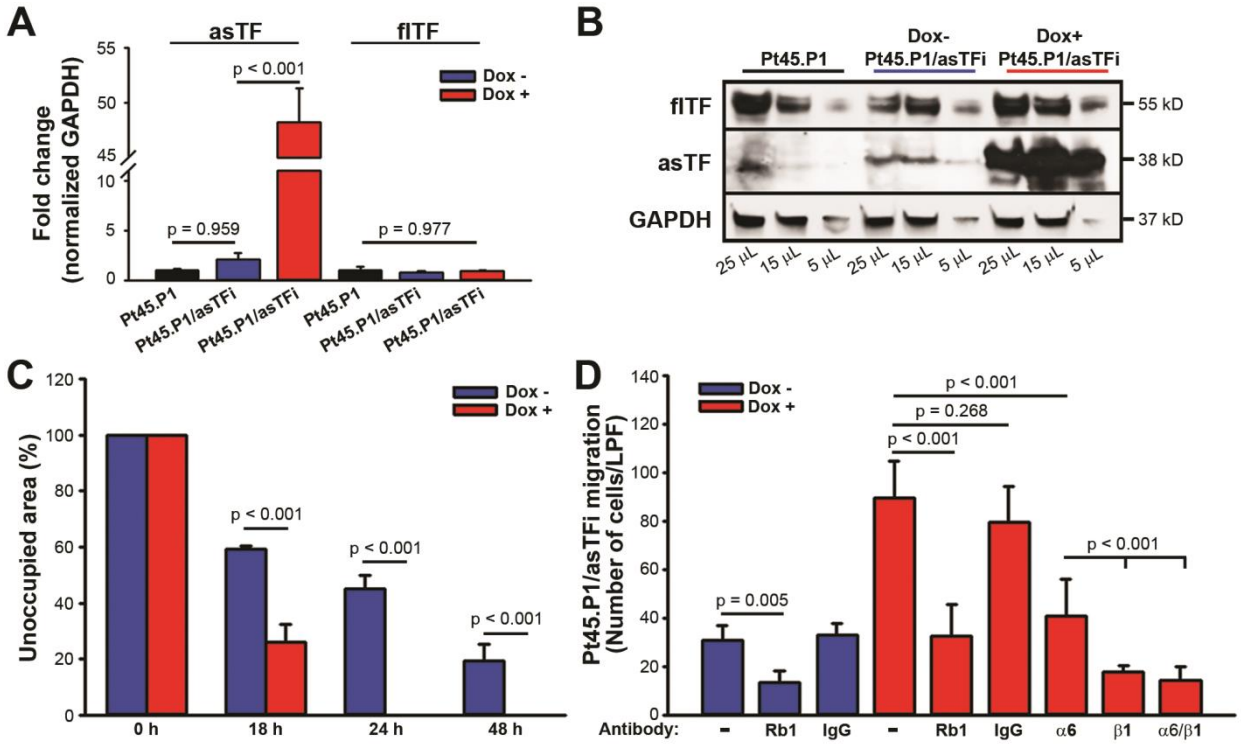

Figure 4.1: TF isoform expression in Pt45.P1/asTFi cells. (***A***) asTF/flTF mRNA expression levels were assessed by quantitative real-time RT-PCR (n=3). (***B***) Western blot, flTF/asTF protein levels in Pt45.P1 and Pt45.P1/asTFi cells; lysates were assessed for total protein concentration and volume was adjusted accordingly. (***C***) Quantification of gap closure / scratch assay, Pt45.P1/asTFi cells treated and untreated (±Dox). Bars depict the area unoccupied by Pt45.P1/asTFi cells (n=3) at 0, 18, 24, and 48 hours. (***D***) Pt45.P1/asTFi cell migration toward serum in a transwell assay: laminin-coated transwell inserts were seeded with Pt45.P1/asTFi cells treated as indicated (n=6 transwells per treatment). (RabMab1 = Rb1)

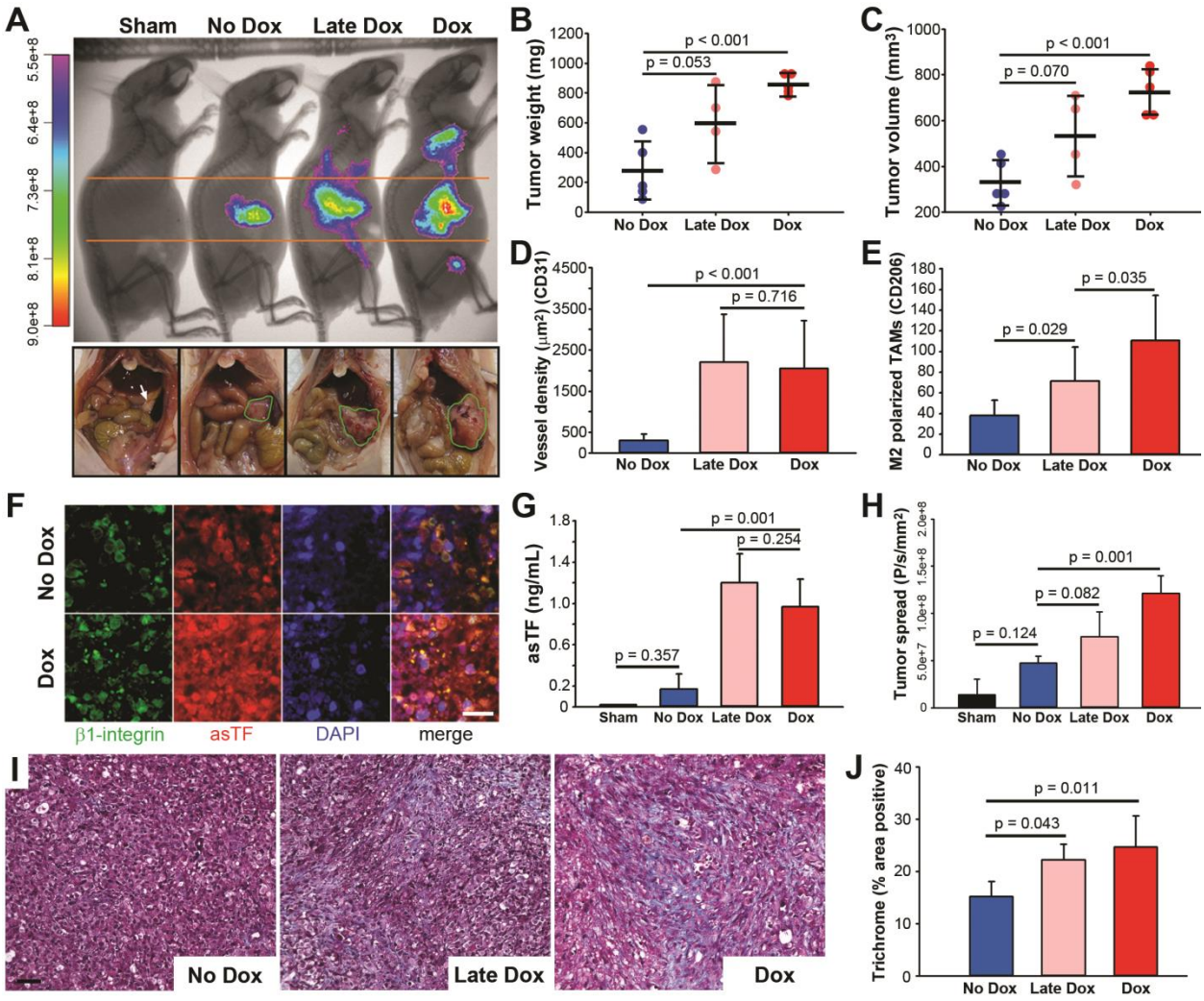

Figure 4.2: Growth of orthotopically implanted Pt45.P1/asTFi cells in nude mice. (*A*) Mice began receiving Dox (2µg/mL) in sucrose at day 1 of the study ("Dox"), day 25 of the study ("late Dox"), or sucrose alone ("No Dox"), and tumor progression were imaged by SapC-DOPS 5 weeks post-surgery (n=5/cohort; top row, representative images). Bottom row, abdominal cavities of nude mice bearing orthotopic Pt45.P1/asTFi tumors. White arrow: normal pancreas; green outlines: tumor. Quantification of tumor weight (***B***) and tumor volume (***C***) in the three groups (n=5). (***D***) 8 view fields per specimen (n=5 per specimen type) were counted and averaged for vessel density as assessed by anti-CD31 staining. (***E***) M2 TAMs were assessed by anti-CD206 staining. (***F***) Expression and co-localization of β1 integrin and asTF in tumors formed by Pt45P1/asTFi cells (scale bar = 20µm). (***G***) Plasma from mice bearing Pt45.P1/asTFi tumors was assayed for asTF using ELISA (n=5). (***H***) Quantification of tumor spread to distal sites in anesthetized mice via CMV-SapC-DOPS imaging. (***I***) Representative images, Masson's Trichrome stain (scale bar = 50µm). (***J***) Quantification of percent area positive for Masson's Trichrome stain, 5 view fields per specimen (n = 5).

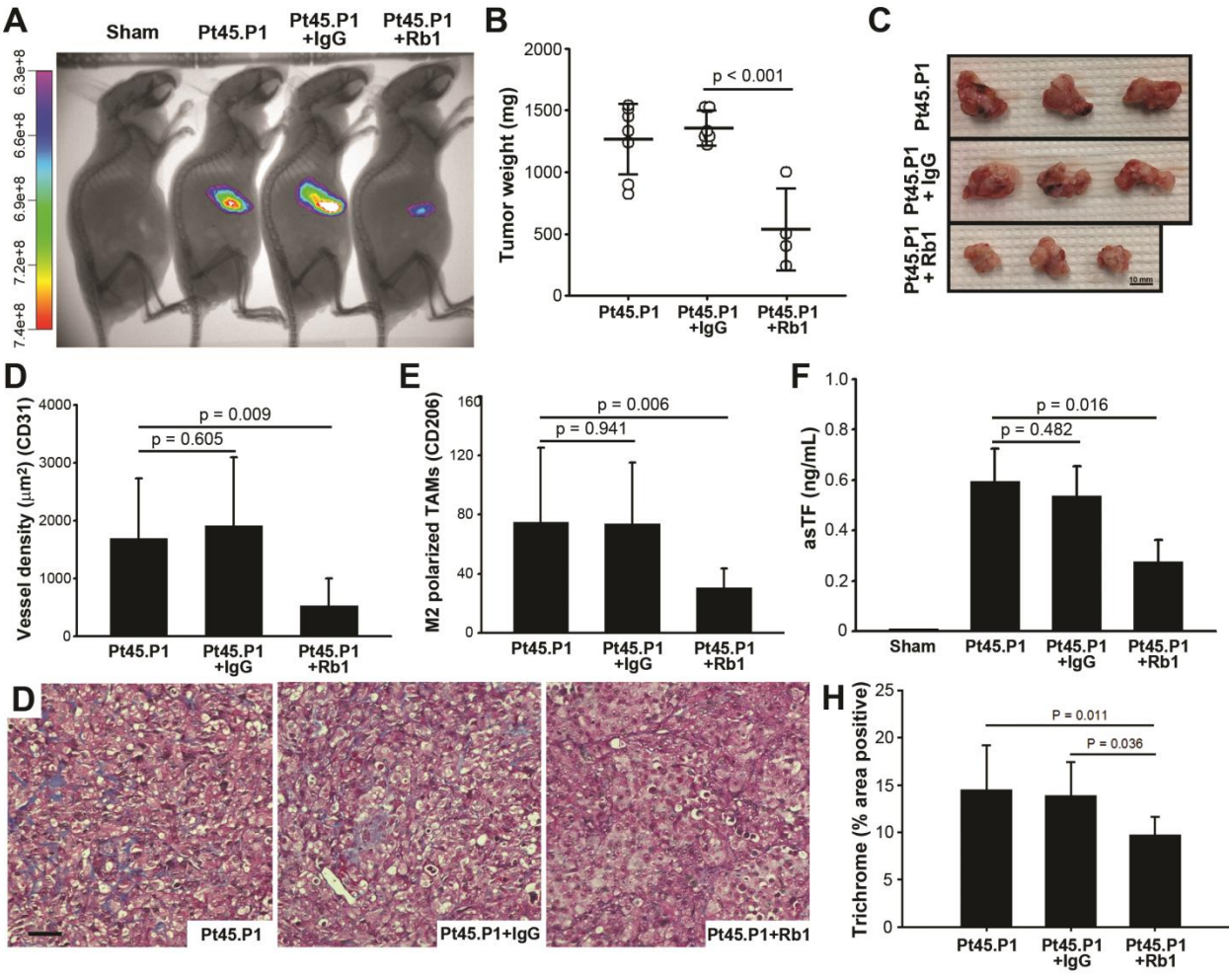

Figure 4.3: Effects of RabMab1 on the growth of orthotopically implanted Pt45.P1 cells in nude mice. (***A)*** Tumor progression was monitored *in vivo* via SapC-DOPS imaging over 7 weeks (n≥3). ***(B)*** Quantification of primary tumor weight (n≥3). ***(C)*** Representative specimens, resected tumors. (***D***) Eight view fields per specimen (n=3 per specimen type) were assessed for vessel density by anti-CD31 staining, and (***E***) for M2 TAMs by anti-Ly6C/anti-CD206 staining. (***F***) Plasma samples from each cohort bearing Pt45.P1 tumors were assayed for asTF using ELISA (n=3). (***D***) Representative images, Masson's Trichrome stain (scale bar = 50μm). (***H***) Quantification of percent area positive for Masson's Trichrome stain. (RabMab1 = Rb1)

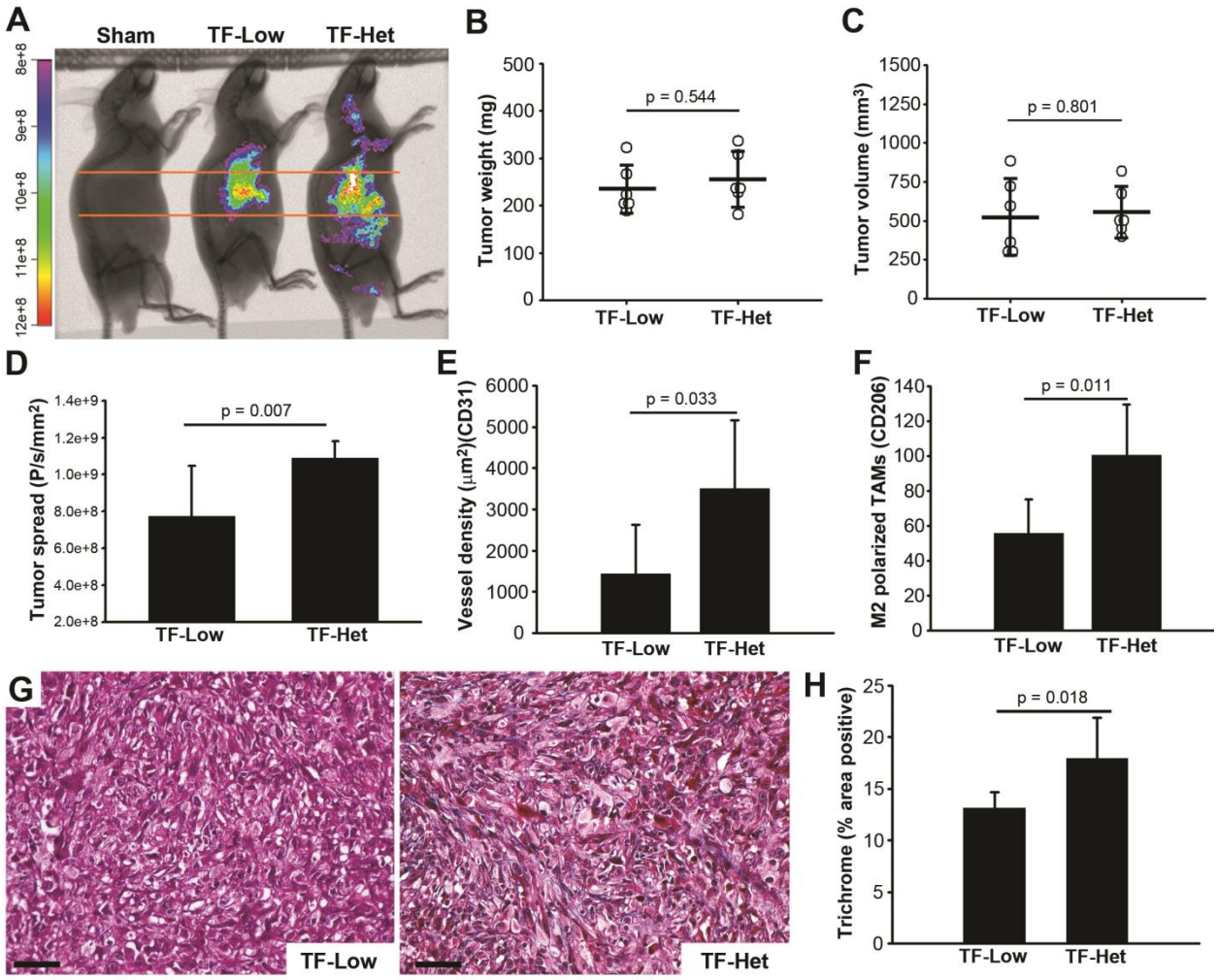

Figure 4.4: Contribution of host-derived TF to tumor progression, orthotopically implanted Pt45.P1 cells. (***A***) Tumor progression was monitored via CVM-SapC-DOPS (n=6).(***B***) Quantification of average primary tumor weight and (***C***) volume in each cohort (n=6). (***D***) Quantification of spread to distal sites. (***E***) Eight view fields per specimen (n=6 per specimen type) were assessed for vessel density by anti-CD31 staining, and (***F***) M2 TAMs by anti-Ly6C/anti-CD206 staining. (***G***) Representative images, Masson's Trichrome stain (scale bar = 50μm). (***H***) Quantification of percent area positive for Masson's Trichrome stain.

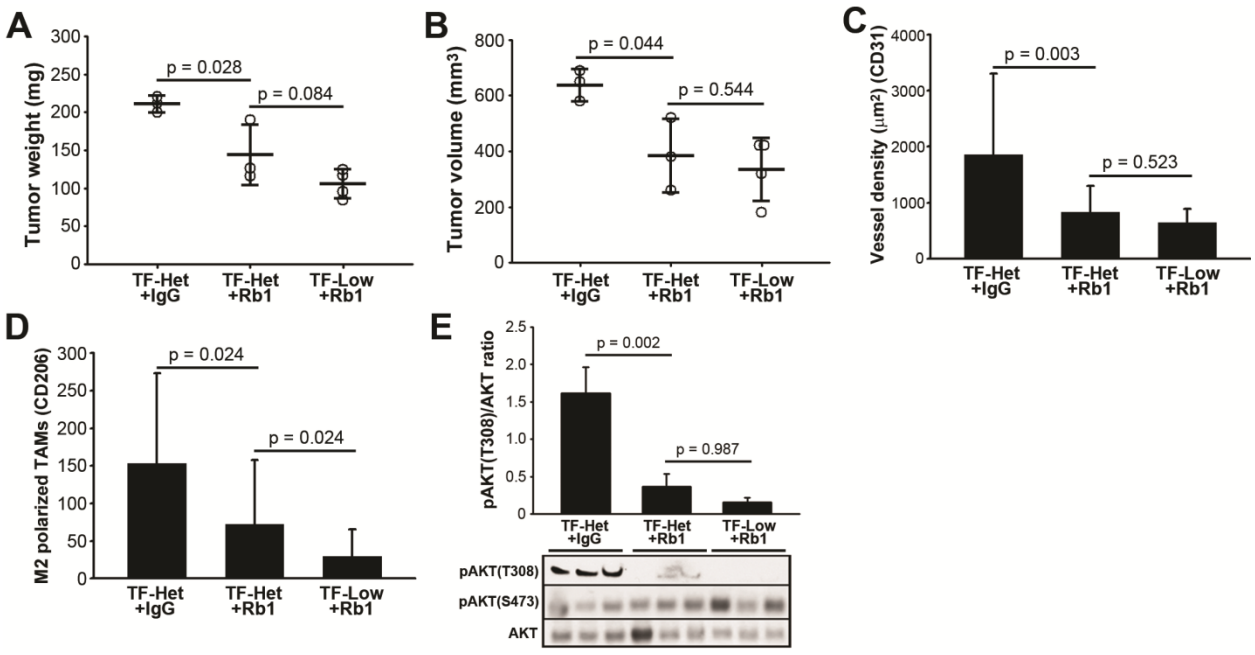

Figure 4.5: RabMab1 suppresses Pt45.P1 growth with equal efficacy in TF-Het and TF-Low mice. (***A)*** Average primary tumor weight, TF-Low and TF-Het SCID mice bearing orthotopic Pt45.P1 tumors (n≥3). (***B***) Average primary tumor volume (n≥3). ***(C)*** Quantification of vessel density as assessed by anti-CD31 staining. (***D***) Eight view fields per each tumor (n≥3 per specimen type) were counted and averaged for M2 TAMs by anti-Ly6C/anti-CD206 staining. (***E***) Western blot, phosphorylation of AKT (T308 & S473) in the three cohorts; each lane is a sample of an individual tumor. (RabMab1 = Rb1)

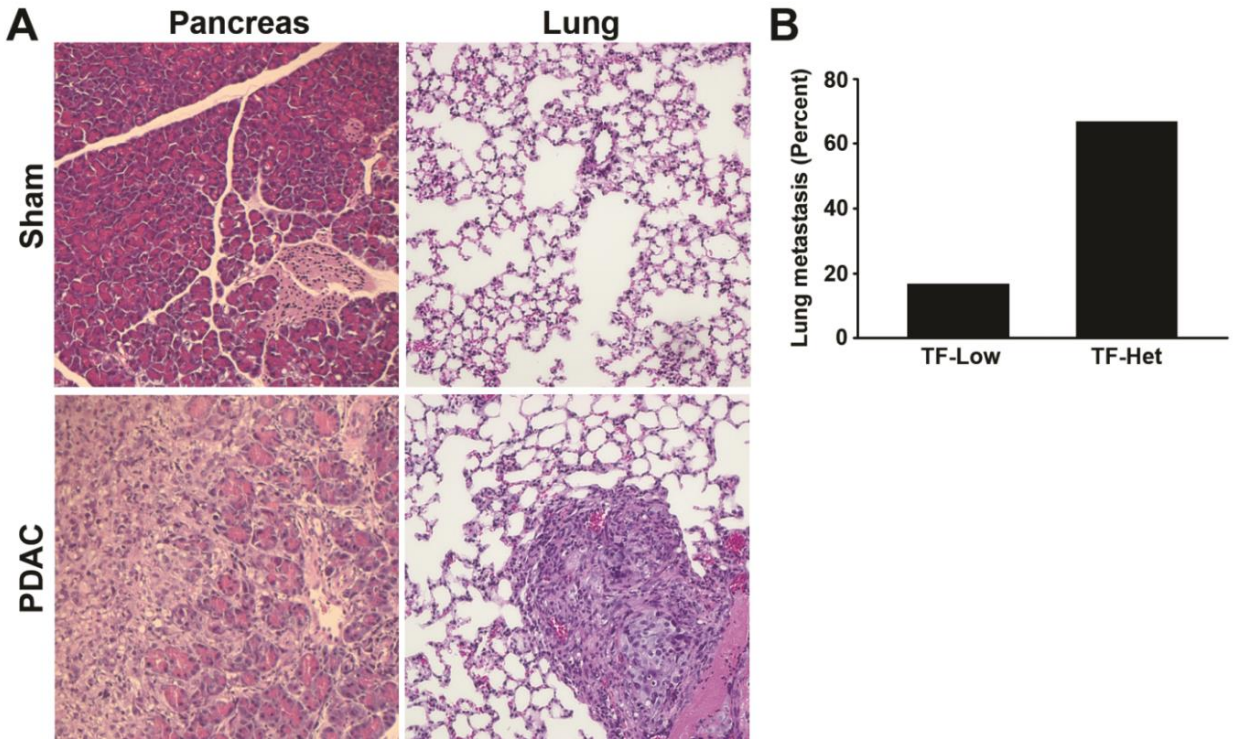

Figure 4.6: Host-derived TF contributes to tumor spread. (A) Representative images, H&E stain: histology of tumors generated via orthotopic implantation of Pt45.P1 cells in the pancreases of SCID mice (left row), and micrometastatic lesions in the lung tissue (right row). (B) Prevalence of micrometastatic lesions in the lung tissue of TF-Low and TF-Het SCID mice, H&E stain (n=6 mice per group).

Chapter 5: Discussion

You do very nice work, young man; too bad you study an artifact

– Yale Nemerson
My Life with Tissue Factor

5.1 Summary

The aim of this dissertation was to improve our understanding of the mechanisms regulating asTF-induced tumor progression, examine circulating levels of asTF in several disease conditions including PDAC, and assess the effectiveness of anti-asTF targeted therapeutics in hopes of improving PDAC treatment.

The work presented in chapter 2 reports that asTF expression is increased in human PDAC lesions, and that asTF protein expression positively correlates with the degree of vessel density and monocyte infiltration. This finding is in agreement with previous reports, which show that asTF exhibits angiogenic activity via integrin ligation and activation of proangiogenic effector pathways such as FAK and AKT (186)(185). Hobbs et al. reported that asTF expression, rather than flTF, induced larger more vascularized tumors in a subcutaneous pancreatic cancer model (185). Van den Berg et al. subsequently reported that asTF ligates integrins α6β1 and αVβ3 on endothelial cells promoting angiogenesis (186). Surprisingly, blocking FVII and thrombin, or deleting PAR2 was unable to abolish asTF-mediated angiogenesis, which suggests that asTF exerts its effects via pathways distinct from flTF. In our model of PDAC we find that asTF promotes tumor spread, and show that asTF exerts autocrine/paracrine changes in PDAC cells, by eliciting a variety of patho(biological) processes such as EGFR signaling, angiogenesis, cell proliferation, EMT, cell migration, and apoptosis resistance. One gene in particular that was highly elevated was *EFEMP1*, whose product is a ligand for EGFR and can activate MAPK and Akt promoting PDAC growth (206). Studies correlate *EFEMP1* levels with microvessel density in a variety of tumors and show that *EFEMP1* promotes the expression of VEGF.

Since its discovery, the role of asTF in health and disease has been highly contentious. Some believe that asTF behaves as a procoagulant protein, while others refute this hypothesis. Whether asTF behaves as a procoagulant protein appears to be highly dependent upon the experimental settings. Studies measuring asTF's procoagulant potential in a setting where flTF is not present fails to recapitulate the biological settings of asTF - since asTF is not found in the absence of flTF, and thus do not take into consideration flTF/asTF synergy. Furthermore, data discrepancies reproducing asTF's role in hemostasis can be attributed to the type of procoagulant assay being used. Current assays for measuring asTF procoagulant potential have significant differences in their sensitivity and specificity. In chapter 2 we use a sensitive and specific two-stage activity assay to measure TF's ability to generate FXa, and show that asTF likely has a synergistic effect with flTF in promoting a pro-thrombotic state in PDAC: PDAC cells that overexpress asTF are more procoagulant, as are the microparticles derived from these cells. Of note, we observed the ability of asTF to be retained on the surface of both PDAC cells and microparticles. Retention of asTF on cell and microparticle surfaces may be due to integrin ligation or through direct interactions with its positively charged C-terminus and anionically charged phospholipids. In chapter 2 we show that asTF mediated signaling may serve as a novel target to treat PDAC and its thrombotic complications.

Chapter 3 examines circulating levels of asTF in patient groups known to be associated with increased TF and thrombosis. Since the late 1990s when Key et al. and Giesen et al. demonstrated that procoagulant TF is present in blood of healthy individuals, it shifted the hypothesis that TF only resides in the adventitia acting as a hemostatic envelope (215)(216). Circulating TF has since then been reported to be elevated in DM (221), ACS (222), and pancreatic

cancer (223). Not surprisingly all of these diseases are associated with an increased risk for VTE. Current available assays for measuring circulating TF antigen have varying sensitivity and specificity (231), with some of these assays having cross-reactivity for both TF isoforms flTF and asTF, and thus measure 'total circulating TF'. In chapter 3 we use a newly developed asTF specific ELISA to detect asTF in the plasma of healthy subjects, and patients with ongoing ACS, DM, ACS + DM, and PDAC. In this study we show circulating asTF levels ≥200 pg/mL were not significantly associated with either ACS and/or DM. A few patients had remarkably high levels of asTF and it still remains to be definitively ascertained whether asTF is elevated in patients with cardiovascular disease. However, circulating levels of asTF ≥200 pg/mL were significantly associated with pancreatic cancer when compared to a healthy cohort matched for age and gender. Pancreatic cancer patients with high asTF levels were significantly less likely to qualify for tumor resection. Plasma levels of asTF were the highest in PDAC patients with distal metastases, and did not correlate with CA19-9 levels. Thus, measuring asTF in plasma may help identify pancreatic cancer patients who have a more aggressive disease, yet have low CA19-9 levels.

Chapter 4 tests the efficacy of targeting asTF with an asTF specific monoclonal antibody termed RabMab1. In chapter 2 we show that asTF influences PDAC disease progression and unlike the highly studied flTF, asTF triggers tumor progression via non-proteolytic mechanisms. asTF signals by binding α6β1 and avβ3 integrins, and thereby activating PI3K/Akt, MAPK, and FAK signaling pathways. asTF-integrin signaling was shown to promote breast cancer cell proliferation and increase microvessel density in a xenograft model of breast cancer. Activation of integrin linked signaling pathways can regulate a variety of biological processes in cancer (270), but they also regulate mechanical cell-cell and cell-ECM interactions. We hypothesize that asTF-

integrin interactions render cells more motile by preventing integrin-ECM protein interactions. Using a transwell migration assay we show for the first time that asTF promotes PDAC cell migration, and that RabMab1 targeting of asTF-integrin interactions prevented the asTF-potentiated migration of PDAC cells. This study also supports the idea that asTF acts a proinflammatory molecule in the tumor microenvironment by increasing the levels of TAMs, vessel density, and collagen deposition. Remarkably, RabMab1 was able to significantly reduce all these asTF-induced inflammatory effects, resulting in smaller tumors and blunted tumor spread. Other novel findings of this study were asTF's ability to promote tumor progression at all stages of the disease, and that host-derived TF contributes to PDAC spread and remodeling of tumor microenvironment. Thus, antibody-based targeting of asTF may comprise a novel therapeutic strategy to stem PDAC progression.

5.2 Targeting TF in cancer

TF plays an important role in cancer progression; multiple reports indicate that TF promotes cancer related coagulopathy, metastasis, tumor growth, and tumor angiogenesis. Currently there are a variety of very unique ways to target TF-mediated cancer progression. One strategy focuses on cancer-related thrombosis. One of the major complications of pancreatic cancer is the development of VTE, which is likely the result of a combination of systemic inflammation, procoagulant microparticles released from cancer cells, and TF expressed by cancer cells themselves (271). Sproul in 1938 was the first to describe thromboembolism as a major complication of pancreatic cancer (272), and it was later reported that pancreatic cancer has an incidence rate of VTE that ranges from 17% to as high as 57% (273). The first study to identify

TF activity as the major mechanism responsible for pancreatic cancer related VTE was Silberberg in 1989, who showed that two PDAC cancer cell lines RWP1 and RWP2 have TF-mediated procoagulant activity and were able to release procoagulant microparticles (274). These studies highlight the clinical relationship between TF and cancer coagulopathy, but do not answer the question of whether activation of coagulation can promote tumor progression, or if the increased procoagulant state is merely a consequence of tumor progression.

Since the "cascade" or "waterfall" theory of blood coagulation proposed almost simultaneously by MacFarlane, and Ratnoff in 1964 (275)(276), we have known that TF-mediated coagulation occurs through sequential proteolytic activation of pro-enzymes (zymogens), that result in the formation of fibrin. The TF-mediated activation of coagulation results in the activation of clotting factors FVII, FX / FIX, and FII (prothrombin), all of which promote inflammation. Elevated levels of FVIIa highten the expression of C-reactive protein (CRP) and IL-6 (277). IL-6 was shown to play a critical role in the maintenance and progression of PanIN lesions to PDAC, so much so that mice expressing mutated K-RAS; which recapitulate the sequential histological progression of PDAC (**Figure 1.2**), yet had IL-6 knocked out ($K\text{-}RAS^{G12D}$,$IL\text{-}6^{-/-}$) did not progress to *in situ* carcinoma (278). FXa was also shown to promote the expression of CRP and IL-6 (279)(280), and it also caused the increase in IL-8, MCP-1, and adhesion molecules ICAM, VCAM, and E-selectin (281). FIIa and fibrin have very similar inflammatory responses: they both promote monocyte adhesion and the production of chemokine/cytokines IL-6, IL-8, and MCP-1 (282)(283). It was also shown that FIIa can promote tumor invasion by inducing matrix metalloproteinase-9 and can promote distal metastasis by making sites more receptive to growth of cancer cells (284)(258). Inhibition of TF-mediated coagulation and inflammation have had

varying results. Several clinical trials that explored the effect of anticoagulation in cancer patients did not significantly reduce or prevent cancer progression – with the exception of prostate cancer that has generated conflicting results with some reports indicating a possible cancer preventative effect (285)(286). The anticoagulant Warfarin inhibits the synthesis of vitamin K dependent clotting factors FII, FVII, FIX, and FX. Studies examining long term use of warfarin show no cancer preventative effect for pancreatic cancer patients, but did show a significant increase in mean survival from 2.3 to 5 months, and in combination with gemcitabine to 7.1 months (287)(288). Although Warfarin treatment generated only a small survival benefit, recent experimental evidence suggests that the non-hemostatic functions of TF may have a greater impact on tumor pathology and allow for targeting TF signaling without concerns of developing bleeding complications.

A variety of new drugs that target TF-mediated signaling pathways are being developed. flTF signals through PARs, which can be cleaved by the formation of either flTF:FVIIa or flTF:FVIIa:FXa complex (289). Inhibition of the ternary complex with monoclonal antibody-5G9 (mAb-5G9) prevents PAR1 signaling and coagulation activity (290). Another inhibitor of flTF is mAb-10H10; and in contrast to mAb-5G9 it has minimal anticoagulant activity and inhibits PAR2 signaling of the binary TF:FVIIa complex (291). The generation of these two selectively inhibitory antibodies allows for the opportunity to address the specific roles of flTF-mediated signaling versus coagulation activity in tumor progression. Surprisingly, inhibition of mAb-5G9 had no effect on tumor growth, but mAb-10H10 was able to significantly inhibit tumor growth in a breast cancer xenograft model (179). The TF:FVIIa:PAR2 signaling nexus induces the expression of proangiogenic molecules and growth factors, such as VEGF, cysteine-rich angiogenic inducer 61

(Cyr61), VEGF-C, CTGF, CXCL1, GM-CSF, macrophage colony-stimulating factor (M-CSF) and IL-8 (292)(293). TF-PAR2 signaling promotes the expression of chemokines GM-CSF and M-CSF, which promote the recruitment of myeloid cells, and Gil-Bernabé et al. report that TF induced coagulation is responsible for macrophage recruitment and promotes tumor metastasis (258). However, the results of the breast cancer xenograft studies report that flTF primarily promotes tumor progression via PAR2-mediated angiogenesis by promoting the expression of VEGF, and that blockade of downstream coagulation factors had little impact on tumor growth (179). The association of flTF expression with vessel density has been reported in gliomas (294), lung cancer (196), breast cancer (295), colon cancer (296), liver (297), prostate cancer (298), and pancreatic cancer (178). Further highlighting the role of flTF:PAR signaling, are genetic studies of mice that spontaneously develop tumors and are either PAR-1 or PAR-2 deficient. PAR-1 deficiency had no effect on tumor progression and in contrast PAR-2 deficiency displayed a decrease in tumor vessel density and had a significant decrease in tumor progression (299). In light of these studies, the proteolytic signaling pathway of flTF may be an attractive therapeutic target by reducing angiogenesis while maintaining normal hemostasis. However, current anti-angiogenic drugs, such as bevacuzimab which targets VEGF and is effective in mouse xenograft models, but in a randomized phase III trial showed no significant benefit for progression-free survival, overall survival, and quality of life (300). The results from this trial may have been due to a delayed therapeutic intervention and that the optimal time to intervene with antiangiogenic agents may be relatively early in the course of cancer. Secondly, angiogenic pathways are numerous, and this redundancy can decrease the dependency on VEGF. Moreover, PDAC tumors are severely desmoplastic and markedly hypovascular rendering them "sensitized" to a hypoxic

environment and more likely to survive without surrounding vasculature and thus likely to be less vulnerable to antiangiogenic therapy.

Other potent flTF inhibitors have been developed to inhibit tumor growth. Nematode anticoagulant protein c2 (NAPc2) isolated from the nematode *Ancylostoma caninum* is a potent flTF:FVIIa inhibitor that prevents the generation of FXa. NAPc2 was shown to have antitumor effect in a xenograft model of colon cancer by blocking PAR-2 signaling (301), while inhibiting FXa with nematode anticoagulant protein 5 (NAP5) did not reduce tumor growth, thus providing more support to the notion that the flTF:PAR2 signaling pathway is the predominant means of flTF-mediated tumor progression (180). However, despite these reports a clinical study examining the effect of NAPc2 to treat colon cancer has been suspended (302). It is unclear whether this clinical study was suspended due to bleeding complications or if NAPc2 lacked therapeutic benefits in the setting of colon cancer. Despite these results, other flTF-targeting drugs are currently being investigated for clinical utility in stemming cancer. These drugs are TF-inhibiting antibody ALT-836 and PCI-27483 (a FVIIa inhibiting molecule). ALT-836 in combination with gemcitabine is currently in phase I trial to test its safety at treating locally advanced and/or metastatic solid tumors (303). PCI-27483 is also being tested in combination with gemcitabine to treat pancreatic cancer (304). Both of these studies are targeting the flTF-mediated PAR2 signaling and coagulant pathways, and the results of these studies will provide very interesting insight on whether targeting flTF nexus will be a viable option to treat cancer.

It still remains to be determined whether flTF-targeting therapies will be useful for clinical applications. One major concern for the majority of flTF therapeutics are the risk for developing

bleeding complications - excluding the mAb-10H10 which targets flTF signaling without affecting hemostasis, but it remains to be determined if mAb-10H10 will be effective in a clinical setting. In 2009 van den Berg et al. discovered an alternative tumor-promoting TF-mediated mechanism (186). This mechanism relies on non-proteolytic (i.e. PAR-independent) integrin-mediated signaling of the alternatively spliced isoform of TF (asTF). The authors report that asTF promotes vessel formation via ligation of β1 and β3 integrins on endothelial cells (186). Surprisingly, in this study the truncated form of flTF (i.e. the extracellular domain of flTF, see **Figure 1.5**) was unable to elicit an integrin-mediated angiogenic response. Moreover, in this report asTF-mediated angiogenesis was shown to be more pro-angiogenic than flTF in an aortic sprouting assay. Shortly after the discovery of asTF-integrin signaling, Srinivasan et al. reported that asTF-β1 integrins on microvascular endothelial cells induces the expression of cell adhesion molecules leading to monocyte adhesion and diapedesis (194). Thus, in light of these reports it is easy to speculate that asTF-integrin signaling could fuel cancer growth and spread by increasing vessel density and macrophage accumulation. In non-small cell lung cancer (NSCLC) asTF mRNA was significantly elevated 6.8 fold versus control, compared to only 3.4 fold increase of flTF mRNA. Interestingly, asTF mRNA and not flTF mRNA levels were significantly associated with patients in stages IIIA/IIIB, while flTF mRNA levels had no such association (196). Until the study by Kocatük et al. in 2013, the function of asTF in the tumor microenvironment was unclear (228). The study reports that asTF is expressed at high levels in breast cancer tissue, and acts via β1 integrins on breast cancer cells to promote tumor progression via cell proliferation, resistance to apoptosis, and vessel density. This study is also the first to show the efficacy of co-implantation of anti-asTF monoclonal inhibitor antibody RabMAb1 with breast cancer cells to reduce tumor growth (228). Chapter 2 of this thesis furthers our understanding of asTF-mediated tumor progression showing

its ability to promote tumor metastasis and autocrine/paracrine signaling that elicits EGFR signaling and EMT in a PDAC setting. Chapter 4 shows the efficacy of RabMab1 to stem PDAC tumor growth and spread, and adds further support to asTF-targeting as a new therapeutic option for TF targeted therapies. However, much work is still needed before RabMab1 therapy can be brought into a clinical setting. First, RabMab1 needs to be administered systemically by intravenous or intraperitoneal injections rather than co-implanted with cancer cells during implantation. Also, new mouse models that recapitulate the histopathology of PDAC should be used - such as human PDAC-derived xenografts, to verify that RabMab1 can be effectively delivered to the severely desmoplastic and hypovascular tumors. It would also be highly significant if RabMab1 could show synergistic effect while administered in combination with cytotoxic chemotherapies, such as gemcitabine. If RabMab1 can systemically inhibit tumor progression using this new PDAC model and/or prove beneficial when administered with already clinically used cytotoxic chemotherapies, it may indeed be the preferred TF isoform to target in cancer since asTF is dispensable to normal hemostasis, highly expressed in malignant tissues, and promotes tumor progression via a variety of signaling pathways.

5.3 Alternative pre-mRNA splicing in cancer

Alternative splicing is one of the primary evolutionary causes of maintaining proteome diversity. It is now estimated that roughly 95% of genes are alternatively spliced in humans (305)(306). Alternative splicing is a mechanism to produce multiple isoforms from a single gene by removing intervening sequences (introns) and joining protein coding regions (exons) through

the use of alternative splice sites. Spliced isoforms can have different functions, and in some cases even have antagonistic properties to the canonical isoform (307). The plasticity afforded by alternative splicing greatly contributes to biological complexity, and failure to express the correct isoform can lead to deleterious consequences. Alternative splicing is regulated, in part, by a family of splicing regulatory / serine-arginine rich (SR) proteins (308). These proteins have an essential function during spliceosome assembly, which is necessary for intron removal, and their activity may result in either enhanced inclusion, or enhanced exclusion of an exon (309). Exon 5 of human TF contains exonic splicing enhancer (ESE) motifs, recognized by SR proteins. It was shown in human monocytic cells that SR proteins serine/arginine-rich splicing factor 2 (ASF/SF2) and splicing regulatory protein 55 (SRp55) bind to ESE motifs and promote the inclusion of exon 5, which results in the biosynthesis of flTF (199). In contrast, splicing regulatory protein 40 (SRp40) and splicing component 35 (SC35) antagonize ASF/SF2 and SRp55 through a competitive binding to overlapping ESE motifs on exon 5, resulting in the exclusion of exon 5, and thus the biosynthesis of asTF (264). Other studies have shown that inhibiting DNA topoisomerase I reduces the activity of ASF/SF2 and SRp55, leading to the reduction of flTF expression and an increase in asTF production by human endothelial cells (310).

Increased expression of various SR proteins promote the progression of a variety of malignancies, such as breast (265), lung (266), colon (267), and ovaries (268). However, very little is known about PDAC alternative pre-mRNA processing. Hypoxia can influence alternative splicing by upregulating SR proteins CDC-like kinase 1 (Clk1) and CDC-like kinase 4 (Clk4), and inhibiting both Clk1 and Clk4, which decrease the expression of both flTF and asTF in lung cancer (311). Since PDAC tumors are highly hypovascular and hypoxic it is easy to speculate that PDAC

cells feature aberrant alternative splicing of TF, thereby altering the levels of asTF, which is highly likely to influence the relative expression of flTF and asTF. Future studies will examine whether there is an 'alternative splicing switch' that occurs during the progression of PanIN to PDAC disease. If this is the case, asTF may be the preferred isoform for targeting in PDAC, a disease which is mainly diagnosed at later stages. Also, new drugs are being developed that deliver anti-tumor compounds to sites with enhanced flTF expression; since flTF is ubiquitously expressed throughout the body, this method will surely lack specificity. Thus, if aberrant alternative splicing does occur in PDAC and since asTF is only minimally expressed in healthy tissues, it may be the preferred isoform to target during end-stage PDAC and/or other malignancies with aberrant alternative splicing.

5.4 TF and integrin interactions in cancer

Integrins are heterodimeric transmembrane glycoprotein receptors that mediate cell-cell and cell-ECM interactions (312). Integrins are composed of an α and β subunit. Currently there are 18 α and 8 β monomer subunits that can complex with each other to form 24 integrin heterodimers that can bind ECM molecules such as collagens, laminins, fibronectin, and tenascin (270). Integrin activity regulation is complex. Extracellular stimuli can induce "outside-in" signaling, whereby integrin cytoplasmic tail act as a signal transduction platform that recruits kinases such as PI3K, FAK, and Src family kinases. Outside-in signaling in turn controls cell attachment, migration, proliferation, and survival (247). Integrins can also perform "inside-out" signaling via intracellular activators, such as talin or kindlins binding to integrin cytoplasmic tails

and causing integrin extracellular conformation changes that lead to an increased affinity for extracellular ligands.

In 2005 Nitori et al., showed that TF expression was found to have a prognostic significance for determining more aggressive PDAC, and patient TF levels positively correlated with tumor invasiveness (176). In this study, immunohistochemical staining revealed that TF was prominent at the invasive tumor front, suggesting a likely causative relationship between TF and tumor invasion. Integrins also localize to the leading edge of invasive tumors and regulate tumor invasion, thus leading to the question of whether TF and integrins interact and influence each other's function. Multiple studies show that TF does indeed interact with a variety of integrins. Co-localization and co-imunoprecipitation studies demonstrate that TF does interact with β1-integrins (179). Versteeg et al. show that integrins α6β1 and α3β1 regulates flTF:PAR2 signaling in cancer, and that their complexation facilitated breast cancer growth (313)(299). Surprisingly, it was discovered that flTF keeps β1 integrins in an inactive state and that flTF β1-integrin dissociation dampens flTF signaling (179).

In contrast to flTF, asTF-integrin interactions are independent of PARs and do not require FVIIa. Ligation of β1 and β3 integrins by asTF promotes angiogenesis both *in vitro* and *in vivo* (186). Moreover, asTF-integrin interactions prevent anoikis (a form of cell death induced by anchorage-dependent cells detaching from ECM) and promote proliferation of breast cancer cells (228). Currently, the protein domain(s) responsible for TF-integrin association are unknown. Interestingly, flTF binds β1-integrins keeping them in an inactive state via its extracellular and intracellular domains, yet asTF binds β1 integrins and activates them. Moreover, Van den Berg et

al. show that sTF (truncated flTF) failed to evoke an angiogenic response. This suggests that the unique C-terminus of asTF may be critical for activating β1-integrins. Future studies examining the protein domain(s) responsible for TF-mediated signaling will provide potentially valuable therapeutic insights for the development of new small molecule inhibitors that will disrupt TF-integrin mediated tumor progression.

TF-integrin complex formation regulating cell migration and other tumor progression processes is still poorly understood. Whether asTF influences tumor cell migration directly or indirectly via ECM molecules such as collagen, fibronectin, and tenascin is unknown. Future studies examining how asTF regulates integrin interaction with ECM molecules would provide further insight into the mechanism behind asTF-mediated cell migration. Does asTF promote PDAC cell migration by acting as an integrin agonist, promoting outside-in signaling and subsequently the activation of kinases that influence cell motility? In contrast, does asTF dampen inside-out signaling, by decreasing the recruitment of intracellular scaffolding proteins or, by binding integrins, does asTF prevent them from interacting with ECM molecules, thus allowing for cancer cells to escape the tumor microenvironment? A study that examines how asTF influences PDAC cell transmigration through ECM molecules fibronectin, collagen, tenascin, and laminin would provide insight necessary to begin answering these questions. asTF binds to α6β1 and αvβ3 integrin heterodimers, which respectively bind laminin and fibronectin. Thus, above studies would allow for the identification of what ECM and integrin interactions asTF interferes with, thus determining whether asTF promotes migration via mechanical adhesion hindrance or by activating cell motility effector signaling pathways. Furthermore, since flTF:β1-integrins mediate cancer signaling in breast cancer and asTF also binds β1-integrins, does asTF interact

competitively with flTF to regulate β1-integrin signaling? The interactions between integrins and TF play an important role in the pathobiology of TF mediated tumor progression, and future studies examining the mechanisms responsible will likely facilitate development of novel and useful strategies to stem cancer progression.

5.5 Conclusions

The studies presented in this thesis demonstrate the critical role that asTF plays in cancer progression. We report that asTF is abundantly expressed in human PDAC tissue, and positively correlates with the degree of monocyte infiltration and vessel density. Tumor cells that express asTF have increased tumor metastasis to distal sites *in vivo* in an orthotopic mouse model of PDAC; *in vitro*, asTF-β1 integrin interaction renders PDAC cells more motile, and importantly, targeting asTF with an inhibitory antibody RabMab1 can inhibit asTF mediated cell migration. In our PDAC orthotopic mouse model, asTF was shown to have a synergistic effect with flTF by increasing the procoagulant potential when expressed in combination with flTF. Unlike flTF, asTF is secreted and can exert autocrine/paracrine effects on PDAC cells resulting in global changes in gene expression implicated in EMT, apoptosis resistance, cell proliferation, and metastatic spread. When RabMab1 is co-implanted with PDAC cells into mice, tumor size was significantly reduced with fewer macrophages and blood vessels, and had a reduction in tumor spread. Thus, antibody-based targeting of asTF may comprise a novel therapeutic strategy to stem PDAC progression as well as its thrombotic complications.

In plasma samples of tumor bearing mice, we were able to detect circulating levels of asTF protein, and when tumor cells were treated with RabMab1, a significant decrease in circulating asTF was observed. We then analyzed plasma of PDAC patients for asTF levels, and found a significant increase in the number of patients who had elevated plasma asTF versus a healthy age and sex matched cohort. Surprisingly, PDAC patients whose asTF levels were greater than or equal to 200 pg/mL had a significantly lower chance to qualify for tumor resection. Thus, asTF may also comprise a novel marker of aggressive PDAC phenotype with a potential utility in patient stratification, warranting prospective evaluation of larger PDAC patient cohorts.

References

1. Fitzgerald PJ. Medical anecdotes concerning some diseases of the pancreas. *Monogr Pathol*. 21:1–29 (1980).

2. Nutton V. (2004). *Ancient medicine*. New York, New York: Routledge.

3. Busnardo a C, DiDio LJ, Tidrick RT, Thomford NR. History of the pancreas. *Am J Surg*. 146(11):539–50 (1983).

4. Howard JM, Hess W, Traverso W. Johann Georg Wirsüng (1589-1643) and the pancreatic duct: the prosector of Padua, Italy. *J Am Coll Surg*. 187(2):201–11 (1998).

5. Bassi C, Malleo G. The unsolved mystery of Johann Georg Wirsung and of (his?) pancreatic duct. *Surgery*. 149(1):153–5 (2011).

6. Jay V. A portrait in history. The legacy of Reinier de Graaf. *Arch Pathol Lab Med*. 124:1115–6 (2000).

7. Longnecker D. Anatomy and Histology of the Pancreas. *Pancreapedia: Exocrine Pancreas Knowledge Base*. 1–29 (2014).

8. Siegel RL, Miller KD, Jemal A. Cancer statistics, 2015. *CA Cancer J Clin*. 65(1):5–29 (2015).

9. Rahib L, Smith BD, Aizenberg R, Rosenzweig AB, Fleshman JM, Matrisian LM. Projecting cancer incidence and deaths to 2030: the unexpected burden of thyroid, liver, and pancreas cancers in the United States. *Cancer Res*. 74(11):2913–21 (2014).

10. Warshaw AL, Castillo CF. Pancreatic Carcinoma. *NEJM*. 326:455-465 (1992).

11. Ryan DP, Hong TS, Bardeesy N. Pancreatic Adenocarcinoma. *NEJM*. 371:1039-1049 (2014).

12. Everhart J, Wright D. Diabetes mellitus as a risk factor for pancreatic cancer: A meta-analysis. *JAMA*. 273(20):1605–9 (1995).

13. Song S, Wang B, Zhang X, Hao L, Hu X, Li Z, et al. Long-Term Diabetes Mellitus Is Associated with an Increased Risk of Pancreatic Cancer: A Meta-Analysis. *PLoS One*. 10(7):e0134321 (2015).

14. Fuchs CS, Colditz GA, Stampfer MJ, Giovannucci EL, Hunter DJ, Rimm EB, et al. A prospective study of cigarette smoking and the risk of pancreatic cancer. *Arch Intern Med*. 156(19):2255–60 (1996).

15. Lowenfels AB, Maisonneuve P. Epidemiology and risk factors for pancreatic cancer. *Best Pract Res Clin Gastroenterol*. 20(2):197–209 (2006).

16. Villeneuve PJ, Johnson KC, Hanley AJ, Mao Y. Alcohol, tobacco and coffee consumption and the risk of pancreatic cancer: results from the Canadian Enhanced Surveillance System case-control project. Canadian Cancer Registries Epidemiology Research Group. *Eur J Cancer Prev*. 9(1):49–58 (2000).

17. Berrington de Gonzalez A, Sweetland S, Spencer E. A meta-analysis of obesity and the risk of pancreatic cancer. *Br J Cancer*. 89(3):519–23 (2003).

18. Special section: Pancreatic cancer. Cancer facts & figures 2013. American Cancer Society.

19. Iacobuzio-Donahue C. Genetic evolution of pancreatic cancer: lessons learnt from the pancreatic cancer genome sequencing project. *Gut*. 61:1085–94 (2012).

20. Bozic I, Antal T, Ohtsuki H, Carter H, Kim D, Chen S, et al. Accumulation of driver and passenger mutations during tumor progression. *Proc Natl Acad Sci USA*. 107(43):18545–50 (2010).

21. Yachida S, Jones S, Bozic I, Antal T, Leary R, Fu B, et al. Distant metastasis occurs late during the genetic evolution of pancreatic cancer. *Nature*. 467(7319):1114–7 (2010).

22. Klein AP, Brune KA, Petersen GM, Goggins M, Tersmette AC, Offerhaus GJA, et al. Prospective risk of pancreatic cancer in familial pancreatic cancer kindreds. *Cancer Res*. 64(7):2634–8 (2004).

23. Klein AP, Hruban RH, Brune KA, Petersen GM, Goggins M. Familial pancreatic cancer. *Cancer J*. 7(4):266–73 (2001).

24. De Snoo FA, Bishop DT, Bergman W, van Leeuwen I, van der Drift C, van Nieuwpoort FA, et al. Increased risk of cancer other than melanoma in CDKN2A founder mutation (p16-Leiden)-positive melanoma families. *Clin Cancer Res*. 14(21):7151–7 (2008).

25. Thompson D, Easton DF. Cancer Incidence in BRCA1 mutation carriers. *J Natl Cancer Inst*. 94(18):1358–65 (2002).

26. Murphy KM, Brune KA, Griffin C, Sollenberger JE, Petersen GM, Bansal R, et al. Evaluation of candidate genes MAP2K4, MADH4, ACVR1B, and BRCA2 in familial pancreatic cancer: deleterious BRCA2 mutations in 17%. *Cancer Res*. 62(13):3789–93 (2002).

27. Hezel AF, Bardeesy N. LKB1; linking cell structure and tumor suppression. *Oncogene*. 27(55):6908–19 (2008).

28. Solomon S, Whitcomb DC, LaRusch J. (2012) *PRSS1*-Related Hereditary Pancreatitis. *Gene Reviews*. Seattle, Washington. University of Washington.

29. Jaffee EM, Hruban RH, Canto M, Kern SE. Focus on pancreas cancer. *Cancer Cell*. 2(1):25–8 (2002).

30. Bardeesy N, DePinho RA. Pancreatic cancer biology and genetics. *Nat Rev Cancer*. 2(12):897–909 (2002).

31. Whitcomb DC, Gorry MC, Preston RA, Furey W, Sossenheimer MJ, Ulrich CD, et al. Hereditary pancreatitis is caused by a mutation in the cationic trypsinogen gene. *Nat Genet*. 14(2):141–5 (1996).

32. Modolell I, Guarner L, Malagelada JR. Vagaries of clinical presentation of pancreatic and biliary tract cancer. *Ann Oncol*. 4:82–4 (1999).

33. Kamisawa T, Isawa T, Koike M, Tsuruta K, Okamoto A. Hematogenous metastases of pancreatic ductal carcinoma. *Pancreas*. 11(4):345–9 (1995).

34. Domenico DR, Hanson DJ, Howard JM. Observations the the of Adenocarcinoma. *Arch Surg*. 130(2):125-34 (1995).

35. Embuscado EE, Laheru D, Ricci F, Yun KJ, de Boom Witzel S, Seigel A, et al. Immortalizing the complexity of cancer metastasis: genetic features of lethal metastatic pancreatic cancer obtained from rapid autopsy. *Cancer Biol Ther*. 4(5):548–54 (2005).

36. Hruban RH, Goggins M, Parsons J, Kern SE. Progression Model for Pancreatic Cancer Progression Model for Pancreatic Cancer. *Clin Cancer Res*. 6(8):2969–72 (2000).

37. Hruban RH. An Illustrated Consensus on the Classification of Pancreatic. *Am J Surg Pathol*. 28(8):977–87 (2004).

38. Stanger BZ, Dor Y. Dissecting the cellular origins of pancreatic cancer. *Cell Cycle*. 5(7):43–6 (2006).

39. Parsa I, Longnecker DS, Scarpelli DG, Pour P, Reddy JK, Lefkowitz M. Ductal metaplasia of human exocrine pancreas and its association with carcinoma. *Cancer Res*. 45(5):1285–90 (1985).

40. De La O JP, Emerson LL, Goodman JL, Froebe SC, Illum BE, Curtis AB, et al. Notch and Kras reprogram pancreatic acinar cells to ductal intraepithelial neoplasia. *Proc Natl Acad Sci USA*. 105(48):18907–12 (2008).

41. Habbe N, Shi G, Meguid R a, Fendrich V, Esni F, Chen H, et al. Spontaneous induction of murine pancreatic intraepithelial neoplasia (mPanIN) by acinar cell targeting of oncogenic Kras in adult mice. *Proc Natl Acad Sci USA*. 105(48):18913–8 (2008).

42. Shi G, DiRenzo D, Qu C, Barney D, Miley D, Konieczny SF. Maintenance of acinar cell organization is critical to preventing Kras-induced acinar-ductal metaplasia. *Oncogene*. 32(15):1950–8 (2013).

43. Ray KC, Bell KM, Yan J, Gu G, Chung CH, Washington MK, et al. Epithelial tissues have varying degrees of susceptibility to KrasG12D-initiated tumorigenesis in a mouse model. *PLoS One*. 6(2):e16786 (2011).

44. Stanger BZ, Stiles B, Lauwers GY, Bardeesy N, Mendoza M, Wang Y, et al. Pten constrains centroacinar cell expansion and malignant transformation in the pancreas. *Cancer Cell*. 8(9):185–95 (2005).

45. Kopp JL, von Figura G, Mayes E, Liu FF, Dubois CL, Morris JP, et al. Identification of Sox9-Dependent Acinar-to-Ductal Reprogramming as the Principal Mechanism for Initiation of Pancreatic Ductal Adenocarcinoma. *Cancer Cell*. 22(6):737–50 (2012).

46. Li C, Heidt DG, Dalerba P, Burant CF, Zhang L, Adsay V, et al. Identification of pancreatic cancer stem cells. *Cancer Res*. 67(3):1030–7 (2007).

47. Van Heek NT, Meeker AK, Kern SE, Yeo CJ, Lillemoe KD, Cameron JL, et al. Telomere shortening is nearly universal in pancreatic intraepithelial neoplasia. *Am J Pathol*. 161(5):1541–7 (2002).

48. Matsuda Y, Ishiwata T, Izumiyama-Shimomura N, Hamayasu H, Fujiwara M, Tomita K-I, et al. Gradual telomere shortening and increasing chromosomal instability among PanIN grades and normal ductal epithelia with and without cancer in the pancreas. *PLoS One*. 10(2):e0117575 (2015).

49. Feijoo P, Dominguez D, Tusell L, Genesca A. Telomere-dependent genomic integrity: evolution of the fusion-bridge-breakage cycle concept. *Curr Pharm Des*. 20(41):6375–85 (2014).

50. Kong CM, Lee XW, Wang X. Telomere shortening in human diseases. *FEBS J*. 280(14):3180–93 (2013).

51. O'Hagan RC, Chang S, Maser RS, Mohan R, Artandi SE, Chin L, et al. Telomere dysfunction provokes regional amplification and deletion in cancer genomes. *Cancer Cell*. 2(2):149–55 (2002).

52. Chin L, Artandi SE, Shen Q, Tam A, Lee SL, Gottlieb GJ, et al. p53 deficiency rescues the adverse effects of telomere loss and cooperates with telomere dysfunction to accelerate carcinogenesis. *Cell*. 97(4):527–38 (1999).

53. Gisselsson D, Jonson T, Petersén A, Strömbeck B, Dal Cin P, Höglund M, et al. Telomere dysfunction triggers extensive DNA fragmentation and evolution of complex chromosome abnormalities in human malignant tumors. *Proc Natl Acad Sci USA*. 98(22):12683–8 (2001).

54. Artandi SE, Chang S, Lee SL, Alson S, Gottlieb GJ, Chin L, et al. Telomere dysfunction promotes non-reciprocal translocations and epithelial cancers in mice. *Nature*. 406(6796):641–5 (2000).

55. Hao X-D, Yang Y, Song X, Zhao X-K, Wang L-D, He J-D, et al. Correlation of telomere length shortening with TP53 somatic mutations, polymorphisms and allelic loss in breast tumors and esophageal cancer. *Oncol Rep*. 29(1):226–36 (2013).

56. Yachida S, Iacobuzio-Donahue CA. Evolution and dynamics of pancreatic cancer progression. *Oncogene*. 32(45):5253–60 (2013).

57. Jones S, Zhang X, Parsons DW, Lin JC-H, Leary RJ, Angenendt P, et al. Core signaling pathways in human pancreatic cancers revealed by global genomic analyses. *Science*. 321(5897):1801–6 (2008).

58. Biankin A V, Waddell N, Kassahn KS, Gingras M-C, Muthuswamy LB, Johns AL, et al. Pancreatic cancer genomes reveal aberrations in axon guidance pathway genes. *Nature*. 491(7424):399–405 (2012).

59. Jones S, Li M, Parsons DW, Zhang X, Wesseling J, Kristel P, et al. Somatic mutations in the chromatin remodeling gene ARID1A occur in several tumor types. *Hum Mutat*. 33(1):100–3 (2012).

60. Shain AH, Giacomini CP, Matsukuma K, Karikari CA, Bashyam MD, Hidalgo M, et al. Convergent structural alterations define SWItch/Sucrose NonFermentable (SWI/SNF) chromatin remodeler as a central tumor suppressive complex in pancreatic cancer. *Proc Natl Acad Sci USA*. 109(5):e252–9 (2012).

61. Shields JM, Pruitt K, McFall A, Shaub A, Der CJ. Understanding Ras: “it ain”t over ’til it’s over’. *Trends Cell Biol*. 10(4):147–54 (2000).

62. Lemoine NR, Jain S, Hughes CM, Staddon SL, Maillet B, Hall PA, et al. Ki-ras oncogene activation in preinvasive pancreatic cancer. *Gastroenterology*. 102(1):230–6 (1992).

63. Klimstra DS, Longnecker DS. K-ras mutations in pancreatic ductal proliferative lesions. *Am J Pathol*. 145(6):1547–50 (1994).

64. Hruban RH, van Mansfeld AD, Offerhaus GJ, van Weering DH, Allison DC, Goodman SN, et al. K-ras oncogene activation in adenocarcinoma of the human pancreas. A study of 82 carcinomas using a combination of mutant-enriched polymerase chain reaction analysis and allele-specific oligonucleotide hybridization. *Am J Pathol*. 143(2):545–54 (1993).

65. Tada M, Ohashi M, Shiratori Y, Okudaira T, Komatsu Y, Kawabe T, et al. Analysis of K-ras gene mutation in hyperplastic duct cells of the pancreas without pancreatic disease. *Gastroenterology*. 110(1):227–31 (1996).

66. Aguirre AJ, Bardeesy N, Sinha M, Lopez L, Tuveson DA, Horner J, et al. Activated Kras and Ink4a/Arf deficiency cooperate to produce metastatic pancreatic ductal adenocarcinoma. *Genes Dev*. 17(24):3112–26 (2003).

67. Hingorani SR, Petricoin EF, Maitra A, Rajapakse V, King C, Jacobetz MA, et al. Preinvasive and invasive ductal pancreatic cancer and its early detection in the mouse. *Cancer Cell*. 4(6):437–50 (2003).

68. Campbell SL, Khosravi-Far R, Rossman KL, Clark GJ, Der CJ. Increasing complexity of Ras signaling. *Oncogene*. 17(11):1395–413 (1998).

69. Godwin P, Baird AM, Heavey S, Barr MP, O'Byrne KJ, Gately K. Targeting nuclear factor-kappa B to overcome resistance to chemotherapy. *Front Oncol*. 3:120 (2013).

70. Hustinx SR, Leoni LM, Yeo CJ, Brown PN, Goggins M, Kern SE, et al. Concordant loss of MTAP and p16/CDKN2A expression in pancreatic intraepithelial neoplasia: evidence of homozygous deletion in a noninvasive precursor lesion. *Mod Pathol*. 18(7):959–63 (2005).

71. Rozenblum E, Schutte M, Goggins M, Hahn SA, Panzer S, Zahurak M, et al. Tumor-suppressive pathways in pancreatic carcinoma. *Cancer Res*. 57(9):1731–4 (1997).

72. Whelan AJ, Bartsch D, Goodfellow PJ. Brief report: a familial syndrome of pancreatic cancer and melanoma with a mutation in the CDKN2 tumor-suppressor gene. *N Engl J Med*. 333(15):975–7 (1995).

73. Goldstein AM, Fraser MC, Struewing JP, Hussussian CJ, Ranade K, Zametkin DP, et al. Increased risk of pancreatic cancer in melanoma-prone kindreds with p16INK4 mutations. *N Engl J Med*. 333(15):970–4 (1995).

74. Sharpless NE, DePinho RA. Cancer: crime and punishment. *Nature*. 436(7051):636–7 (2005).

75. Yachida S, Iacobuzio-Donahue CA. The pathology and genetics of metastatic pancreatic cancer. *Arch Pathol Lab Med*. 133(3):413–22 (2009).

76. Dunne RF, Hezel AF. Genetics and Biology of Pancreatic Ductal Adenocarcinoma. *Hematol Oncol Clin North Am*. 29(4):595–608 (2015).

77. Maitra A, Adsay NV, Argani P, Iacobuzio-Donahue C, De Marzo A, Cameron JL, et al. Multicomponent analysis of the pancreatic adenocarcinoma progression model using a pancreatic intraepithelial neoplasia tissue microarray. *Mod Pathol*. 16(9):902–12 (2003).

78. Boschman CR, Stryker S, Reddy JK, Rao MS. Expression of p53 protein in precursor lesions and adenocarcinoma of human pancreas. *Am J Pathol*. 145(6):1291–5 (1994).

79. Maitra A, Fukushima N, Takaori K, Hruban RH. Precursors to invasive pancreatic cancer. *Adv Anat Pathol*. 12(2):81–91 (2005).

80. Morton JP, Timpson P, Karim SA, Ridgway RA, Athineos D, Doyle B, et al. Mutant p53 drives metastasis and overcomes growth arrest/senescence in pancreatic cancer. *Proc Natl Acad Sci USA*. 107(1):246–51 (2010).

81. Weissmueller S, Manchado E, Saborowski M, Morris JP, Wagenblast E, Davis CA, et al. Mutant p53 drives pancreatic cancer metastasis through cell-autonomous PDGF receptor β signaling. *Cell*. 157(2):382–94 (2014).

82. Massagué J, Blain SW, Lo RS. TGFbeta signaling in growth control, cancer, and heritable disorders. *Cell*. 103(2):295–309 (2000).

83. Massagué J. TGF-beta in Cancer. *Cell*. 134(2):215–30 (2008).

84. Xu J, Lamouille S, Derynck R. TGF-beta-induced epithelial to mesenchymal transition. *Cell Res*. 19(2):156–72 (2009).

85. Clark RA, McCoy GA, Folkvord JM, McPherson JM. TGF-beta 1 stimulates cultured human fibroblasts to proliferate and produce tissue-like fibroplasia: a fibronectin matrix-dependent event. *J Cell Physiol*. 170(1):69–80 (1997).

86. Wilentz RE, Iacobuzio-Donahue CA, Argani P, McCarthy DM, Parsons JL, Yeo CJ, et al. Loss of expression of Dpc4 in pancreatic intraepithelial neoplasia: evidence that DPC4 inactivation occurs late in neoplastic progression. *Cancer Res*. 60(7):2002–6 (2000).

87. Hahn SA, Schutte M, Hoque AT, Moskaluk CA, da Costa LT, Rozenblum E, et al. DPC4, a candidate tumor suppressor gene at human chromosome 18q21.1. *Science*. 271(5247):350–3 (1996).

88. Wilentz RE, Su GH, Dai JL, Sparks AB, Argani P, Sohn TA, et al. Immunohistochemical labeling for dpc4 mirrors genetic status in pancreatic adenocarcinomas : a new marker of DPC4 inactivation. *Am J Pathol*. 156(1):37–43 (2000).

89. Ellenrieder V, Hendler SF, Boeck W, Seufferlein T, Menke A, Ruhland C, et al. Transforming growth factor beta1 treatment leads to an epithelial-mesenchymal transdifferentiation of pancreatic cancer cells requiring extracellular signal-regulated kinase 2 activation. *Cancer Res*. 61(10):4222–8 (2001).

90. Ellenrieder V, Hendler SF, Ruhland C, Boeck W, Adler G, Gress TM. TGF-beta-induced invasiveness of pancreatic cancer cells is mediated by matrix metalloproteinase-2 and the urokinase plasminogen activator system. *Int J Cancer*. 93(2):204–11 (2001).

91. Murakami M, Suzuki M, Nishino Y, Funaba M. Regulatory expression of genes related to metastasis by TGF-beta and activin A in B16 murine melanoma cells. *Mol Biol Rep*. 37(3):1279–86 (2010).

92. Nishimori H, Ehata S, Suzuki HI, Katsuno Y, Miyazono K. Prostate cancer cells and bone stromal cells mutually interact with each other through bone morphogenetic protein-mediated signals. *J Biol Chem*. 287(24):20037–46 (2012).

93. Karagiannis GS, Musrap N, Saraon P, Treacy A, Schaeffer DF, Kirsch R, et al. Bone morphogenetic protein antagonist gremlin-1 regulates colon cancer progression. *Biol Chem*. 396(2):163–83 (2015).

94. Alarmo E-L, Kallioniemi A. Bone morphogenetic proteins in breast cancer: dual role in tumourigenesis? *Endocr Relat Cancer*. 17(2):R123–39 (2010).

95. Watanabe I, Sasaki S, Konishi M, Nakagohri T, Inoue K, Oda T, et al. Onset symptoms and tumor locations as prognostic factors of pancreatic cancer. *Pancreas*. 28(2):160–5 (2004).

96. Artinyan A, Soriano PA, Prendergast C, Low T, Ellenhorn JDI, Kim J. The anatomic location of pancreatic cancer is a prognostic factor for survival. *HPB* (Oxford). 10(5):371–6 (2008).

97. Porta M, Fabregat X, Malats N, Guarner L, Carrato A, de Miguel A, et al. Exocrine pancreatic cancer: symptoms at presentation and their relation to tumour site and stage. *Clin Transl Oncol*. 7(5):189–97 (2005).

98. Smith EB. Carcinoma of the pancreas--early diagnostic presumptive signs. *J Natl Med Assoc*. 66(6):496–8 (1974).

99. Chari ST, Leibson CL, Rabe KG, Ransom J, de Andrade M, Petersen GM. Probability of pancreatic cancer following diabetes: a population-based study. *Gastroenterology*. 129(2):504–11 (2005).

100. Pezzilli R, Pagano N. Is diabetes mellitus a risk factor for pancreatic cancer? World J *Gastroenterology*. 19(30):4861–6 (2013).

101. Pinzon R, Drewinko B, Trujillo JM, Guinee V, Giacco G. Pancreatic carcinoma and Trousseau's syndrome: experience at a large cancer center. *J Clin Oncol*. 4(4):509–14 (1986).

102. Goonetilleke KS, Siriwardena AK. Systematic review of carbohydrate antigen (CA 19-9) as a biochemical marker in the diagnosis of pancreatic cancer. *Eur J Surg Oncol*. 33(3):266–70 (2007).

103. Guo Q, Kang M, Zhang B, Chen Y, Dong X, Wu Y. Elevated levels of CA 19-9 and CEA in pancreatic cancer-associated diabetes. *J Cancer Res Clin Oncol*. 136(11):1627–31 (2010).

104. Brand RE, Nolen BM, Zeh HJ, Allen PJ, Eloubeidi MA, Goldberg M, et al. Serum biomarker panels for the detection of pancreatic cancer. *Clin Cancer Res*. 17(4):805–16 (2011).

105. Safi F, Schlosser W, Falkenreck S, Beger HG. Prognostic value of CA 19-9 serum course in pancreatic cancer. *Hepatogastroenterology*. 45(19):253–9 (1998).

106. Montgomery RC, Hoffman JP, Riley LB, Rogatko A, Ridge JA, Eisenberg BL. Prediction of recurrence and survival by post-resection CA 19-9 values in patients with adenocarcinoma of the pancreas. *Ann Surg Oncol*. 4(7):551–6 (1997).

107. Narimatsu H, Iwasaki H, Nakayama F, Ikehara Y, Kudo T, Nishihara S, et al. Lewis and secretor gene dosages affect CA19-9 and DU-PAN-2 serum levels in normal individuals and colorectal cancer patients. *Cancer Res*. 58(3):512–8 (1998).

108. Tempero MA, Uchida E, Takasaki H, Burnett DA, Steplewski Z, Pour PM. Relationship of carbohydrate antigen 19-9 and Lewis antigens in pancreatic cancer. *Cancer Res*. 47(20):5501–3 (1987).

109. Fong ZV, Winter JM. Biomarkers in pancreatic cancer: diagnostic, prognostic, and predictive. *Cancer J*. 18(6):530–8 (2012).

110. Raman SP, Horton KM, Fishman EK. Multimodality imaging of pancreatic cancer-computed tomography, magnetic resonance imaging, and positron emission tomography. *Cancer J*. 18(6):511–22 (2012).

111. Ahn SS, Kim M-J, Choi J-Y, Hong H-S, Chung YE, Lim JS. Indicative findings of pancreatic cancer in prediagnostic CT. *Eur Radiol*. 19(10):2448–55 (2009).

112. Tummala P, Junaidi O, Agarwal B. Imaging of pancreatic cancer: An overview. *J Gastrointest Oncol*. 2(3):168–74 (2011).

113. Horton KM, Fishman EK. Adenocarcinoma of the pancreas: CT imaging. *Radiol Clin North Am*. 40(6):1263–72 (2002).

114. Buchs NC, Chilcott M, Poletti P-A, Buhler LH, Morel P. Vascular invasion in pancreatic cancer: Imaging modalities, preoperative diagnosis and surgical management. *World J Gastroenterol*. 16(7):818–31 (2010).

115. Arvold ND, Niemierko A, Mamon HJ, Fernandez-del Castillo C, Hong TS. Pancreatic cancer tumor size on CT scan versus pathologic specimen: implications for radiation treatment planning. *Int J Radiat Oncol Biol Phys*. 80(5):1383–90 (2011).

116. Miura F, Takada T, Amano H, Yoshida M, Furui S, Takeshita K. Diagnosis of pancreatic cancer. *HPB* (Oxford). 8(5):337–42 (2006).

117. Grassetto G, Rubello D. Role of FDG-PET/CT in diagnosis, staging, response to treatment, and prognosis of pancreatic cancer. *Am J Clin Oncol*. 34(2):111–4 (2011).

118. Vauthey J-N, Dixon E. AHPBA/SSO/SSAT Consensus Conference on Resectable and Borderline Resectable Pancreatic Cancer: rationale and overview of the conference. *Ann Surg Oncol*. 16(7):1725–6 (2009).

119. Konstantinidis IT, Warshaw AL, Allen JN, Blaszkowsky LS, Castillo CF-D, Deshpande V, et al. Pancreatic ductal adenocarcinoma: is there a survival difference for R1 resections versus locally advanced unresectable tumors? What is a "true" R0 resection? *Ann Surg*. 257(4):731–6 (2013).

120. Badger SA, Brant JL, Jones C, McClements J, Loughrey MB, Taylor MA, et al. The role of surgery for pancreatic cancer: a 12-year review of patient outcome. *Ulster Med J*. 79(2):70–5 (2010).

121. Bachmann J, Michalski CW, Martignoni ME, Büchler MW, Friess H. Pancreatic resection for pancreatic cancer. *HPB* (Oxford). 8(5):346–51 (2006).

122. Yeo TP, Hruban RH, Leach SD, Wilentz RE, Sohn TA, Kern SE, et al. Pancreatic cancer. *Curr Probl Cancer*. 26(4):176–275 (2002).

123. Ghaneh P, Costello E, Neoptolemos JP. Biology and management of pancreatic cancer. *Postgrad Med J*. 84(995):478–97 (2008).

124. Beger HG, Rau B, Gansauge F, Leder G, Schwarz M, Poch B. Pancreatic cancer--low survival rates. *Dtsch Arztebl Int*. 105(14):255–62 (2008).

125. Ying J-E, Zhu L-M, Liu B-X. Developments in metastatic pancreatic cancer: is gemcitabine still the standard? *World J Gastroenterol*. 18(8):736–45 (2012).

126. Walker EJ, Ko AH. Beyond first-line chemotherapy for advanced pancreatic cancer: an expanding array of therapeutic options? *World J Gastroenterol*. 20(9):2224–36 (2014).

127. Ko a. H. Progress in the Treatment of Metastatic Pancreatic Cancer and the Search for Next Opportunities. *J Clin Oncol*. 33(16):1779-86 (2015).

128. Gourgou-Bourgade S, Bascoul-Mollevi C, Desseigne F, Ychou M, Bouché O, Guimbaud R, et al. Impact of FOLFIRINOX compared with gemcitabine on quality of life in patients with metastatic pancreatic cancer: results from the PRODIGE 4/ACCORD 11 randomized trial. *J Clin Oncol*. 31(1):23–9 (2013).

129. Von Hoff DD, Ervin T, Arena FP, Chiorean EG, Infante J, Moore M, et al. Increased survival in pancreatic cancer with nab-paclitaxel plus gemcitabine. *N Engl J Med*. 369(18):1691–703 (2013).

130. Troiani T, Martinelli E, Capasso A, Morgillo F, Orditura M, De Vita F, et al. Targeting EGFR in pancreatic cancer treatment. *Curr Drug Targets*. 13(6):802–10 (2012).

131. Moore MJ, Goldstein D, Hamm J, Figer A, Hecht JR, Gallinger S, et al. Erlotinib plus gemcitabine compared with gemcitabine alone in patients with advanced pancreatic cancer: a phase III trial of the National Cancer Institute of Canada Clinical Trials Group. *J Clin Oncol*. 25(15):1960–6 (2007).

132. Minchinton AI, Tannock IF. Drug penetration in solid tumours. *Nat Rev Cancer*. 6(8):583–92 (2006).

133. Trédan O, Galmarini CM, Patel K, Tannock IF. Drug resistance and the solid tumor microenvironment. *J Natl Cancer Inst*. 99(19):1441–54 (2007).

134. Feig C, Gopinathan A, Neesse A, Chan DS, Cook N, Tuveson DA. The pancreas cancer microenvironment. *Clin Cancer Res*. 18(16):4266–76 (2012).

135. Wang Z, Li J, Chen X, Duan W, Ma Q, Li X. Disrupting the balance between tumor epithelia and stroma is a possible therapeutic approach for pancreatic cancer. *Med Sci Monit*. 20:2002–6 (2014).

136. Rhim AD, Oberstein PE, Thomas DH, Mirek ET, Palermo CF, Sastra SA, et al. Stromal elements act to restrain, rather than support, pancreatic ductal adenocarcinoma. *Cancer Cell*. 25(6):735–47 (2014).

137. Clark CE, Beatty GL, Vonderheide RH. Immunosurveillance of pancreatic adenocarcinoma: insights from genetically engineered mouse models of cancer. *Cancer Lett*. 279(1):1–7 (2009).

138. Royal RE, Levy C, Turner K, Mathur A, Hughes M, Kammula US, et al. Phase 2 trial of single agent Ipilimumab (anti-CTLA-4) for locally advanced or metastatic pancreatic adenocarcinoma. *J Immunother*. 33(8):828–33 (2010).

139. Ungefroren H, Voss M, Bernstorff W V, Schmid A, Kremer B, Kalthoff H. Immunological escape mechanisms in pancreatic carcinoma. *Ann N Y Acad Sci*. 880:243–51 (1999).

140. Von Bernstorff W, Voss M, Freichel S, Schmid A, Vogel I, Jöhnk C, et al. Systemic and local immunosuppression in pancreatic cancer patients. *Clin Cancer Res*. 7(3):925s – 932s (2001).

141. Bernstorff W V, Glickman JN, Odze RD, Farraye FA, Joo HG, Goedegebuure PS, et al. Fas (CD95/APO-1) and Fas ligand expression in normal pancreas and pancreatic tumors. Implications for immune privilege and immune escape. *Cancer*. 94(10):2552–60 (2002).

142. Collins MA, Bednar F, Zhang Y, Brisset J-C, Galbán S, Galbán CJ, et al. Oncogenic Kras is required for both the initiation and maintenance of pancreatic cancer in mice. *J Clin Invest*. 122(2):639–53 (2012).

143. Eser S, Schnieke A, Schneider G, Saur D. Oncogenic KRAS signalling in pancreatic cancer. *Br J Cancer*. 111(5):817–22 (2014).

144. Stephen AG, Esposito D, Bagni RK, McCormick F. Dragging ras back in the ring. *Cancer Cell*. 25(3):272–81 (2014).

145. Ostrem JM, Peters U, Sos ML, Wells JA, Shokat KM. K-Ras(G12C) inhibitors allosterically control GTP affinity and effector interactions. *Nature*. 503(7477):548–51 (2013).

146. Lim SM, Westover KD, Ficarro SB, Harrison RA, Choi HG, Pacold ME, et al. Therapeutic targeting of oncogenic K-Ras by a covalent catalytic site inhibitor. *Angew Chem Int Ed Engl*. 53(1):199–204 (2014).

147. Boulton F. A hundred years of cascading - started by Paul Morawitz (1879-1936), a pioneer of haemostasis and of transfusion. *Transfus Med*. 16(1):1–10 (2006).

148. Bach R, Nemerson Y, Konigsberg W. Purification and characterization of bovine tissue factor. *J Biol Chem*. 256(16):8324–31 (1981).

149. Spicer EK, Horton R, Bloem L, Bach R, Williams KR, Guha A, et al. Isolation of cDNA clones coding for human tissue factor: primary structure of the protein and cDNA. *Proc Natl Acad Sci USA*. 84(15):5148–52 (1987).

150. Morrissey JH, Fakhrai H, Edgington TS. Molecular cloning of the cDNA for tissue factor, the cellular receptor for the initiation of the coagulation protease cascade. *Cell*. 50(1):129–35 (1987).

151. Mackman N. Role of tissue factor in hemostasis, thrombosis, and vascular development. *Arterioscler Thromb Vasc Biol*. 24(6):1015–22 (2004).

152. Fisher KL, Gorman CM, Vehar GA, O'Brien DP, Lawn RM. Cloning and expression of human tissue factor cDNA. *Thromb Res*. 48(1):89–99 (1987).

153. Scarpati EM, Wen D, Broze GJ, Miletich JP, Flandermeyer RR, Siegel NR, et al. Human tissue factor: cDNA sequence and chromosome localization of the gene. *Biochemistry*. 26(17):5234–8 (1987).

154. Chen VM, Hogg PJ. Allosteric disulfide bonds in thrombosis and thrombolysis. *J Thromb Haemost*. 4(12):2533–41 (2006).

155. Bogdanov VY, Balasubramanian V, Hathcock J, Vele O, Lieb M, Nemerson Y. Alternatively spliced human tissue factor: a circulating, soluble, thrombogenic protein. *Nat Med*. 9(4):458–62 (2003).

156. Bogdanov VY, Osterud B. Cardiovascular complications of diabetes mellitus: The Tissue Factor perspective. *Thromb Res*. 125(2):112–8 (2010).

157. Szotowski B, Antoniak S, Poller W, Schultheiss H-P, Rauch U. Procoagulant soluble tissue factor is released from endothelial cells in response to inflammatory cytokines. *Circ Res*. 96(12):1233–9 (2005).

158. Censarek P, Bobbe A, Grandoch M, Schrör K, Weber A-A. Alternatively spliced human tissue factor (asHTF) is not pro-coagulant. *Thromb Haemost*. 97(1):11–4 (2007).

159. Srinivasan R, Bogdanov VY. Splice variants of Tissue Factor and integrin-mediated signaling. *Thromb Res*. 129(2):S34–7 (2012).

160. Osterud B, Breimo ES, Olsen JO. Blood borne tissue factor revisited. *Thromb Res*. 122(3):432–4 (2008).

161. Bogdanov VY, Cimmino G, Tardos JG, Tunstead JR, Badimon JJ. Assessment of plasma tissue factor activity in patients presenting with coronary artery disease: limitations of a commercial assay. *J Thromb Haemost*. 7(5):894–7 (2009).

162. Van den Berg YW, Osanto S, Reitsma PH, Versteeg HH. The relationship between tissue factor and cancer progression: insights from bench and bedside. *Blood*. 119(4):924–32 (2012).

163. Butenas S, Orfeo T, Mann KG. Tissue factor in coagulation: Which? Where? When? *Arterioscler Thromb Vasc Biol*. 29(12):1989–96 (2009).

164. Konigsberg W, Kirchhofer D, Riederer MA, Nemerson Y. The TF:VIIa complex: clinical significance, structure-function relationships and its role in signaling and metastasis. *Thromb Haemost*. 86(3):757–71 (2001).

165. Khorana AA, Fine RL. Pancreatic cancer and thromboembolic disease. *Lancet Oncol*. 5(11):655–63 (2004).

166. Noble S, Pasi J. Epidemiology and pathophysiology of cancer-associated thrombosis. *Br J Cancer*. 102(1):S2–9 (2010).

167. Blom JW. Malignancies, Prothrombotic Mutations, and the Risk of Venous Thrombosis. *JAMA*. 293(6):715 (2005).

168. Yu JL, May L, Lhotak V, Shahrzad S, Shirasawa S, Weitz JI, et al. Oncogenic events regulate tissue factor expression in colorectal cancer cells: implications for tumor progression and angiogenesis. *Blood*. 105(4):1734–41 (2005).

169. Rao B, Gao Y, Huang J, Gao X, Fu X, Huang M, et al. Mutations of p53 and K-ras correlate TF expression in human colorectal carcinomas: TF downregulation as a marker of poor prognosis. *Int J Colorectal Dis*. 26(5):593–601 (2011).

170. Magnus N, Garnier D, Rak J. Oncogenic epidermal growth factor receptor up-regulates multiple elements of the tissue factor signaling pathway in human glioma cells. *Blood*. 116(5):815–8 (2010).

171. Rong Y, Post DE, Pieper RO, Durden DL, Van Meir EG, Brat DJ. PTEN and hypoxia regulate tissue factor expression and plasma coagulation by glioblastoma. *Cancer Res*. 65(4):1406–13 (2005).

172. Vrana JA, Stang MT, Grande JP, Getz MJ. Expression of tissue factor in tumor stroma correlates with progression to invasive human breast cancer: paracrine regulation by carcinoma cell-derived members of the transforming growth factor beta family. *Cancer Res*. 56(21):5063–70 (1996).

173. Sun L, Liu Y, Lin S, Shang J, Liu J, Li J, et al. Early growth response gene-1 and hypoxia-inducible factor-1α affect tumor metastasis via regulation of tissue factor. *Acta Oncol*. 52(4):842–51 (2013).

174. Bastarache JA, Sebag SC, Grove BS, Ware LB. Interferon-γ and tumor necrosis factor-α act synergistically to up-regulate tissue factor in alveolar epithelial cells. *Exp Lung Res*. 37(8):509–17 (2011).

175. Kakkar AK, Lemoine NR, Scully MF, Tebbutt S, Williamson RC. Tissue factor expression correlates with histological grade in human pancreatic cancer. *Br J Surg*. 82(8):1101–4 (1995).

176. Nitori N, Ino Y, Nakanishi Y, Yamada T, Honda K, Yanagihara K, et al. Prognostic significance of tissue factor in pancreatic ductal adenocarcinoma. *Clin Cancer Res*. 11(7):2531–9 (2005).

177. Koomägi R, Volm M. Tissue-factor expression in human non-small-cell lung carcinoma measured by immunohistochemistry: correlation between tissue factor and angiogenesis. *Int J Cancer*. 79(1):19–22 (1998).

178. Khorana AA, Ahrendt SA, Ryan CK, Francis CW, Hruban RH, Hu YC, et al. Tissue factor expression, angiogenesis, and thrombosis in pancreatic cancer. *Clin Cancer Res*. 13(10):2870–5 (2007).

179. Versteeg HH, Schaffner F, Kerver M, Petersen HH, Ahamed J, Felding-Habermann B, et al. Inhibition of tissue factor signaling suppresses tumor growth. *Blood*. 111(1):190–9 (2008).

180. Hembrough TA, Swartz GM, Papathanassiu A, Vlasuk GP, Rote WE, Green SJ, et al. Tissue factor/factor VIIa inhibitors block angiogenesis and tumor growth through a nonhemostatic mechanism. *Cancer Res*. 63(11):2997–3000 (2003).

181. Abe K, Shoji M, Chen J, Bierhaus A, Danave I, Micko C, et al. Regulation of vascular endothelial growth factor production and angiogenesis by the cytoplasmic tail of tissue factor. *Proc Natl Acad Sci USA*. 96(15):8663–8 (1999).

182. Müller M, Albrecht S, Gölfert F, Hofer A, Funk RH, Magdolen V, et al. Localization of tissue factor in actin-filament-rich membrane areas of epithelial cells. *Exp Cell Res*. 248(1):136–47 (1999).

183. Marutsuka K, Hatakeyama K, Sato Y, Yamashita A, Sumiyoshi A, Asada Y. Protease-activated receptor 2 (PAR2) mediates vascular smooth muscle cell migration induced by tissue factor/factor VIIa complex. *Thromb Res*. 107(5):271–6 (2002).

184. Zhu T, Mancini JA, Sapieha P, Yang C, Joyal J-S, Honoré J-C, et al. Cortactin activation by FVIIa/tissue factor and PAR2 promotes endothelial cell migration. *Am J Physiol Regul Integr Comp Physiol*. 300(3):R577–85 (2011).

185. Hobbs JE, Zakarija A, Cundiff DL, Doll J a, Hymen E, Cornwell M, et al. Alternatively spliced human tissue factor promotes tumor growth and angiogenesis in a pancreatic cancer tumor model. *Thromb Res*. Jan;120(1):S13–21 (2007).

186. Van den Berg YW, van den Hengel LG, Myers HR, Ayachi O, Jordanova E, Ruf W, et al. Alternatively spliced tissue factor induces angiogenesis through integrin ligation. *Proc Natl Acad Sci USA*. 106(46):19497–502 (2009).

187. Millard M, Odde S, Neamati N. Integrin targeted therapeutics. *Theranostics*. 1:154–88 (2011).

188. Hood JD, Cheresh DA. Role of integrins in cell invasion and migration. *Nat Rev Cancer*. 2(2):91–100 (2002).

189. Jemal A, Siegel R, Ward E, Hao Y, Xu J, Murray T, et al. Cancer statistics. *Cancer J Clin*. 58(2):71–96 (2008).

190. Rak J, Yu JL, Luyendyk J, Mackman N. Oncogenes, trousseau syndrome, and cancer-related changes in the coagulome of mice and humans. *Cancer Res*. 66(22):10643–6 (2006).

191. Tesselaar MET, Romijn FPHTM, Van Der Linden IK, Prins F a., Bertina RM, Osanto S. Microparticle-associated tissue factor activity: A link between cancer and thrombosis? *J Thromb Haemost*. 5:520–7 (2007).

192. Zwicker JI, Liebman HA, Neuberg D, Lacroix R, Bauer KA, Furie BC, et al. Tumor-derived tissue factor-bearing microparticles are associated with venous thromboembolic events in malignancy. *Clin Cancer Res*. 15(22):6830–40 (2009).

193. Thomas GM, Panicot-Dubois L, Lacroix R, Dignat-George F, Lombardo D, Dubois C. Cancer cell-derived microparticles bearing P-selectin glycoprotein ligand 1 accelerate thrombus formation in vivo. *J Exp Med*. 206(9):1913–27 (2009).

194. Srinivasan R, Ozhegov E, van den Berg YW, Aronow BJ, Franco RS, Palascak MB, et al. Splice variants of tissue factor promote monocyte-endothelial interactions by triggering the expression of cell adhesion molecules via integrin-mediated signaling. *J Thromb Haemost*. 9(10):2087–96 (2011).

195. Sawai H, Okada Y, Funahashi H, Matsuo Y, Takahashi H, Takeyama H, et al. Interleukin-1alpha enhances the aggressive behavior of pancreatic cancer cells by regulating the alpha6beta1-integrin and urokinase plasminogen activator receptor expression. *BMC Cell Biol*. 7:8 (2006).

196. Goldin-Lang P, Tran Q-V, Fichtner I, Eisenreich A, Antoniak S, Schulze K, et al. Tissue factor expression pattern in human non-small cell lung cancer tissues indicate increased blood thrombogenicity and tumor metastasis. *Oncol Rep*. 20(1):123–8 (2008).

197. Rollin J, Regina S, Gruel Y. Tumor expression of alternatively spliced tissue factor is a prognostic marker in non-small cell lung cancer. *J Thromb Haemost*. 8(3):607–10 (2010).

198. Haas SL, Jesnowski R, Steiner M, Hummel F, Ringel J, Burstein C, et al. Expression of tissue factor in pancreatic adenocarcinoma is associated with activation of coagulation. *World J Gastroenterol*. 12(30):4843–9 (2006).

199. Tardos JG, Eisenreich a, Deikus G, Bechhofer DH, Chandradas S, Zafar U, et al. SR proteins ASF/SF2 and SRp55 participate in tissue factor biosynthesis in human monocytic cells. *J Thromb Haemost*. 6(5):877–84 (2008).

200. Kirchhofer D, Moran P, Chiang N, Kim J, Riederer MA, Eigenbrot C, et al. Epitope location on tissue factor determines the anticoagulant potency of monoclonal anti-tissue factor antibodies. *Thromb Haemost*. 84(6):1072–81 (2000).

201. Sipos B, Möser S, Kalthoff H, Török V, Löhr M, Klöppel G. A comprehensive characterization of pancreatic ductal carcinoma cell lines: towards the establishment of an in vitro research platform. *Virchows Arch*. 442(5):444–52 (2003).

202. Qi X, Chu Z, Mahller YY, Stringer KF, Witte DP, Cripe TP. Cancer-selective targeting and cytotoxicity by liposomal-coupled lysosomal saposin C protein. *Clin Cancer Res*. 15(18):5840–51 (2009).

203. Olive KP, Jacobetz MA, Davidson CJ, Gopinathan A, McIntyre D, Honess D, et al. Inhibition of Hedgehog signaling enhances delivery of chemotherapy in a mouse model of pancreatic cancer. *Science*. 324(5933):1457–61 (2009).

204. Morello V, Cabodi S, Sigismund S, Camacho-Leal MP, Repetto D, Volante M, et al. β1 integrin controls EGFR signaling and tumorigenic properties of lung cancer cells. *Oncogene*. 30(39):4087–96 (2011).

205. Balanis N, Yoshigi M, Wendt MK, Schiemann WP, Carlin CR. β3 integrin-EGF receptor cross-talk activates p190RhoGAP in mouse mammary gland epithelial cells. *Mol Biol Cell*. 22(22):4288–301 (2011).

206. Seeliger H, Camaj P, Ischenko I, Kleespies A, De Toni EN, Thieme SE, et al. EFEMP1 expression promotes in vivo tumor growth in human pancreatic adenocarcinoma. *Mol Cancer Res*. 7(2):189–98 (2009).

207. Yotsumoto F, Fukami T, Yagi H, Funakoshi A, Yoshizato T, Kuroki M, et al. Amphiregulin regulates the activation of ERK and Akt through epidermal growth factor receptor and HER3 signals involved in the progression of pancreatic cancer. *Cancer Sci*. 101(11):2351–60 (2010).

208. Schoppmann SF, Birner P, Stöckl J, Kalt R, Ullrich R, Caucig C, et al. Tumor-associated macrophages express lymphatic endothelial growth factors and are related to peritumoral lymphangiogenesis. *Am J Pathol*. 161(3):947–56 (2002).

209. Camaj P, Seeliger H, Ischenko I, Krebs S, Blum H, De Toni EN, et al. EFEMP1 binds the EGF receptor and activates MAPK and Akt pathways in pancreatic carcinoma cells. Biol Chem [Internet]. Dec [cited 2015 Jul 28];390(12):1293–302. Available from: http://www.ncbi.nlm.nih.gov/pubmed/19804359

210. Mizukami Y. Bone marrow-derived proangiogenic cells in pancreatic cancer. *J Gastroenterol Hepatol*. 27 Suppl 2:23–6 (2009).

211. Thaler J, Ay C, Mackman N, Bertina RM, Kaider A, Marosi C, et al. Microparticle-associated tissue factor activity, venous thromboembolism and mortality in pancreatic, gastric, colorectal and brain cancer patients. *J Thromb Haemost*. 10(7):1363–70 (2012).

212. Wang J-G, Geddings JE, Aleman MM, Cardenas JC, Chantrathammachart P, Williams JC, et al. Tumor-derived tissue factor activates coagulation and enhances thrombosis in a mouse xenograft model of human pancreatic cancer. *Blood*. 119(23):5543–52 (2012).

213. Ettelaie C, Collier MEW, Mei MP, Xiao YP, Maraveyas A. Enhanced binding of tissue factor-microparticles to collagen-IV and fibronectin leads to increased tissue factor activity in vitro. *Thromb Haemost*. 109(1):61–71 (2013).

214. Garnier D, Magnus N, Lee TH, Bentley V, Meehan B, Milsom C, et al. Cancer cells induced to express mesenchymal phenotype release exosome-like extracellular vesicles carrying tissue factor. *J Biol Chem*. 287(52):43565–72 (2012).

215. Key NS, Slungaard a, Dandelet L, Nelson SC, Moertel C, Styles L a, et al. Whole blood tissue factor procoagulant activity is elevated in patients with sickle cell disease. *Blood*. 91(11):4216–23 (1998).

216. Giesen PL, Rauch U, Bohrmann B, Kling D, Roqué M, Fallon JT, et al. Blood-borne tissue factor: another view of thrombosis. *Proc Natl Acad Sci USA*. 96(5):2311–5 (1999).

217. Egorina EM, Sovershaev M a, Bjørkøy G, Gruber FXE, Olsen JO, Parhami-Seren B, et al. Intracellular and surface distribution of monocyte tissue factor: application to intersubject variability. *Arterioscler Thromb Vasc Biol*. 25(7):1493–8 (2005).

218. Bogdanov VY. Blood coagulation and alternative pre-mRNA splicing: an overview. *Curr Mol Med*. 6(8):859–69 (2006).

219. Bogdanov VY, Kirk RI, Miller C, Hathcock JJ, Vele S, Gazdoiu M, et al. Identification and characterization of murine alternatively spliced tissue factor. *J Thromb Haemost*. 4(1):158–67 (2006).

220. Srinivasan R, Bogdanov VY. Alternatively spliced tissue factor: discovery, insights, clinical implications. *Front Biosci*. 16:3061–71 (2011).

221. Zumbach M, Hofmann M, Borcea V, Luther T, Kotzsch M, Müller M, et al. Tissue factor antigen is elevated in patients with microvascular complications of diabetes mellitus. *Exp Clin Endocrinol Diabetes*. 105(4):206–12 (1997).

222. Suefuji H, Ogawa H, Yasue H, Kaikita K, Soejima H, Motoyama T, et al. Increased plasma tissue factor levels in acute myocardial infarction. *Am Heart J*. 134(1):253–9 (1997).

223. Khorana a a, Francis CW, Menzies KE, Wang J-G, Hyrien O, Hathcock J, et al. Plasma tissue factor may be predictive of venous thromboembolism in pancreatic cancer. *J Thromb Haemost*. 6(11):1983–5 (2008).

224. Soejima H, Ogawa H, Yasue H, Kaikita K, Nishiyama K, Misumi K, et al. Heightened Tissue Factor Associated With Tissue Factor Pathway Inhibitor and Prognosis in Patients With Unstable Angina. *Circulation*. 99(22):2908–13 (1999).

225. Vaidyula VR, Rao a K, Mozzoli M, Homko C, Cheung P, Boden G. Effects of hyperglycemia and hyperinsulinemia on circulating tissue factor procoagulant activity and platelet CD40 ligand. *Diabetes*. 55(1):202–8 (2006).

226. Carr ME. Diabetes mellitus: a hypercoagulable state. *J Diabetes Complications*. 15(1):44–54 (2001).

227. Sambola A. Role of Risk Factors in the Modulation of Tissue Factor Activity and Blood Thrombogenicity. *Circulation*. 107(7):973–7 (2003).

228. Kocatürk B, Van den Berg YW, Tieken C, Mieog JSD, de Kruijf EM, Engels CC, et al. Alternatively spliced tissue factor promotes breast cancer growth in a β1 integrin-dependent manner. *Proc Natl Acad Sci USA*. 110(28):11517–22 (2013).

229. Unruh D, Turner K, Srinivasan R, Kocatürk B, Qi X, Chu Z, et al. Alternatively spliced tissue factor contributes to tumor spread and activation of coagulation in pancreatic ductal adenocarcinoma. *Int J Cancer*. 134:9–20 (2014).

230. Maithel SK, Maloney S, Winston C, Gönen M, D'Angelica MI, Dematteo RP, et al. Preoperative CA 19-9 and the yield of staging laparoscopy in patients with radiographically resectable pancreatic adenocarcinoma. *Ann Surg Oncol*. 15(12):3512–20 (2008).

231. Key NS, Mackman N, Ph D. Tissue Factor and Its Measurement in Whole. *Semin Thromb Hemost*. 36(8):865–75 (2010).

232. Davila M, Robles-Carrillo L, Unruh D, Huo Q, Gardiner C, Sargent IL, et al. Microparticle association and heterogeneity of tumor-derived tissue factor in plasma: is it important for coagulation activation? *J Thromb Haemost*. 12(2):186–96 (2014).

233. Ryan RJ, Lindsell CJ, Hollander JE, O'Neil B, Jackson R, Schreiber D, et al. A multicenter randomized controlled trial comparing central laboratory and point-of-care cardiac marker testing strategies: the Disposition Impacted by Serial Point of Care Markers in Acute Coronary Syndromes (DISPO-ACS) trial. *Ann Emerg Med*. 53(3):321–8 (2009).

234. Zawaski S, Hammes M, Balasubramanian V. Alternatively Spliced Human Tissue Factor and Thrombotic Tendencies in Hemodialysis Patients. *Int J Nephrol Urol*. 2(1):193–9 (2010).

235. Kim YC, Kim HJ, Park JH, Park D Il, Cho YK, Sohn C Il, et al. Can preoperative CA19-9 and CEA levels predict the resectability of patients with pancreatic adenocarcinoma? *J Gastroenterol Hepatol*. 24(12):1869–75 (2009).

236. Ueno H, Kosuge T, Matsuyama Y, Yamamoto J, Nakao A, Egawa S, et al. A randomised phase III trial comparing gemcitabine with surgery-only in patients with resected pancreatic cancer: Japanese Study Group of Adjuvant Therapy for Pancreatic Cancer. *Br J Cancer*. 101(6):908–15 (2009).

237. Winter JM, Yeo CJ, Brody JR. Diagnostic, prognostic, and predictive biomarkers in pancreatic cancer. *J Surg Oncol*. 107(1):15–22 (2013).

238. Ugorski M, Laskowska A. Sialyl Lewis(a): a tumor-associated carbohydrate antigen involved in adhesion and metastatic potential of cancer cells. *Acta Biochim Pol*. 49(2):303–11 (2002).

239. Rahib L, Smith BD, Aizenberg R, Rosenzweig AB, Fleshman JM, Matrisian LM. Projecting cancer incidence and deaths to 2030: The unexpected burden of thyroid, liver, and pancreas cancers in the united states. *Cancer Res*. 74:2913–21 (2014).

240. Emmerich J. Epidemiology of venous thrombosis. *Bull Acad Natl Med*. 187(10):19–32 (2003).

241. Rickles FR, Falanga A. Molecular basis for the relationship between thrombosis and cancer. *Thromb Res*. 102:215–24 (2001).

242. Falanga A, Panova-Noeva M, Russo L. Procoagulant mechanisms in tumour cells. *Best Pract Res Clin Haematol*. 22(1):49–60 (2009).

243. Grzesiak JJ, Ho JC, Moossa AR, Bouvet M. The integrin-extracellular matrix axis in pancreatic cancer. *Pancreas*. 35(4):293–301 (2007).

244. DeNardo DG, Brennan DJ, Rexhepaj E, Ruffell B, Shiao SL, Madden SF, et al. Leukocyte complexity predicts breast cancer survival and functionally regulates response to chemotherapy. *Cancer Discov*. 1(6):54–67 (2011).

245. Parry GCN, Erlich JH, Carmeliet P, Luther T, Mackman N. Low levels of tissue factor are compatible with development and hemostasis in mice. *J Clin Invest*. 101:560–9 (1998).

246. Yu J, May L, Milsom C, Anderson GM, Weitz JI, Luyendyk JP, et al. Contribution of host-derived tissue factor to tumor neovascularization. *Arterioscler Thromb Vasc Biol*. 28:1975–81 (2008).

247. Hynes RO. Integrins: Bidirectional, allosteric signaling machines. *Cell*. 110(1):673–87 (2002).

248. Courtney KD, Corcoran RB, Engelman JA. The PI3K pathway as drug target in human cancer. *J Clin Oncol*. 28(6):1075–83 (2010).

249. Stegeman H, Span PN, Kaanders JH a. M, Bussink J. Improving chemoradiation efficacy by PI3-K/AKT inhibition. *Cancer Treat Rev*. 40(10):1182–91 (2014).

250. Wei F, Zhang Y, Geng L, Zhang P, Wang G, Liu Y. mTOR inhibition induces EGFR feedback activation in association with its resistance to human pancreatic cancer. *Int J Mol Sci*. 16(2):3267–82 (2015).

251. Islam MR, Ellis IR, Macluskey M, Cochrane L, Jones SJ. Activation of Akt at T308 and S473 in alcohol, tobacco and HPV-induced HNSCC: is there evidence to support a prognostic or diagnostic role? *Exp Hematol Oncol*. 3(1):25 (2014).

252. Ruffell B, Coussens LM. Macrophages and Therapeutic Resistance in Cancer. *Cancer Cell*. 27(4):462–72 (2015).

253. Zhang Q, Liu L, Gong C, Shi H, Zeng Y, Wang X, et al. Prognostic significance of tumor-associated macrophages in solid tumor: a meta-analysis of the literature. *PLoS One*. 7(12):e50946 (2012).

254. Liu C-Y, Xu J-Y, Shi X-Y, Huang W, Ruan T-Y, Xie P, et al. M2-polarized tumor-associated macrophages promoted epithelial-mesenchymal transition in pancreatic cancer cells, partially through TLR4/IL-10 signaling pathway. *Lab Invest*. 93(7):844–54 (2013).

255. Mantovani A, Sozzani S, Locati M, Allavena P, Sica A. Macrophage polarization: Tumor-associated macrophages as a paradigm for polarized M2 mononuclear phagocytes. *Trends Immunol*. 23(11):549–55 (2002).

256. Le Page C, Marineau A, Bonza PK, Rahimi K, Cyr L, Labouba I, et al. BTN3A2 expression in epithelial ovarian cancer is associated with higher tumor infiltrating T cells and a better prognosis. *PLoS One*. 7(6):e38541 (2012).

257. Komohara Y, Jinushi M, Takeya M. Clinical significance of macrophage heterogeneity in human malignant tumors. *Cancer Sci*. 105(1):1–8 (2014).

258. Gil-Bernabé AM, Ferjančič Š, Tlalka M, Zhao L, Allen PD, Im JH, et al. Recruitment of monocytes/macrophages by tissue factor-mediated coagulation is essential for metastatic cell survival and premetastatic niche establishment in mice. *Blood*. 119(13):3164–75 (2012).

259. Simon DI, Chen Z, Xu H, Li CQ, Dong JF, McIntire L V, et al. Platelet glycoprotein ibalpha is a counterreceptor for the leukocyte integrin Mac-1 (CD11b/CD18). *J Exp Med*. 192(2):193–204 (2000).

260. Guerra C, Collado M, Navas C, Schuhmacher AJ, Hernández-Porras I, Cañamero M, et al. Pancreatitis-induced inflammation contributes to pancreatic cancer by inhibiting oncogene-induced senescence. *Cancer Cell*. 19:728–39 (2011).

261. Masamune A, Watanabe T, Kikuta K, Shimosegawa T. Roles of Pancreatic Stellate Cells in Pancreatic Inflammation and Fibrosis. *Clin Gastroenterol Hepatol*. 7(11):S48–54 (2009).

262. Erkan M, Hausmann S, Michalski CW, Fingerle AA, Dobritz M, Kleeff J, et al. The role of stroma in pancreatic cancer: diagnostic and therapeutic implications. *Nat Rev Gastroenterol Hepatol*. 9(8):454–67 (2012).

263. Tesselaar MET, Romijn FPHTM, Van Der Linden IK, Prins FA, Bertina RM, Osanto S. Microparticle-associated tissue factor activity: a link between cancer and thrombosis? *J Thromb Haemost*. 5(3):520–7 (2007).

264. Chandradas S, Deikus G, Tardos JG, Bogdanov VY. Antagonistic roles of four SR proteins in the biosynthesis of alternatively spliced tissue factor transcripts in monocytic cells. *J Leukoc Biol*. 87(1):147–52 (2010).

265. Stickeler E, Kittrell F, Medina D, Berget SM. Stage-specific changes in SR splicing factors and alternative splicing in mammary tumorigenesis. *Oncogene*. 18:3574–82 (1999).

266. Zerbe LK, Pino I, Pio R, Cosper PF, Dwyer-Nield LD, Meyer AM, et al. Relative amounts of antagonistic splicing factors, hnRNP A1 and ASF/SF2, change during neoplastic lung growth: Implications for pre-mRNA processing. *Mol Carcinog*. 41(4):187–96 (2004).

267. Hamdollah Zadeh M a., Amin EM, Hoareau-Aveilla C, Domingo E, Symonds KE, Ye X, et al. Alternative splicing of TIA-1 in human colon cancer regulates VEGF isoform expression, angiogenesis, tumour growth and bevacizumab resistance. *Mol Oncol*. 9:167–78 (2015).

268. He X, Arslan a D, Pool MD, Ho T-T, Darcy KM, Coon JS, et al. Knockdown of splicing factor SRp20 causes apoptosis in ovarian cancer cells and its expression is associated with malignancy of epithelial ovarian cancer. *Oncogene*. 30(7):356–65 (2011).

269. Unruh D, Sagin F, Adam M, Van Dreden P, Woodhams BJ, Hart K, et al. Levels of Alternatively Spliced Tissue Factor in the Plasma of Patients with Pancreatic Cancer May Help Predict Aggressive Tumor Phenotype. *Ann Surg Oncol*. May 12 epub ahead of print (2015).

270. Goodman SL, Picard M. Integrins as therapeutic targets. *Trends Pharmacol Sci*. 33(7):405–12 (2012).

271. Elyamany G, Alzahrani AM, Bukhary E. Cancer-associated thrombosis: an overview. *Clin Med Insights Oncol*. 8:129–37 (2014).

272. Sproul EE. Carcinoma and Venous Thrombosis: The Frequency of Association of Carcinoma in the Body or Tail of the Pancreas with Multiple Venous Thrombosis. *Am J Cancer*. 34(4):566–85 (1938).

273. Khorana AA, Fine RL. Pancreatic cancer and thromboembolic disease. *Lancet Oncol*. 5(11):655–63 (2004).

274. Silberberg JM, Gordon S, Zucker S. Identification of tissue factor in two human pancreatic cancer cell lines. *Cancer Res*. 49(19):5443–7 (1989).

275. Macfarlane RG. An enzyme cascade in the blood clotting mechanism, and its function as a biochemical amplifier. *Nature*. 202:498–9 (1964).

276. Davie EW, Ratnoff OD. Waterfall sequence for intrinsic blood clotting. *Science*. 145(3638):1310–2 (1964).

277. Porreca E, Di Febbo C, di Castelnuovo A, Baccante G, Amore C, Angelini A, et al. Association of factor VII levels with inflammatory parameters in hypercholesterolemic patients. *Atherosclerosis*. 165(1):159–66 (2002).

278. Zhang Y, Yan W, Collins MA, Bednar F, Rakshit S, Zetter BR, et al. Interleukin-6 is required for pancreatic cancer progression by promoting MAPK signaling activation and oxidative stress resistance. *Cancer Res*. 73(20):6359–74 (2013).

279. Kruithof EK, Agay D, Mestries JC, Gascon MP, Ythier A. The effect of factor Xa/phospholipid infusion on the acute phase response in baboons. *Thromb Haemost*. 77(2):308–11 (1997).

280. McLean K, Schirm S, Johns A, Morser J, Light DR. FXa-induced responses in vascular wall cells are PAR-mediated and inhibited by ZK-807834. *Thromb Res*. 103(4):281–97 (2001).

281. Senden NH, Jeunhomme TM, Heemskerk JW, Wagenvoord R, van't Veer C, Hemker HC, et al. Factor Xa induces cytokine production and expression of adhesion molecules by human umbilical vein endothelial cells. *J Immunol*. 161(8):4318–24 (1998).

282. Szaba FM, Smiley ST. Roles for thrombin and fibrin(ogen) in cytokine/chemokine production and macrophage adhesion in vivo. *Blood*. 99(3):1053–9 (2002).

283. Johnson K, Choi Y, DeGroot E, Samuels I, Creasey A, Aarden L. Potential mechanisms for a proinflammatory vascular cytokine response to coagulation activation. *J Immunol*. 160(10):5130–5 (1998).

284. Radjabi AR, Sawada K, Jagadeeswaran S, Eichbichler A, Kenny HA, Montag A, et al. Thrombin induces tumor invasion through the induction and association of matrix metalloproteinase-9 and beta1-integrin on the cell surface. *J Biol Chem*. 283(5):2822–34 (2008).

285. Pottegård A, Friis S, Hallas J. Cancer risk in long-term users of vitamin K antagonists: a population-based case-control study. *Int J Cancer*. 132(11):2606–12 (2013).

286. Barsam SJ, Patel R, Arya R. Anticoagulation for prevention and treatment of cancer-related venous thromboembolism. *Br J Haematol*. 161(6):764–77 (2013).

287. Nakchbandi W, Müller H, Singer M V, Löhr M, Nakchbandi IA. Effects of low-dose warfarin and regional chemotherapy on survival in patients with pancreatic carcinoma. *Scand J Gastroenterol*. 41(9):1095–104 (2006).

288. Nakchbandi W, Müller H, Singer M V, Lohr JM, Nakchbandi IA. Prospective study on warfarin and regional chemotherapy in patients with pancreatic carcinoma. *J Gastrointestin Liver Dis*. 17(3):285–90 (2008).

289. Camerer E, Huang W, Coughlin SR. Tissue factor- and factor X-dependent activation of protease-activated receptor 2 by factor VIIa. *Proc Natl Acad Sci USA*. 97(10):5255–60 (2000).

290. Huang M, Syed R, Stura EA, Stone MJ, Stefanko RS, Ruf W, et al. The mechanism of an inhibitory antibody on TF-initiated blood coagulation revealed by the crystal structures of human tissue factor, Fab 5G9 and TF.G9 complex. *J Mol Biol*. 275(5):873–94 (1998).

291. Ahamed J, Versteeg HH, Kerver M, Chen VM, Mueller BM, Hogg PJ, et al. Disulfide isomerization switches tissue factor from coagulation to cell signaling. *Proc Natl Acad Sci USA*. 103(38):13932–7 (2006).

292. Albrektsen T, Sørensen BB, Hjortø GM, Fleckner J, Rao LVM, Petersen LC. Transcriptional program induced by factor VIIa-tissue factor, PAR1 and PAR2 in MDA-MB-231 cells. *J Thromb Haemost*. 5(8):1588-97 (2007).

293. Schaffner F, Ruf W. Tissue factor and PAR2 signaling in the tumor microenvironment. *Arterioscler Thromb Vasc Biol*. 29(12):1999–2004 (2009).

294. Guan M, Jin J, Su B, Liu WW, Lu Y. Tissue factor expression and angiogenesis in human glioma. *Clin Biochem*. 35(4):321–5 (2002).

295. Rydén L, Grabau D, Schaffner F, Jönsson P-E, Ruf W, Belting M. Evidence for tissue factor phosphorylation and its correlation with protease-activated receptor expression and the prognosis of primary breast cancer. *Int J Cancer*. 126(10):2330–40 (2010).

296. Nakasaki T, Wada H, Shigemori C, Miki C, Gabazza EC, Nobori T, et al. Expression of tissue factor and vascular endothelial growth factor is associated with angiogenesis in colorectal cancer. *Am J Hematol*. 69(4):247–54 (2002).

297. Poon RT-P, Lau CP-Y, Ho JW-Y, Yu W-C, Fan S-T, Wong J. Tissue factor expression correlates with tumor angiogenesis and invasiveness in human hepatocellular carcinoma. *Clin Cancer Res*. 9(14):5339–45 (2003).

298. Abdulkadir SA, Carvalhal GF, Kaleem Z, Kisiel W, Humphrey PA, Catalona WJ, et al. Tissue factor expression and angiogenesis in human prostate carcinoma. *Hum Pathol*. 31(4):443–7 (2000).

299. Versteeg HH, Schaffner F, Kerver M, Ellies LG, Andrade-Gordon P, Mueller BM, et al. Protease-activated receptor (PAR) 2, but not PAR1, signaling promotes the development of mammary adenocarcinoma in polyoma middle T mice. *Cancer Res*. 68(17):7219–27 (2008).

300. Miller KD, Chap LI, Holmes FA, Cobleigh MA, Marcom PK, Fehrenbacher L, et al. Randomized phase III trial of capecitabine compared with bevacizumab plus capecitabine in patients with previously treated metastatic breast cancer. *J Clin Oncol*. 23(4):792–9 (2005).

301. Zhao J, Aguilar G, Palencia S, Newton E, Abo A. rNAPc2 inhibits colorectal cancer in mice through tissue factor. *Clin Cancer Res*. 15(1):208–16 (2009).

302. Love TE. Safety Study of Recombinant NAPc2 to Prevent Tumor Progression and Metastases in Metastatic Colon Cancer - ClinicalTrials.gov [Internet]. Available from: https://clinicaltrials.gov/ct2/show/NCT00443573.

303. Wong HC. A Study of ALT-836 in Combination With Gemcitabine for Locally Advanced or Metastatic Solid Tumors - Full Text View - ClinicalTrials.gov [Internet]. Available from: https://clinicaltrials.gov/ct2/show/NCT01325558.

304. Hedrick E. Study of Safety and Tolerability of PCI-27483 in Patients With Pancreatic Cancer Patients Receiving Treatment With Gemcitabine - ClinicalTrials.gov [Internet]. Available from: https://clinicaltrials.gov/ct2/show/NCT01020006.

305. Pan Q, Shai O, Lee LJ, Frey BJ, Blencowe BJ. Deep surveying of alternative splicing complexity in the human transcriptome by high-throughput sequencing. *Nat Genet*. 40(12):1413–5 (2008).

306. Wang ET, Sandberg R, Luo S, Khrebtukova I, Zhang L, Mayr C, et al. Alternative isoform regulation in human tissue transcriptomes. *Nature*. 456(7221):470–6 (2008).

307. David CJ, Manley JL. Alternative pre-mRNA splicing regulation in cancer: pathways and programs unhinged. *Genes Dev*. 24(21):2343-64 (2010).

308. Bourgeois CF, Lejeune F, Stévenin J. Broad specificity of SR (serine/arginine) proteins in the regulation of alternative splicing of pre-messenger RNA. *Prog Nucleic Acid Res Mol Biol*. 78:37–88 (2004).

309. Chen M, Manley JL. Mechanisms of alternative splicing regulation: insights from molecular and genomics approaches. *Nat Rev Mol Cell Biol*. 10(11):741–54 (2009).

310. Eisenreich A, Bogdanov VY, Zakrzewicz A, Pries A, Antoniak S, Poller W, et al. Cdc2-like kinases and DNA topoisomerase I regulate alternative splicing of tissue factor in human endothelial cells. *Circ Res*. 104:589–99 (2009).

311. Eisenreich A, Zakrzewicz A, Huber K, Thierbach H, Pepke W, Goldin-Lang P, et al. Regulation of pro-angiogenic tissue factor expression in hypoxia-induced human lung cancer cells. *Oncol Rep*. 30:462–70 (2013).

312. Hynes RO. Integrins: versatility, modulation, and signaling in cell adhesion. *Cell*. 69(1):11–25 (1992).

313. Dorfleutner A, Hintermann E, Tarui T, Takada Y, Ruf W. Cross-talk of integrin alpha3beta1 and tissue factor in cell migration. *Mol Biol Cell*. 15(10):4416–25 (2004).

314. Windsor JA. Anatomy and Physiology of the Pancreas. ACS Surg Princ Pract. 2012;1-14.